Biochemical studies of aromatic amino acid decarboxylase and acetaldehyde synthase

Jing Liang

Dissertation submitted to the faculty of the Virginia Polytechnic Institute and State University in partial fulfillment of the requirements for the degree of

Doctor of Philosophy
In
Biochemistry

Jianyong Li, Chair

David R. Bevan

Timothy J. Larson

Jinsong Zhu

April 16, 2018
Blacksburg, Virginia

Keywords: 3,4-dihydroxyphenylacetaldehyde synthase; tyrosine decarboxylase, 3,4-dihydroxyphenylalanine decarboxylase; pyridoxal 5'-phosphate; structure-function relationship

Biochemical studies of aromatic amino acid decarboxylase and acetaldehyde synthase

Jing Liang

ACADEMIC ABSTRACT

Pyridoxal 5'-phosphate (PLP)-dependent enzymes widely exist in most living organisms from bacteria to human. Among different types of PLP-dependent enzymes, aromatic amino acid decarboxylases play critical physiological roles because many aromatic amines are essential neurotransmitters. This dissertation concerns the biochemical characterization of several PLP-dependent decarboxylases and aims to understand the structure-function relationships, especially critical residues involved in their catalysis. L-3, 4-dihydroxyphenylalanine (L-dopa) decarboxylase (DDC) is one well-established decarboxylase. We previously identified two annotated DDC-like proteins from *Drosophila* indeed catalyzing a decarboxylation-oxidative deamination reaction of L-dopa to form 3,4-dihydroxyphenylacetaldehyde (DHPA), CO_2, NH_3, and H_2O_2 and we named these proteins as DHPA synthases due to the physiological importance of DHPA for cuticle protein crosslinking. Our results indicate that DHPA synthase reuse H_2O_2 as an oxidizing agent, and provide an efficient way to identify more DHPA synthase enzymes from DDC based on sequence identity and the signature residues we identified (Asn192 in DHPA synthase versus His192 in DDC), and we also propose a reasonable explanation of the mechanism. We then studied one tyrosine decarboxylase (TyDC). As the enzyme catalyzing the

first step of insect neurotransmitter tyramine/octopamine synthesis, the biochemical characteristics of insect TyDC have not been thoroughly elucidated yet because of the expression difficulty. We expressed one insect TyDC and analyzed its biochemical properties and compared with DDC, especially on the absorbance spectra and substrate selectivity. Site-directed mutagenesis indicates that the interactions between residue Asn304 and PLP is primarily responsible for its spectra differences of TyDC as compared to those of DDC and also is involved in higher substrate affinity to L-tyrosine. Another active site residue (Ser353) has the main effect on substrate selectivity. Our results show the biochemical properties of TyDC for the first time, and also provide some insights into the mechanism of its substrate selectivity.

Biochemical studies of aromatic amino acid decarboxylase and acetaldehyde synthase

Jing Liang

PUBLIC ABSTRACT

Pyridoxal 5'-phosphate (PLP) is a coenzyme for many enzymatic reactions. Among PLP-dependent enzymes, aromatic amino acid decarboxylase plays critical physiological roles, because many aromatic amines produced by decarboxylation of aromatic amino acids are essential neurotransmitters. L-3, 4-dihydroxyphenylalanine (L-dopa) decarboxylase (DDC) is one well-established decarboxylase, and we use DDC as a reference enzyme for comparative study with other decarboxylases. We analyzed the catalytic characteristics of several PLP-dependent decarboxylases, with a focus on the active site residues important for the catalysis and substrate specificity. We previously identified that two annotated *Drosophila* L-3, 4-dihydroxyphenylalanine (L-dopa) decarboxylase (DDC) indeed catalyzed a decarboxylation-oxidative deamination reaction of L-dopa to form 3,4-dihydroxyphenylacetaldehyde (DHPA), CO_2, NH_3, and H_2O_2 and we named these proteins as DHPA synthases due to the physiological importance of DHPA for cuticle protein crosslinking. We also functionally expressed one insect tyrosine decarboxylase (TyDC) and analyzed its biochemical properties. Our results indicate that Asn192 in DHPA synthase versus His192 in DDC are important for DHPA synthase activity and DDC activity respectively, and the roles of these two residues in both enzymes were also

proposed. In addition, DHPA synthase can reuse H_2O_2 as the oxidizing agent, and the oxidative stress of accumulated H_2O_2 may be avoided in this way. Our biochemical analyses of TyDC reveal its substrate specificity and spectra characteristics. Site-directed mutagenesis suggests the interactions between Asn304 with PLP is primarily responsible for TyDC spectra differences compared with those of DDC, and Asn304 is also involved in higher substrate affinity of TyDC to L-tyrosine. Another active site residue (Ser353) has the main effect on the substrate selectivity. Our results show the biochemical properties of insect TyDC for the first time, including the substrate specificity, spectra characteristics, and suggest some key residues involved in the substrate specificity and spectra of insect TyDC.

Acknowledgments

Here, I would like to appreciate people who have helped me tremendously during my graduate study.

First, I want to express my thanks to my advisor, Dr. Jianyong Li, who provided me a chance to study in his laboratory for Ph.D. training, especially when I was looking for a laboratory to learn protein expression, purification and characterization, the topics and skills of which attract me so much. Dr. Li provided me an excellent opportunity and environment to learn the protein research, develop one's own scientific interest and great guidance. Dr. Li taught me a lot diligently in how to conduct experiments efficiently and organizing data in manuscript logically and reasonably. Without his generous help, the two manuscripts would not be in shape so well. He also always encourages me to pursue what I want to do. I am always grateful for all I have learned during these years and all the help I get here. The only one laboratory member I have is Haizhen Ding, and she also contributed to my work and offered tremendous support in my education. I also want to appreciate Dr. Qian Han who has worked here before. I would also thank all my committee members for their brilliant advice and prompt help not only in my Ph.D. academic growth but also future career plan. They are Dr. David R. Bevan, Dr. Timothy J. Larson, and Dr. Jinsong Zhu. Many faculty members have helped me in selecting the lab to join in and planning my graduate study and career in the future, including Dr. Glenda Gillaspy, Dr. Michael Klemba, Dr. Zachary Mackey, Dr. Zhijian Tu, Dr. Bin Xu. Finally, I would like to thank Biochemistry Department for helping me with the whole graduate study.

Finally, I am so grateful to my family members and my husband who always support and encourage me to pursue my Ph.D. education. I also thank numerous friends in Blacksburg who give me so much happiness and encouragement.

Attribution

Chapter 2-4:

Qian Han (Laboratory of Tropical Veterinary Medicine and Vector Biology, Hainan Key Laboratory of Sustainable Utilization of Tropical Bioresources, Institute of Agriculture and Forestry, Hainan University, Haikou, 570228, Hainan, China.): contributed to reviewing and modifying the manuscript.

Haizhen Ding (Department of Biochemistry, Virginia Polytechnic Institute and State University, Blacksburg, VA24060, United States): contributed to technical support and guidance for protein expression.

Jianyong Li (Department of Biochemistry, Virginia Polytechnic Institute and State University, Blacksburg, VA24060, United States): contributed to modifying the manuscript and TyDC expression and purification

Table of Contents

List of Figures

List of Diagrams

List of Tables

List of Abbreviations

L-dopa	L-3, 4-dihydroxyphenylalanine
5-HTP	5-hydroxytryptophan
AAAD	aromatic amino acid decarboxylase
AMD	α-methyl dopa
AMD-r	α-methyl dopa-resistant
DDC	L-3, 4-dihydroxyphenylalanine decarboxylase
DHPA	3, 4-dihydroxylphenylacetaldehyde
HPLC	high-performance liquid chromatography
IPTG	isopropyl-β-thiogalactopyranoside
PLP	pyridoxal 5'-phosphate
SDS-PAGE	sodium dodecyl sulfate polyacrylamide gel electrophoresis
TyDC	tyrosine decarboxylase
PDB	protein data bank
WT	wild type

Chapter 1

Introduction

Pyridoxal 5'-phosphate (PLP)-dependent enzymes exist from bacteria to human, and they play multiple important roles in aromatic amino acid metabolism. PLP-dependent enzymes usually have one lysine residue conserved in the active site. PLP forms an internal aldimine with the lysine residue through a Schiff base. After substrate binding, the internal aldimine breaks up to form an external aldimine between PLP and amino group of substrates through a new Schiff base. After substrate binding and external aldimine formation in the active site, through different interactions between external aldimine and active site residues, reaction types catalyzed by PLP-dependent enzymes differ. Reaction types catalyzed by PLP-dependent enzymes include decarboxylation, racemization, transamination, deamination, etc. (1). The reaction specificity of PLP-dependent enzymes seems to be dictated primarily by stereoelectronic effects and PLP protonation status (2, 3). The stereoelectronic effect of PLP enzyme is that the enzyme binds substrates in an orientation to make the bond to be broken parallel to π system p-orbital to make it more labile (3). The PLP protonation status may also be a way by which PLP enzymes can control reaction specificity, e.g., the role of pyridine N protonation in the possibility of Cα and C4' protonation (2, 4)

In addition to the reaction specificity, these enzymes also have different substrate specificity. The enzyme active site, after substrate binding, likely has some conformational change to make the active site isolated from the effect of solvent. Otherwise, different reaction types could not be

so specific from each other. Therefore, both factors (the stereoelectronic effect and protonation status of PLP-substrate external aldimine) that mainly contribute to the reaction specificity and substrate specificity highly depend on the structures of the enzymes and interactions between substrate and active site residues. This generates an intriguing question as to what kinds of structural factors can contribute to the different reaction specificity and substrate specificity. Moreover, PLP-dependent enzymes have multiple critical physiological roles. Accordingly, PLP-dependent enzymes are an ideal group of enzymes for structure-function analysis.

The structure-function relationship of several PLP-dependent enzymes is reviewed in Chapter 2. The PLP-dependent enzymes we studied include insect L-3,4-dihydroxyphenylalanine decarboxylase (DDC), L-tyrosine decarboxylase (TyDC) and 3,4-dihydroxyphenylacetaldehyde (DHPA) synthase. DDC and TyDC belong to the insect aromatic amino acid decarboxylase (AAAD) family. DDC catalyzes the decarboxylation of L-dopa and 5-hydroxytryptophan to produce dopamine and serotonin, respectively. TyDC was proposed to catalyze decarboxylation of tyrosine to produce tyramine and was identified based on the impacted level of the tyramine in the insects with mutated proposed TyDC genes. DHPA synthase is annotated as α-methyldopa-resistant protein (AMD-r) in *Drosophila* because increased expression or mutation of this DDC-like gene leads to resistant or vulnerable phenotype of mutants to α-methyldopa added in their food (5, 6). In other insect species genomes, DHPA synthase is annotated as AAAD enzyme or DDC-like protein. Our previous study identified that DHPA synthase catalyzes decarboxylation-oxidative deamination reaction to produce DHPA, CO_2, NH_3, and H_2O_2, which is entirely different from typical decarboxylation catalyzed by DDC and other AAAD enzymes.

DDC shares high sequence identity (>30%) with TyDC and DHPA synthase. Dopamine and serotonin, produced through DDC catalyzed-decarboxylation of L-dopa and 5-hydroxytryptophan (5-HTP) respectively, are classical neurotransmitters important for both vertebrates and invertebrates. Besides, dopamine has multiple physiological functions essential for insect cuticle and eggshell hardening and immune responses (7-10). Therefore, the functional roles of DDC are relatively well established, while the DHPA synthase mechanism and the structural characteristics, leading to the deviation of the reaction type from the same substrate, are far from clearly elucidated. In addition, the biochemical characteristics of insect TyDC have not been fully analyzed because of the failure in expressing functional enzyme. Therefore, DDC is a good reference for comparative study with DHPA synthase and TyDC. The comparative study of DDC, DHPA synthase, and TyDC respectively will lead to a better understanding of their substrate specificity, catalysis specificity, and enzymatic mechanisms.

The first annotated PLP-dependent enzyme studied in this dissertation is DHPA synthase. DHPA, the product of DHPA synthase, is involved in cuticle protein crosslinking through reacting with free amino group of protein residues, leading to the hardening of colorless soft cuticle (11). DHPA synthase shares the same substrate with DDC but catalyzes decarboxylation-oxidative deamination, which is in contrast with the typical decarboxylation catalyzed by DDC. With sequence alignment of DDC and DHPA synthase from different species separately and together, combined with homology modeling and structural analysis, some potential residues crucial for typical decarboxylation and decarboxylation-oxidative deamination of L-dopa are predicted. With subsequent site-directed mutagenesis and biochemical analysis of the wild-type and mutated enzymes, our results suggest that conserved His192 and Asn192 in DDC and DHPA

synthase are signature residues respectively for distinguishing true DHPA synthase from other DDC-like proteins (e.g., DDC and TyDC) and many other typical PLP-dependent decarboxylases. Our comparative study between DDC and DHPA synthase also leads to a better understanding of the enzymatic mechanism of DHPA synthase and also complements the currently proposed mechanism for DDC-catalyzed reaction and leads to the identification of more DHPA synthases from most of the sequenced insect genomes. The comparative study also offers some basis for analyzing how functional evolution of enzymes leads to deviation of reaction types and results in different kinds of cuticle hardening (Chapter 3).

DHPA synthase vs. DDC comparison leads to a better understanding of the catalytic specificity of PLP-dependent enzymes regarding typical decarboxylation or decarboxylation-oxidative deamination from aromatic amino acids. TyDC is another member of PLP-dependent decarboxylase. TyDC gene sequence is identified and annotated based on the experimental results that the mutation of the relevant gene leads to lower level of tyramine. Tyrosine, as the substrate of TyDC, is quite similar with L-dopa except for one additional 3-OH group. DDC catalyzes decarboxylation of L-dopa and 5-HTP but has no activity to L-tyrosine. This generates an interesting question regarding whether TyDC can only catalyze decarboxylation of L-tyrosine or has an activity to L-dopa and 5-HTP as well. With the functional expression of the recombinant TyDC protein from insects, biochemical studies of TyDC suggests that the enzyme has similar catalytic specificity (typical decarboxylation) with DDC, but TyDC is active to L-tyrosine and L-dopa with better affinity to both substrates as compared with DDC. The spectra of TyDC proteins are also different from those of DDC. Subsequent sequence alignment, homology modeling, and structural analysis provide some predicted active site residues that likely are

responsible for the spectral differences and substrate specificity between TyDC and DDC. Site-directed mutagenesis identified that Asn304 and His301 in TyDC and DDC are residues important for their spectral differences and also involved in different binding affinity toward L-dopa and L-tyrosine. In addition, Ser353 makes the active site of the TyDC smaller than the active site of DDC to exclude 5-HTP as a substrate of TyDC. The biochemical study of TyDC provides some reasonable explanations of the substrate specificity of aromatic amino acid decarboxylases. The study also provides some biochemical basis for the study of the physiological functions of insect TyDC enzymes and the tyrosine/octopamine synthesis pathway (Chapter 4).

The whole dissertation is related to three PLP-dependent decarboxylases or acetaldehyde synthase. This research provides some biochemical basis for the study of the function of DHPA synthase in insect cuticle hardening and regulation of DHPA synthase in cuticle formation process and also some details in the mechanism. Additionally, as the first functionally expressed insect TyDC enzyme, the biochemical characteristics of TyDC aid in developing further study about the physiological function and regulation of this enzyme.

1.1 References

1. Eliot AC, Kirsch JF. Pyridoxal phosphate enzymes: mechanistic, structural, and evolutionary considerations. Annu Rev Biochem. 2004;73:383-415
2. Toney MD. Controlling reaction specificity in pyridoxal phosphate enzymes. Biochim Biophys Acta. 2011;1814(11):1407-1418
3. Dunathan HC. Conformation and reaction specificity in pyridoxal phosphate enzymes. Proc Natl Acad Sci U S A. 1966;55:712-716
4. Casasnovas R, Salvà A, Frau J, Donoso J, Muñoz F. Theoretical study on the distribution of atomic charges in the Schiff bases of 3-hydroxypyridine-4-aldehyde and alanine. The effect of

the protonation state of the pyridine and imine nitrogen atoms. Chem Phys. 2009;355(2-3):149-156
5. Sparrow JC, Wright TRF. The Selection for Mutants in *Drosophila melanogaster* Hypersensitive to alpha-Methyl Dopa, a Dopa Decarboxylase Inhibitor. Molec gen Genet 1974(130):127-141
6. Sherald AF, Wright TRF. The Analog Inhibitor, alpha-Methyl Dopa, as a Screening Agent for Mutants Elevating Levels of Dopa Decarboxylase Activity in *Drosophila melanogaste*. Molec gen Genet 1974(133):25-36
7. Davis MM, Primrose DA, Hodgetts RB. A member of the p38 mitogen-activated protein kinase family is responsible for transcriptional induction of Dopa decarboxylase in the epidermis of Drosophila melanogaster during the innate immune response. Mol Cell Biol. 2008;28(15):4883-4895
8. Ferdlg MT, Li J, Severson DW, Chritensen BM. Mosquito dopa decarboxylase cDNA characterization and blood-meal-induced ovarian expression. Insect Mol Biol. 1996;5(2):119-126
9. Sideri M, Tsakas S, Markoutsa E, Lampropoulou M, Marmaras VJ. Innate immunity in insects: surface-associated dopa decarboxylase-dependent pathways regulate phagocytosis, nodulation and melanization in medfly haemocytes. Immunology. 2007(123):528-537
10. Huang CY, Chou SY, Bartholomay LC, Christensen BM, Chen CC. The use of gene silencing to study the role of dopa decarboxylase in mosquito melanization reactions. Insect Mol Biol. 2005;14(3):237-244
11. Vavricka C, Han Q, Huang Y, Erickson SM, Harich K, Christensen BM, Li J. From L-dopa to dihydroxyphenylacetaldehyde: a toxic biochemical pathway plays a vital physiological function in insects. PLoS One. 2011;6(1):e16124

Chapter 2

Current Opinions on Structure-function Relationships of Pyridoxal 5'-phosphate-dependent Enzymes

Jing Liang [a], Qian Han[b], Haizhen Ding [a], Jianyong Li [a*]

[a] Department of Biochemistry, Virginia Polytechnic Institute and State University, Blacksburg, VA24060, United States

[b] Laboratory of Tropical Veterinary Medicine and Vector Biology, Hainan Key Laboratory of Sustainable Utilization of Tropical Bioresources, Institute of Agriculture and Forestry, Hainan University, Haikou, 570228, Hainan, China.

[*] Correspondence to Prof. Jianyong Li (lij@vt.edu; Tel: 540-231-5779; Fax: 540-231-9070)

Abstract

Pyridoxal 5'-phosphate (PLP) functions as a coenzyme in many enzymatic processes, including decarboxylation, deamination, transamination, racemization, etc. Enzymes requiring PLP are commonly termed PLP-dependent enzymes, and they are widely involved in crucial cellular metabolic pathways in virtually all living organisms from bacteria to human. The chemical mechanisms for PLP-mediated reactions have been well elaborated and accepted, but this coenzyme must be associated with proteins to be functional, and the three-dimensional structures,

particularly the active site residues dictate the reaction directions, i.e., transamination or decarboxylation, etc. Although chemical reaction mechanism for any given enzyme may have been well described, the specific mechanism of an enzyme in relation to the one for the similar class of enzymes seems scarcely described or discussed. This discussion aims to link the specific mechanism described for the individual enzyme to the same types of enzymes from different species with aminotransferases, decarboxylases, and aromatic acetaldehyde synthase as models.

Keywords

pyridoxal 5'-phosphate, structure-function relationship, reaction mechanism, amino acid residues, reaction specificity

2.1 Introduction

Pyridoxal 5'-phosphate (PLP) is one biologically active type of vitamin B_6 through the catalysis of pyridoxal kinase. PLP-dependent enzymes catalyze a wide variety of reaction types and usually have one conserved lysine residue in the active site for PLP binding. The lysine residue ε-amino group and PLP aldehyde group form an internal aldimine through one Schiff base. After substrate binding (amino acid or amine), the internal aldimine breaks up, and a new Schiff base is formed between the amino group in the substrate and aldehyde group in PLP cofactor. This newly formed Schiff base is called external aldimine. The external aldimine formation after substrate binding is the common step of most PLP-dependent enzymes, but reaction types differ after external aldimine formation through interacting with the specific enzymatic environment.

PLP-dependent enzymes participate in many critical cellular processes and metabolism. These enzymes are involved in the amino acid metabolism and production of amino acid-derived metabolites. For example, L-3,4-dihydroxyphenylalanine (L-dopa) decarboxylase (DDC) catalyzes the decarboxylation of L-dopa and 5-hydroxytryptophan to produce dopamine and serotonin respectively, which are the neurotransmitters for not only mammals but also insects. The regulation problems and deficits of PLP-dependent enzymes caused probably by pathogenic mutations result in several metabolism symptoms. For instance, the deficiencies of DDC lead to the development delay, abnormal movement, and other neurotransmitter-related symptoms (1). Deficits of alanine-glyoxylate aminotransferase are involved in hyperoxaluria Type I disease while ornithine aminotransferase deficiency contributes to the vision problem in the dim light situations (1). The blood PLP level and the risk of colorectal cancer are also inversely related (2). Besides, it is evaluated recently, for the first time that the insufficient PLP or B_6 intake from food may contribute to pancreatic islet autoimmunity and the development of type I diabetes (3).

As a result of the diverse reaction specificity and the physiological significance, there are more research regarding the mechanisms of PLP-dependent enzyme activity, especially the mechanisms based on structure-function relationship. With the technological and methodological development, especially the sequencing of genomes, technical progress of protein expression and purification, and the determination of more enzyme crystal structures, an increasing number of PLP-dependent enzymes are revealed and a better understanding of enzymatic catalysis is achieved, especially how the active site residues facilitate the specific reaction and at the same time decrease the possibility of side reactions. In this review, we summarized the mechanisms of several PLP-dependent enzymes and discussed our current opinions on the PLP-dependent

enzymes we have analyzed through structural analysis and site-directed mutagenesis, with the focus on the roles of the crucial active site residues involved in reaction specificity.

2.2 New insights of PLP chemistry in catalysis

PLP has one heteroaromatic pyridine ring, one aldehyde group, one hydroxyl group, and a phosphate group. The aldehyde group of PLP makes it possible to form imine with the free amino group (e.g., the internal aldimine, formed between PLP and conserved lysine residue and external aldimine formed between PLP and substrate amino group). The internal aldimine or external aldimine are formed through one Schiff base, which can be attacked by another unprotonated primary amino group, making the internal or external aldimine reversible with the presence of an unprotonated amino group. The ability to form reversible imine allows the PLP binding, substrate binding, product releasing and regeneration of enzyme with PLP bound in the active site.

The heteroaromatic pyridine ring of PLP enables PLP to stabilize carbanionic intermediate formed during most (if not all) of the PLP-dependent enzymes, except aminomutase family (radical-initiated reaction) (4). In most reactions catalyzed by PLP-dependent enzymes, a carbanionic intermediate or quinonoid intermediate is formed. The electrons of the carbanionic intermediate are resonance stabilized and delocalized by the Schiff base and electron-sink of PLP. Quinonoid intermediate, proposed as the key intermediate in many PLP-dependent catalytic mechanisms, is one resonance form of the carbanionic intermediates. The heteroaromatic pyridine ring N1 also contributes to the electron-sink effect of PLP by affecting the electron

density shifting toward N1 as compared with the benzene ring. The protonated N1 of PLP can better attract electrons from the Cα or C4', and help delocalization and stabilization of the carbanionic intermediate (5).

The aldehyde group and pyridine ring of PLP are well studied as the important groups participating in catalysis. The hydroxyl group could also function as proton donor or acceptor, which will be discussed in detail in this chapter. The role of 5'-phosphate group was less mentioned or elaborated, but recently the importance of the phosphate group in PLP was discussed through comparative analysis using pyridoxal or pyridoxal 5'-phosphate as the cofactor in serine palmitoyltransferase. Research indicated that the removal of the phosphate lowered the activity more than 10-fold although external aldimine formation is not prevented (6). Their research suggested that the phosphate group of PLP interacted with the substrate L-serine hydroxyl group and contributed to the critical intermediate formation and stereospecific orientation of formed quinonoid or carbanionic intermediate after deprotonation for the acyl-CoA thioester attack of next step (6). The phosphate group is also found to function as one acid/base catalyst to promote proton transfer with the substrate and to aid in external aldimine formation and acceleration of *gem-diol* intermediate formation in kynureninase-mediated hydrolytic cleavage reaction (7).

Due to those functional groups, PLP-dependent enzymes catalyze diverse reactions (e.g., decarboxylation, racemization, transamination, elimination, replacement, etc.) for amino acid and amine metabolism and approximately 4% of all classified enzyme activities are PLP-dependent (8, 9). Based on the chemical role of PLP, through different interactions with the

enzymatic environment (e.g., active site residues), PLP-dependent enzymes catalyze different reactions. For example, racemization is through deprotonation and reprotonation of Cα on the opposite side of the position where deprotonation occurs, while reprotonation at C4' of PLP after deprotonation at Cα is the critical step of transamination for a ketimine intermediate formation. Decarboxylation is through removal of $-COO^-$ group from the external aldimine to form a carbanionic or quinonoid intermediate and followed by protonation of the intermediate at Cα after decarboxylation to form amine. Retro-aldol condensation is through bond breaking between Cα and Cβ to form carbanionic intermediate. Some enzymes catalyze a combination of different reaction types, e.g., dialkylglycine decarboxylase (DGD) catalyzes the decarboxylation-dependent transamination (10, 11).

2.3 Mechanism of reaction specificity

2.3.1 Stereoelectronic effects: unifying enzymatic mechanism

PLP is currently accepted to have the electron sink role for delocalization and resonance stabilization of the electrons or negative charges developed from bond breaking at Cα, as well as to form the aldimine through the aldehyde group of PLP. However, in the buffer, mixing of only PLP and amino acid or amine does not lead to evident specific reactions (the rate of reaction is too slow to be physiologically or enzymatically relevant) as compared with reactions catalyzed by PLP-dependent enzymes. The aldimine can be formed between PLP and amino acid or amine without adding protein component, but the aldimine formed is not stable and undergoes dynamic break up and formation. Only the combination of protein components and PLP make the PLP-

dependent enzyme work efficiently on the specific substrate and promotes reaction of specific direction. One might ask how a given enzyme controls the reaction specificity because PLP functions in most of PLP-dependent reactions to delocalize and resonance stabilizes the electrons or negative charges (developed from bond breaking at Cα) in the transition state.

In 1966, Dunathan raised a unifying theory to explain the reaction specificity of the PLP-dependent enzymes (12). It was hypothesized that if the delocalization energy was gained after the loss of one group from Cα, the PLP-dependent enzyme should bind substrates in specific geometry to have the bond to be broken in a perpendicular plane of the plane defined by pyridoxal imine (the π system) to make the bond labile to be broken (12). For example, the α-decarboxylase binds the substrates in a specific orientation to have the $-COO^-$ group perpendicular to the plane of Schiff base and PLP ring. This orientation was proposed to facilitate decarboxylation process, and the carboxyl group, in this orientation, was more labile than the other bonds at Cα.

2.3.2 External aldimine formation is a prepared step

Most PLP-dependent enzymes have the PLP binding in the active site through forming one internal aldimine, although PLP could also be anchored in the active site through phosphate group in some exceptions (13). The internal aldimine is formed through a Schiff base linkage between active site Lys residue ε-amino group and PLP aldehyde carbon atom (C4' atom). The internal aldimine formation is shared in most PLP-dependent enzymes and critical for anchoring PLP in the active site for external aldimine formation. Oliveira et al. (14) found that internal

aldimine formation was not as simple as just a single step of nucleophilic attack of Lys ε-amino group on the aldehyde carbon of PLP. Instead, they found that internal aldimine formation was a complicated process involving different intermediates formation. They indicated that the full process contained three steps. First, the active site Lys residue should be aligned with the ring of PLP to pre-activate the Lys residue and the nucleophilic attack of Lys on PLP should occur spontaneously. Second, one carbinolamine intermediate was detected experimentally to be formed in the process through proton transfer from Lys residue to Cys360 (in human ornithine decarboxylase) with subsequent proton transfer from Cys360 to PLP hydroxyl group. Third, internal aldimine was formed. At the same time, one water molecule was formed and trapped inside the active site. The third step was considered being a rate-limiting step (13.5 kcal/mol activation energy). Moreover, Cys360 seemed to have on and off conformations in the reaction. For "on" conformation, the rotamer of Cys360 pointed toward PLP, and this conformation was present prior to forming carbinolamine intermediate. In contrast, the "off" conformation corresponded to the more distance of Cys from PLP by pointing to the opposite direction (14).

Oliveira et al.'s research provides a detailed process for the first time regarding the internal aldimine formation mechanism from interactions with enzymatic environment point of view. Through the internal aldimine formation, PLP is anchored in the active site. After substrate binding, the external aldimine will form through transimination process, and this is the first step shared by most of the PLP-dependent reactions. The internal aldimine between PLP and Lys residue is relatively stable through protein expression and purification. The external aldimine formation is basically the reverse reaction of internal aldimine break up from a chemical point of view. This generates a question regarding how the transimination toward external aldimine

formation direction is favored. Recently, the researches of Milić et al. (15) and Chan-Huot et al. (16) have given some clues to this question.

Milić et al. (15) crystallized the tyrosine phenol-lyase which is one PLP-dependent enzyme catalyzing β-elimination of L-tyrosine. The structure of tyrosine phenol-lyase and site-directed mutagenesis results determined that Asp214 residue near the pyridine ring nitrogen formed a hydrogen bond with the pyridine ring N1 atom and mutation of Asp214 led to deprotonation of pyridine ring N1. Furthermore, Asp214 seemed to play a role in stabilizing a distorted strain of the internal aldimine, and this state was probably crucial for accelerating the first step, transimination (15). Milić, et al.'s research (15) suggests that Asp and protonation of pyridine ring favor external aldimine formation. Not all PLP-dependent enzymes have one Asp residue or Asp equivalent (such as glutamate) to favor the protonation of pyridine ring and stabilize one distorted strain of internal aldimine to facilitate external aldimine formation, e.g., racemase. Chan-Huot et al. suggested that for enzymes that cannot protonate pyridine nitrogen, the protonation of the phenolic oxygen would activate PLP and prepare for the transimination step when substrate entered the active site by enhancing proton transfer from phenolic oxygen to the Schiff base nitrogen, which is thought to be the prerequisite of transimination (16).

These analyses offer some clues on the specific mechanism of internal aldimine formation and how the internal aldimine protonation state or interactions with the active site residues could favor external aldmine formation, suggesting that the external aldimine formation is already prepared in internal aldimine formation stage. After substrate binding, the external aldmine formation is through a nucleophilic attack. Nucleophilic attack of the amino group of substrate

on PLP C4' atom is possible only when the substrate amino group is not protonated and therefore can serve as a nucleophile. In the reaction mixture under physiological condition (pH around 7), the substrate amino group is usually protonated according to the pKa of the amino group. The protonated amino group invalidates the nucleophilic attack of substrate and inhibits external aldimine formation. This raises the first fundamental question that how the amino group of a substrate is deprotonated.

In 2014, Ngo et al. crystallized and analyzed the snapshot of different intermediates of one PLP-dependent enzyme in its L-serine dehydratase reaction through transferring crystals into a solution containing substrate L-serine for various time durations (17). Their results provided some insights as to how nucleophilic attack of the substrate is achieved by the molecular switch of the dihedral angle between PLP ring and Schiff base and how this angle is affected and restrained by active site residues. Their results suggested that PLP formed one internal aldimine with active site conserved Lys210 residue, and Tyr112 was involved in PLP binding by π-π stacking through the phenyl ring of Tyr112. The substrate-soaked structure identified two substrate electron densities, one is entry site (E site) for substrate entering the active site through the channel and another one is near PLP called active site (A site) (17). Intriguingly, the dihedral angle (angle between the pyridine ring of PLP and Schiff base linkage) is 34° in native structure while when substrate enters the active site, the ring of Tyr112 moved toward E site by 1.4 Å, which resulted in a loss of π-π stacking effect with the PLP ring. Then the substrate seemed to move to A site, and its amino group could be deprotonated by O3' atom of PLP. The dihedral angle in this process was distorted to 52°, which disrupted the π bond system of Schiff base and PLP. Lys210 restricts the further increase of the angle beyond 52° (17). The disrupted π bond

system enables the Schiff base double bond between lysine amino N and PLP aldehyde C4' to have some single bond characteristics, resulting in PLP aldehyde C4' atom to have some positive charge characteristics (17). These changes enable the deprotonated amino group of substrate to undergo nucleophilic attack on the PLP C4', which caused 11.4° tilt of PLP ring toward serine amino group to facilitate a new Schiff base formation between PLP and serine amino group and also at the same time restored the previously lost interactions between PLP and Tyr112 (17). The external aldimine formation through the variation of the dihedral angle also inspires future research of other PLP-dependent enzymes. It is well known that after substrate binding, the enzymes may undergo conformational changes to exclude the substrate from the solvent solution, which could be especially true for PLP-dependent enzymes to ensure the reaction specificity. It is worthwhile to study whether other PLP-dependent enzymes have similar dihedral angle change to facilitate external aldimine formation. Moreover, the ability of PLP O3' as a proton acceptor in L-serine dehydratase external aldimine formation suggests a way of how the availability of nucleophile of Lys residue is enabled. Whether this is the typical way or mechanism for deprotonation of substrate amino group in other PLP-dependent enzymes need to be analyzed.

2.3.3 Aminotransferase

Aminotransferase catalyzes the reversible transformation between an amino acid and α-keto acid. For example, aspartate aminotransferase catalyzes the reversible conversion from L-aspartate and α-ketoglutarate to oxaloacetate and L-glutamate. The two half-reactions of aspartate aminotransferase are under a ping-pong mechanism. PLP forms a Schiff base with a conserved

Lys residue. After substrate binding, the external aldimine is formed, and deprotonation at Cα and reprotonation at C4' position of PLP leads to a ketimine intermediate formation and one H_2O molecule is added to the intermediate Cα. Then the half reaction proceeds to have α-keto acid involved to regenerate PLP and another amino acid. This is the generally accepted reaction mechanism.

The proton transfer between Cα of substrate and aldehyde carbon C4' of PLP is a central process in transamination. In forward reaction, deprotonation is at substrate Cα and reprotonation is at C4' while deprotonation is at C4' and reprotonation is at Cα in the reverse reaction. The proton transfer between Cα and C4' was considered to be through the conserved Lys residue that is in charge of PLP binding in the active site by forming internal aldimine. The role Lys residue plays in proton transfer was indicated by the mutation results, which showed that the impacted catalysis could be restored by adding simple primary amine (18).

In literature, there is a debate regarding whether the proton transfer by Lys residue between Cα and C4' is through a concerted process or stepwise process (needs an interconverting carbanionic intermediate) (19, 20). The quinonoid intermediate has been commonly accepted as the stabilized intermediate for PLP-dependent enzymes. The existence of quinonoid intermediate evidenced by light enhancement of aspartate aminotransferase-catalyzed reaction and the low concentration of quinonoid intermediate in the steady state favor the stepwise mechanism (19).

Both concerted mechanism and stepwise mechanism is dependent on Lys residue and quinonoid intermediate while stepwise mechanism probably needs quinonoid intermediate as one

interconverting intermediate and thus require a relatively long lifetime of the quinonoid intermediate. Both Lys residue and quinonoid intermediate are shared by most of the PLP-dependent enzymes, and only Lys residue and quinonoid intermediate are not enough for mediating the proton transfer between Cα and C4'. There should be other factors that also contribute to the reaction specificity catalyzed by aminotransferase.

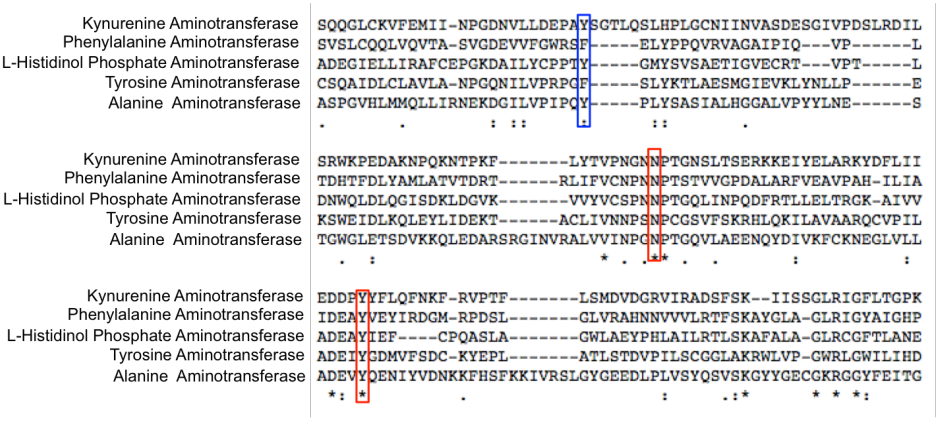

Figure 2.1: Partial sequence alignment of aminotransferase. **Partial sequence alignment of kynurenine aminotransferase (PDB: 2R2N) (21), phenylalanine aminotransferase (PDB: 4R5Z) (22), L-histidinol phosphate aminotransferase (PDB: 1IJI) (23), tyrosine aminotransferase (PDB: 3DYD) (24) and alanine aminotransferase (PDB: 3TCM) (25) is shown. The uncharged aromatic amino acid residues for π-π stacking with PLP ring are highlighted in blue box, and the Asn and Tyr residues forming hydrogen bonds with PLP O3' are highlighted in red boxes.**

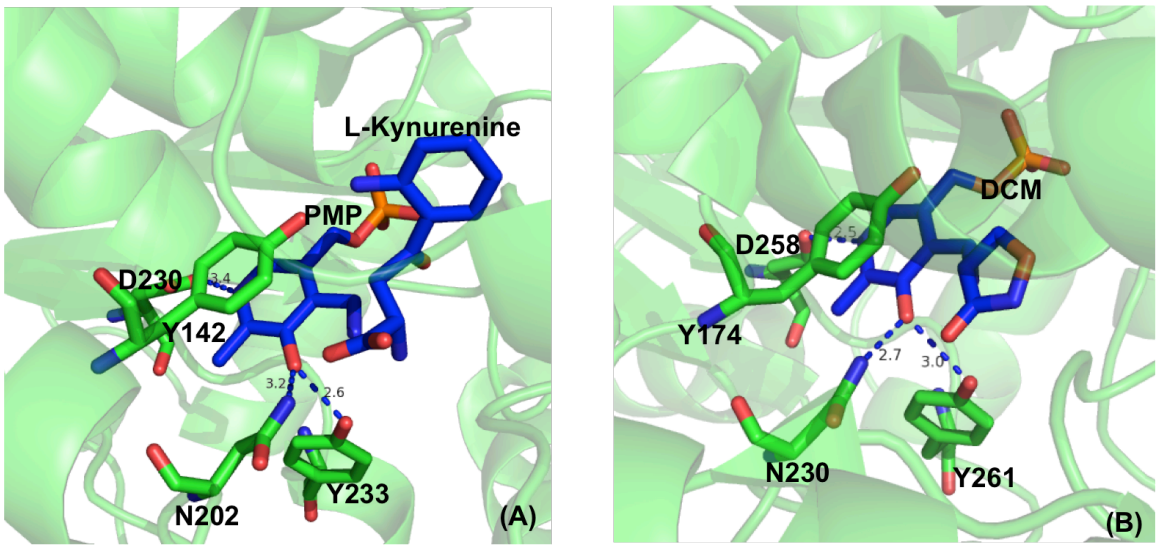

Figure 2.2: The positions of Asn and Tyr residues and the distances for forming hydrogen bonds with O3' of PLP. **The Asn and Tyr residues forming hydrogen bonds with O3' of PLP are shown in green sticks while the PMP, L-kynurenine and external aldimine analog D-pyridoxyl-N,O-cycloserylamide-5-monophosphate (DCM) are shown in blue sticks. The uncharged aromatic amino acid residues forming π-π stacking with PLP pyridine ring and the Asp residue near pyridine ring N atom are also shown in green sticks. The distances between PLP O3' and Asn or Tyr and the distances between pyridine ring N and Asp side chain are in blue dashed line and labeled (Unit: Å). L-kynurenine aminotransferase (PDB: 2R2N) (21) (A) and alanine aminotransferase (PDB: 3TCM) (25) (B) are presented as two examples.**

To analyze how the aminotransferase could proceed proton transfer between Cα and C4' specifically, we analyzed several aminotransferase crystal structures (21-28). Based on those crystal structures, it was found that no other residues are in proximity to transfer a proton except Lys residue as generally accepted. The aminotransferases also have an uncharged aromatic amino acid residue conserved (Phe or Tyr or Trp depending on different aminotransferases) for π-π stacking of the PLP ring (Figure 2.1 and Figure 2.2). In contrast, His residue, a good proton donor and acceptor, is conserved in α-decarboxylases at the equivalent position (28, 29). Sequence alignment (Figure 2.1) and structural analysis (Figure 2.2) also suggest that one Asn

residue and one Tyr residue are highly conserved in the active sites of aminotransferases and are near PLP O3' atom to form hydrogen bonds.

The presence of an uncharged aromatic amino acid residue (Trp, Tyr, or Phe) for π-π stacking (Figure 2.2) likely enables the proton transfer between Cα and C4' through Lys residue by making the relatively long lifetime possible. Once carbanionic intermediate is formed after deprotonation at Cα, it is highly reactive. If His residue is at the equivalent position, the carbanionic intermediate or quinonoid intermediate could be quickly protonated by His residue. This quick protonation may compete with the protonation by Lys residue and impact the catalysis. The proton transfer needs Lys to move between Cα and C4' to deliver the proton. Uncharged aromatic amino acid residue enables a longer lifetime of the carbanionic intermediate or quinonoid intermediate, which leaves time for proton transfer by Lys residue.

In addition to the uncharged aromatic amino acid for π-π stacking with PLP, there are two active site residues Asn and Tyr highly conserved in aminotransferases and forming hydrogen bonds and in proximity with phenol group O3' of PLP (Figure 2.1 and Figure 2.2). The 3'-OH has electrostatic interactions with the Schiff base nitrogen atom and also has hydrogen bond with the Schiff base. The interactions between O3' and Schiff base also likely restrict the flexibility of the groups (e.g., C4') in Schiff base, which may facilitate the electron delocalization and stabilization effect. Furthermore, compared with racemase with Arg residue near O3' of PLP, the neutral characteristics of Tyr and Asn in proximity with O3' atom make the strong hydrogen bond formation possible and make the higher possibility for the O3' group to be neutral or not ionized.

In the enzymatic conditions, as discussed above, the O3' plays a role by serving as one proton acceptor to remove the proton from the substrate amino group to enable the internal aldimine formation (14, 17). O3' group was also reported to participate in catalysis as a proton donor or acceptor (30). The 3'-OH group serves as both proton donor and acceptor because the 3'-OH phenol group is more acidic than the alcohol hydrogen atom (pKa of cyclohexanol is around 16). The delocalization effects of the aromatic ring (pKa of tyrosine is around 10) by forming resonance structures also contributes to the acidity of 3'-OH group (https://chem.libretexts.org/Textbook_Maps/Organic_Chemistry_Textbook_Maps/Map%3A_Organic_Chemistry_(31)/16%3A_Reactions_of_Substituted_Benzenes/16.05_The_Effect_of_Substituents_on_pKa). Compared with the benzene ring in tyrosine, the pyridine ring of PLP has one nitrogen atom to substitute one carbon on the ring. When the pyridine nitrogen is protonated, the electronegative nitrogen atom in pyridine ring has a better effect for electron-withdrawing and delocalization effect than carbon atom in the ring. The negative charge of ionized O3' can also be delocalized through the pyridine ring (Figure 2.3, form I and II).

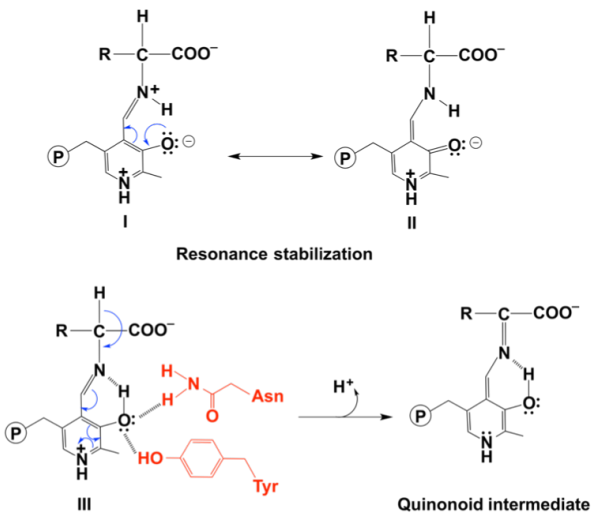

Figure 2.3: The effect of protonation states of O3' on delocalization. **The stabilization of ionized O3' (form I) through resonance structure (form II). The electron withdrawing effect of PLP with a neutral O3' (form III) and formation of quinonoid intermediate are shown.**

The existence of Tyr and Asn near O3' makes the neutral form of 3'-OH favorable for facilitating the delocalization of electrons. An ionized form of phenol group could also possibly exist, but the neutral form should be predominant. Moreover, the strong hydrogen bonds, favoring the neutral form of 3'-OH group, have contributed to the catalysis of aminotransferase by favoring the delocalization effect. This is due to that the ionized O3' has more lone pairs of electrons (Figure 2.3, form I) than that of the neutral form (Figure 2.3, form III) and needs to be delocalized into the pyridine ring for stabilization (Figure 2.3, I and II). The increased lone pairs of electrons may have some electron donating effect to counteract with the delocalization effect (Figure 2.3, form I). In contrast, the neutral 3'-OH group stabilized by the hydrogen bonds with neutral Tyr and Asn likely better favor carbanionic intermediate formation and delocalization of electrons (Figure 2.3, form III) and thus may contribute to the deprotonation of Cα (Figure 2.3,

form III and quinonoid intermediate) as compared with the ionized form, which is the first critical step of aminotransferase-catalyzed reaction after external aldimine formation.

The evidence regarding aminotransferase favors the stepwise mechanism that proton transfer between Cα and C4' needs one stabilized intermediate serving as an interconverting carbanionic intermediate (19). Although other PLP-dependent enzymes also have the carbanionic intermediate formed and stabilized, the necessity of stabilized intermediate in aminotransferase-catalyzed reaction and the detection of low concentration of quinonoid intermediate in steady state (19) indicates that the stabilized carbanionic intermediate likely is more critical for aminotransferase-catalyzed reaction. Tyr and Asn, forming hydrogen bonds with 3'-OH group and stabilizing the neutral form of 3'-OH, by contributing to the delocalization effect, have an important role for the formation and stability of the interconverting intermediate for proton transfer between two sites in reactions catalyzed by aminotransferases. It is noticed that most of the aspartate aminotransferases usually have a λ_{max} around 422 nm, indicating the internal aldimine PLP predominantly in ketoenamine form (O3' is ionized) (Figure 2.4). However, the predominant ketoenamine form of internal aldimine, or even the enolimine/ketoenamine form of the external aldimine, does not necessarily lead to a conclusion regarding the carbanionic intermediate protonation state of the O3' because the process of carbanionic intermediate formation may change the protonation state. The protonation state in the carbanionic intermediate is the one that indeed relates to reaction specificity because it affects the next step by affecting the electron distribution of the whole intermediate. Even the internal aldimine has the ketoenamine form predominant, the O3' should be in the neutral form (enolimine form) in

carbanionic intermediate to promote deprotonation and help with the stability of the quinonoid intermediate to serve as one interconverting intermediate.

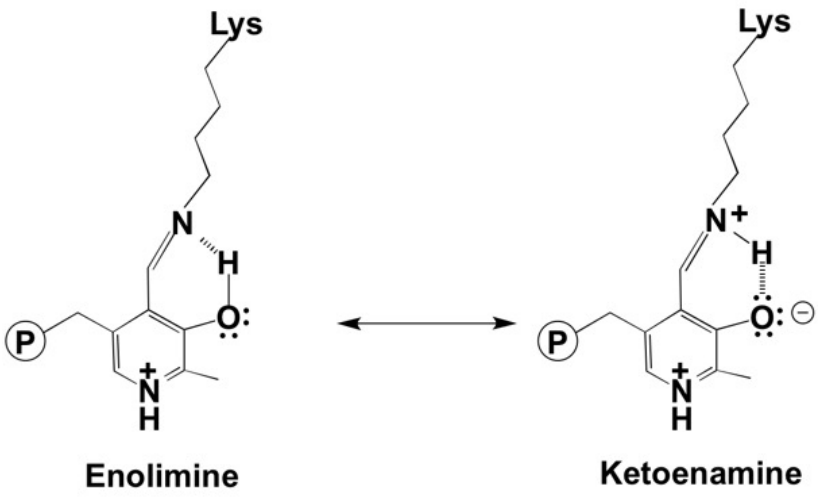

Figure 2.4: Enolimine and ketoenamine forms of internal aldimine. **The interaction between O3' and Schiff base N is shown in dashed line.**

The protonation state of pyridine ring, fulfilled by the nearby Asp residue (Figure 2.2), has been considered necessary for aminotransferase. For the same reason with the protonated O3', the protonated pyridine nitrogen likely reduces the lone pair electrons of the pyridine nitrogen and facilitates the delocalization and stabilization of carbanionic intermediate. The protonated pyridine nitrogen makes the pyridine ring to attract electrons better, and the electron density at C4' of PLP higher than that at Cα and thus promote deprotonation at Cα and facilitate reprotonation at C4'. The synthesized 1-deazaPLP with a carbon atom at the same position to substitute the pyridine ring nitrogen has been utilized as the cofactor to analyze the role of pyridine ring protonation (5). The extremely low reaction rate affected by this PLP analog

indicated the importance of pyridine ring nitrogen on protonation of carbanion intermediate in the reaction catalyzed by aminotransferase.

2.3.4 PLP-dependent decarboxylase

In PLP-dependent decarboxylase, PLP serves as an electron sink to delocalize the unbound electrons and to orientate enzyme-substrate in a specific orientation, both of which contribute to the decarboxylation and the release of CO_2 and formation of a quinonoid intermediate. The protonation at Cα leads to an imine formation, which is attacked by Lys amino group to lead to one Schiff base formed between Lys residue and the PLP. At the same time, the amine product is released. This is the generally accepted mechanism for the decarboxylation process.

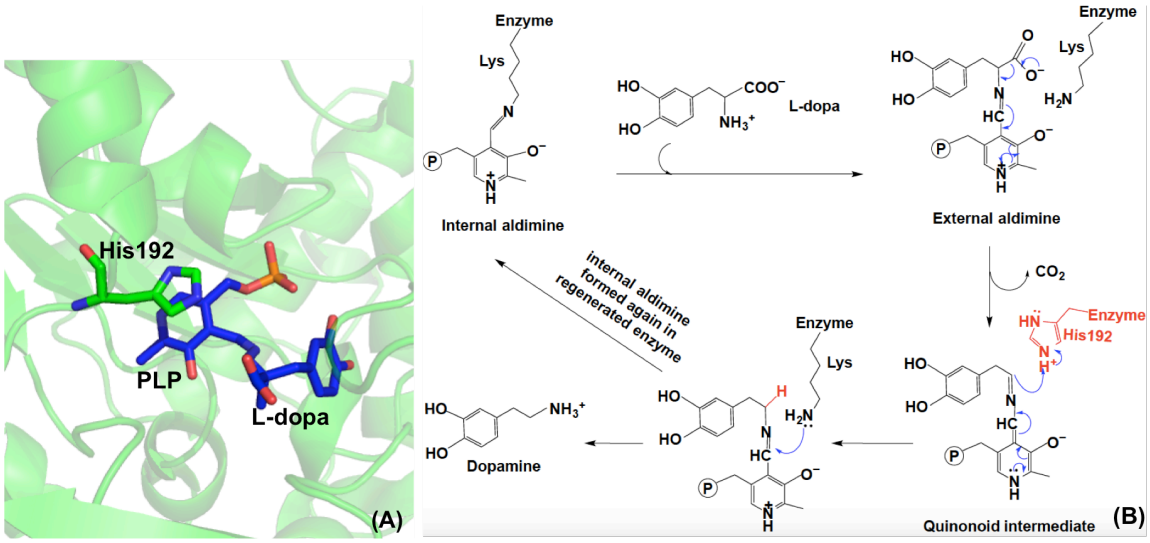

Figure 2.5: The mechanistic role of His192 residue in *Drosophila* DDC. **The His192 residue position in the active site of DDC (PDB: 3K40) (28) is shown with His residue in green sticks and external aldimine formed by PLP and L-dopa in blue sticks (A). The mechanistic role of His192 residue in typical decarboxylation is shown (B).**

The intermediate formed after decarboxylation is unstable and highly reactive, but the residues or other factors that contribute to the Cα protonation are not clear. We have crystallized the *Drosophila melanogaster* 3,4-dihydroxyphenylalanine (dopa) decarboxylase (DDC) before (PDB: 3K40) (28). Our recent study on DDC identified that His192 is the residue that protonates the quinonoid intermediate after decarboxylation (29). His residue is a good proton donor and is in close proximity with the PLP ring and also the Schiff base (Figure 2.5A). After decarboxylation, the carbanion intermediate or quinonoid intermediate (resonance structure of carbanion) is stabilized by the PLP electron sink through electron delocalization. The protonation of Cα by His192 promotes electron shift of the quinonoid intermediate and formation of a new double bond between N atom and C4'. The intermediate after protonation undergoes rapid hydrolysis to release dopamine and regenerate PLP-enzyme complex (internal aldimine). The high efficiency of His192 on promoting protonation of Cα likely is the most important step for the intermediates going through the typical DDC-mediated process (Figure 2.5B) (29).

Except the typical decarboxylation as the main reaction, the side reaction oxidative-deamination of DDC to produce acetaldehyde is also observed. The side reaction is less than 1% of the typical decarboxylation. The operation of both main reaction and side reaction in DDC suggests that even with the fast protonation of His residue, there are still some intermediates that escaped from the typical decarboxylation and were attacked by oxygen, indicating the reactivity of quinonoid intermediate. Our mutation of His192 to Asn192 increased the acetaldehyde formation (side reaction) from negligible to a major pathway by mutated DDC H192N. The existence of both decarboxylation and oxidative deamination in DDC H192N mutation supports the role of fast protonation by His192 in typical decarboxylation (29).

Similar to the His192 residue for decarboxylation at Cα, the structure and mechanism study on β-decarboxylase in *Pseudomonas dacunhae* showed that fast protonation of the carbanionic intermediate also is essential for this enzyme. Instead of His192 to protonate intermediate in DDC, an arginine residue in the active site probably plays a similar role in the intermediate protonation (32).

The pig kidney DDC Y332F mutation makes the mutated DDC have decarboxylation-dependent deamination activity of L-dopa substrate (33). It is likely that Tyr332 residue is in flexible loop region, which could form a hydrogen bond with the His residue to stabilize the proton on His residue by the movement of flexible loop. The Y332F mutation could affect the protonation effect of His residue by removing the hydrogen bond between Tyr332 and His residue.

2.3.5 O_2-using PLP-dependent enzymes

Among PLP-dependent enzymes, the members that use oxygen as a substrate are rarely reported. In contrast, the oxygen is a common substrate for the enzymes dependent on redox cofactor (e.g., flavin or pterin) or transition metal ions to activate oxygen (34-37). For PLP-dependent enzymes, it is well known that the ability for catalysis is dependent on the delocalization of electrons to the PLP ring and the stabilization of the carbanionic intermediate formed. Thus, PLP-dependent enzymes and other enzymes that mediate carbanion formation during the catalysis should develop a specific mechanism to protect intermediates from undesirable electrophiles, e.g., oxygen (38). Taking the DDC enzyme as one example, our recent study indicated that DDC

catalyzed typical non-oxidative decarboxylation as the main reaction through fast protonation at the Cα by His192 residue (in *Drosophila* enzyme). Even the rapid protonation can protect the intermediate from being attacked by oxygen, there are still some intermediates that escape from the typical decarboxylation to undergo oxidative side reaction, the rate of which is negligible and less than 1% of the rate of the main reaction (29). PLP-catalyzed oxidation with oxygen is not the typical type of reaction of PLP-dependent enzymes (39), and also it is unclear how the oxygen is activated by the PLP-dependent enzyme.

Kaminaga et al. (40) have reported one plant phenylacetaldehyde synthase catalyzing oxidative decarboxylation of phenylalanine to generate CO_2, NH_3, phenylacetaldehyde, and H_2O_2 stoichiometrically. Most PLP-dependent reactions have been thought to be via a non-radical mechanism by forming a quinonoid intermediate. Their results indicated the possibilities of radical-involved mechanism as reflected by the isotope labeling results. In the isotope labeling analyses, half of the deuterium was found in the aldehyde group in the acetaldehyde product (40). They suggested that the quinonoid intermediate could have some biradical character to react with oxygen (40).

The study on plant phenylacetaldehyde synthase is the first study that described the coupling of decarboxylation and oxidation stoichiometrically. Our recent work provides insight regarding the differences in the structural characteristics between DDC and acetaldehyde synthase. We identified some enzymes to have the activity of decarboxylation-oxidative deamination using aromatic amino acids as substrates (29, 41). These enzymes are annotated as aromatic amino acid decarboxylases or decarboxylase-like proteins in the dataset. Our previous study demonstrated

that these enzymes catalyze decarboxylation-oxidative deamination to produce the corresponding acetaldehyde synthase, CO_2, H_2O_2 and NH_3, which is in contrast to the typical decarboxylation producing aromatic amine and CO_2. Based on the different types of reactions catalyzed by these enzymes, we named them as acetaldehyde synthase based on the corresponding acetaldehyde formed (41).

Based on our data, the acetaldehyde synthase using aromatic amino acid as a substrate is quite similar in terms of active site residues and structure with the corresponding decarboxylase that uses the same substrate. We propose that the mechanism of decarboxylation-oxidative deamination catalyzed by acetaldehyde synthase is quite similar with decarboxylase for the steps of internal aldimine formation and break up, external aldimine formation and decarboxylation steps. After decarboxylation, the carbanionic intermediate or quinonoid intermediate is quite reactive and needs to be stabilized or reacted. The deviation of decarboxylation-oxidative deamination from typical decarboxylation is dependent on whether the carbanionic intermediate or quinonoid intermediate is protonated efficiently (29).

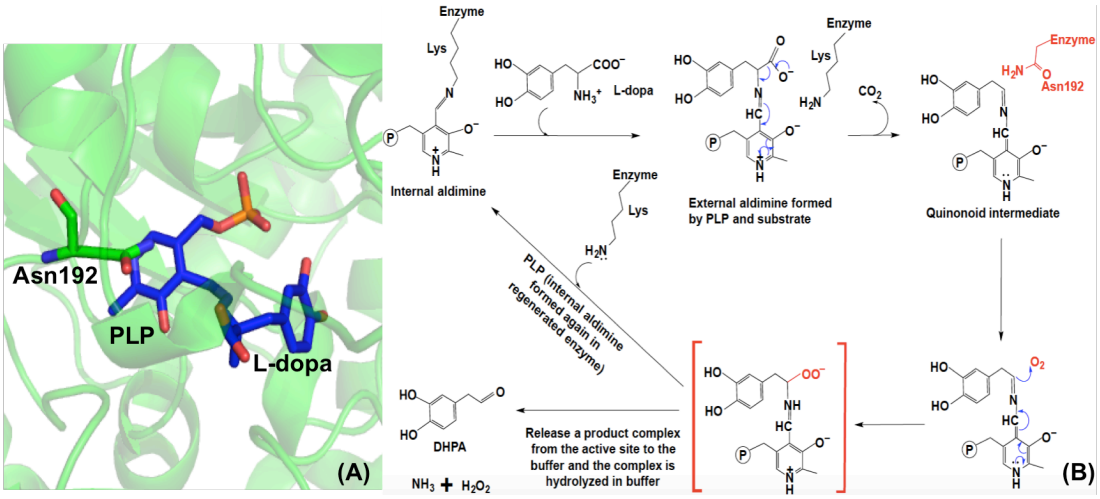

Figure 2.6: The mechanistic role of Asn192 residue in *Drosophila* DHPA synthase. **The Asn192 residue position in the active site of DHPA synthase (model generated by Phyre2 (42)) is shown with Asn residue in green sticks and external aldmine formed by PLP and L-dopa in blue sticks (A). The mechanistic role of Asn192 residue in DHPA synthase-catalyzed reaction is shown (B).**

In decarboxylation as discussed above, the His192 residue is not only involved in π-π stacking of PLP pyridine ring, but also protonates the carbanionic intermediate or quinonoid intermediate quickly after decarboxylation to protect the intermediate from being attacked by oxygen or other factors and then Lys residue is involved in the transamination process after protonation to release the amine and regenerate Schiff base between PLP and Lys residue. The acetaldehyde synthase, in contrast, cannot efficiently protonate the carbanionic intermediate or quinonoid intermediate efficiently and leave the opportunity for oxygen attack. If we take the *Drosophila* 3,4-dihydroxyphenylacetaldehyde (DHPA) synthase which we have recently studied as one example, the DHPA synthase catalyzes the synthesis of 3,4-dihydroxyphenylacetaldehyde using L-dopa as a substrate. DHPA synthase has one Asn192 residue conserved at the equivalent position as His192 in *Drosophila* DDC (Figure 2.6A) (29).

The differences in the ability for protonation of the intermediate between DDC and DHPA synthase are supported by more than one magnitude lower DHPA synthase-mediated reaction than DDC activity. Once carbanion intermediates are formed, the limited ability of Asn192 for reprotonation of Cα may slightly extend their lifetime and force these reactive intermediates going through other reaction routes, e.g., attacked by oxygen. After oxygen addition, the product complex likely is released from the active site of the enzyme and disintegrates rapidly in buffer environment. Our site-directed mutagenesis determined that N192H mutation of DHPA synthase increased the DDC-activity one magnitude and decreased the DHPA synthase activity at the same time to make both dopamine and DHPA production by DHPA synthase N192H mutation to be comparable in magnitude. The site-directed mutagenesis also suggested the crucial roles of Asn192 in DHPA synthase and His192 in DDC (29). Another interesting finding is that DHPA synthase could also reuse H_2O_2, one of the products, as one oxidizing agent during oxidative deamination.

Our analyses suggest that the ineffective ability of Asn192 for protonation of the intermediate hinders rapid protonation of carbanionic intermediate and increases the lifetime of intermediate, leading to oxygen attack, which results in the formation of acetaldehyde (DHPA), NH_3 and H_2O_2 (Figure 2.6B), instead of aromatic amine and CO_2 formation in DDC-catalyzed reaction. The ability to reuse H_2O_2 as an oxidizing agent in DHPA synthase is an example of how enzyme could prevent toxic compounds from accumulation. Furthermore, the acetaldehyde is also very reactive, readily combines with the amino group of proteins for crosslinking. The reactivity of DHPA may explain the physiological meaning of the slow reaction rate of DHPA synthase.

Different from insect acetaldehyde synthase to have the Asn192 residue conserved at the equivalent position with His192 residue in DDC to differentiate decarboxylation-oxidative deamination from typical decarboxylation, the plant acetaldehyde synthases have His residue conserved at equivalent position in both decarboxylase and acetaldehyde synthase. However, the conserved tyrosine or phenylalanine in a flexible loop region function to discriminate typical decarboxylation and acetaldehyde synthase respectively. Tyrosine residue in the plant decarboxylase could not directly protonate the intermediate, but it could stabilize the proton transfer process from His residue to Cα after decarboxylation. In contrast, phenylalanine has no stabilizing effect for proton transfer to leave the intermediate being attacked by oxygen (43).

Du et al. (39) reported one PLP-dependent indolmycin biosynthetic enzyme Ind4, could use O_2 to mediate a four-electron oxidative dehydrogenation and oxidative deamination of L-arginine. One unactivated carbon-carbon bond (C4-C5) was oxidized in the reaction while oxygen is stoichiometrically reduced to H_2O_2. The reaction is oxygen dependent, and no product was detected when oxygen is excluded. Their results indicated that L-arginine had two pathways under the catalysis of this enzyme: 1) oxidative deamination with one equivalent of oxygen involved, 2) oxidative dehydrogenation followed by oxidative deamination with two equivalents of oxygen required (39). After experimentally excluding the possibility of bound metal ions to activate oxygen, they suggested that the Ind4 enzyme was able to use PLP to stabilize the anion formed in the first step by deprotonation of the substrate, similar to other PLP-dependent enzymes. Then oxygen was activated by the growing conjugation of the complex formed by PLP to form the superoxide and combine with the substrate-cofactor radical to form hydroperoxy intermediate (39). They suggest that the activation of oxygen in the Ind4-catalyzed reaction is

probably similar to the cofactor-independent oxidase because of apparent similarities shared between each other (39, 44).

The Ind4 study suggested the radical mechanism of the intermediate, how the oxygen is activated in those reactions still waiting for more details. The mechanism of the oxygen activation and whether the activation is through a mechanism similar to the cofactorless oxidase still needs to be analyzed. There are still no crystal structures available for these PLP-dependent enzymes using oxygen as a substrate while there are many crystal structures of the aminotransferase, decarboxylase, racemase, and other PLP-dependent enzymes. More crystal structural information and captured intermediates may provide more insight regarding the oxygen activation pathway, oxygen attack, the stabilization of the intermediate, the possible radical formation, and the growing conjugation of the complex.

2.4 Conclusion

PLP-dependent enzymes are involved in cellular activities and metabolisms of different species, from bacteria to human. The structure-function relationship and the mechanism study of the PLP-dependent enzymes also provide a basis for the discovery of specific inhibitors or drugs. All these essential roles of PLP-dependent enzymes make the structure-function and mechanism study of PLP-dependent enzymes an attractive field of research attracting more and more attention for recent years.

The catalytic power of PLP relies on delocalization and stabilization of intermediates while the reaction specificity depends on the specific cluster of active site residues to avoid side-reactions and to facilitate certain specific reactions. Although a better understanding of mechanisms of PLP-dependent enzymes has been achieved, especially the fate of carbanionic intermediate with interactions with the active site residues through subtle differences in structures, some detailed information is still needed. For example, the detailed mechanism of some PLP-dependent enzymes still needs to be further characterized with the capture of key intermediates, the annotated uncharacterized PLP-dependent enzymes may have critical functions, and the inaccurate annotation (relying only on sequence similarity) of some PLP-dependent enzymes may also hinder the study of the true functions (e.g., DHPA synthase).

Recently, with the sequencing of more genomes, more protein sequences were annotated as uncharacterized protein or with an inaccurate annotation. Among these proteins, there are many PLP-dependent enzymes. The analyses of their biochemical functions will contribute to a true understanding of these unexplored proteins and may identify novel activities of PLP-dependent enzymes. Based on the sequence and structure information, more key residues involved in reaction specificity will be identified, which may be used as signature residues for a more efficient way to identify specific PLP-dependent enzymes from the relevant misleading annotation and may help understanding the reaction mechanism in an enzymatic environment point of view. A comprehensive study and understanding of the functionally closely related enzymes will give some basis for analyzing how the closely related enzymes are evolved.

2.5 References

1. Cellini B, Montioli R, Oppici E, Astegno A, Voltattorni CB. The chaperone role of the pyridoxal 5'-phosphate and its implications for rare diseases involving B6-dependent enzymes. Clin Biochem. 2014;47(3):158-165
2. Larsson SC, Orsini N, Wolk A. Vitamin B6 and Risk of Colorectal Cancer: A Meta-analysis of Prospective Studies. The Journal of the American Medical Association. 2010;303(11):1077-1083
3. Rubi B. Pyridoxal 5'-phosphate (PLP) deficiency might contribute to the onset of type I diabetes. Med Hypotheses. 2012;78(1):179-182
4. Frey PA. Radicalmechanisms of enzymatic catalysis. Annu Rev Biochem. 2001(70):121-148
5. Griswold WR, Toney MD. Chemoenzymatic synthesis of 1-deaza-pyridoxal 5'-phosphate. Bioorg Med Chem Lett. 2010;20(4):1352-1354
6. Beattie AE, Clarke DJ, Wadsworth JM, Lowther J, Sin HL, Campopiano DJ. Reconstitution of the pyridoxal 5'-phosphate (PLP) dependent enzyme serine palmitoyltransferase (SPT) with pyridoxal reveals a crucial role for the phosphate during catalysis. Chem Commun (Camb). 2013;49(63):7058-7060
7. Phillips RS, Scott I, Paulose R, Patel A, Barron TC. The phosphate of pyridoxal-5'-phosphate is an acid/base catalyst in the mechanism of Pseudomonas fluorescens kynureninase. FEBS J. 2014;281(4):1100-1109
8. Percudani R, Peracchi A. The B6 database: a tool for the description and classification of vitamin B6-dependent enzymatic activities and of the corresponding protein families. BMC Bioinformatics. 2009;10:273
9. Clausen T, Huber R, Laber B, Pohlenz H-D, Messerschmidt A. Crystal Structure of the Pyridoxal-5'-phosphate Dependent Cystathionine beta-lyase from *Escherichia coli* at 1.83 Å. J Mol Biol. 1996(262):202-224
10. Fogle EJ, Toney MD. Mutational analysis of substrate interactions with the active site of dialkylglycine decarboxylase. Biochemistry. 2010;49(30):6485-6493
11. Taylor JL, Price JE, Toney MD. Directed evolution of the substrate specificity of dialkylglycine decarboxylase. Biochim Biophys Acta. 2015;1854(2):146-155
12. Dunathan HC. Conformation and reaction specificity in pyridoxal phosphate enzymes. Proc Natl Acad Sci U S A. 1966;55:712-716
13. Eliot AC, Kirsch JF. Pyridoxal phosphate enzymes: mechanistic, structural, and evolutionary considerations. Annu Rev Biochem. 2004;73:383-415
14. Oliveira EF, Cerqueira NM, Fernandes PA, Ramos MJ. Mechanism of formation of the internal aldimine in pyridoxal 5'-phosphate-dependent enzymes. J Am Chem Soc. 2011;133(39):15496-15505
15. Milić D, V. Demidkina T, N. Zakomirdina L, Matković-Čalogović D, A. Antson A. Crystal Structure of Citrobacter freundii Asp214Ala Tyrosine Phenollyase Reveals that Asp214 is Critical for Maintaining a Strain in the Internal Aldimine. Croatica Chemica Acta. 2012;85(3):283-288
16. Chan-Huot M, Dos A, Zander R, Sharif S, Tolstoy PM, Compton S, Fogle E, Toney MD, Shenderovich I, Denisov GS, Limbach HH. NMR studies of protonation and hydrogen bond

states of internal aldimines of pyridoxal 5'-phosphate acid-base in alanine racemase, aspartate aminotransferase, and poly-L-lysine. J Am Chem Soc. 2013;135(48):18160-18175
17. Ngo HP, Cerqueira NM, Kim JK, Hong MK, Fernandes PA, Ramos MJ, Kang LW. PLP undergoes conformational changes during the course of an enzymatic reaction. Acta Crystallogr D Biol Crystallogr. 2014;70(Pt 2):596-606
18. Toney MD, Kirsch JF. Lysine 258 in aspartate aminotransferase: Enforcer of the Circe effect for amino acid substrates and the general-base catalyst for the 1,3-prototropic shift. Biochemistry. 1993;32(6):1471-1479
19. Toney MD. Aspartate aminotransferase: an old dog teaches new tricks. Arch Biochem Biophys. 2014;544:119-127
20. Goldberg JM, Kirsch JF. The Reaction Catalyzed by *Escherichia coli* Aspartate Aminotransferase Has Multiple Partially Rate-Determining Steps, While That Catalyzed by the Y225F Mutant Is Dominated by Ketimine Hydrolysis. Biochemistry. 1996;35(16):5280-5291
21. Han Q, Robinson H, Li J. Crystal structure of human kynurenine aminotransferase II. J Biol Chem. 2008;283(6):3567-3573
22. Nasir N, Anant A, Vyas R, Biswal BK. Crystal structures of Mycobacterium tuberculosis HspAT and ArAT reveal structural basis of their distinct substrate specificities. Sci Rep. 2016;6:18880
23. Sivaraman J, Li Y, Larocque R, Schrag JD, Cygler M, Matte A. Crystal structure of histidinol phosphate aminotransferase (HisC) from Escherichia coli, and its covalent complex with pyridoxal-5'-phosphate and l-histidinol phosphate. J Mol Biol. 2001;311(4):761-776
24. Karlberg T, Moche, M., Andersson, J., Arrowsmith, C.H., Berglund, H., Collins, R., Dahlgren, L.G., Edwards, A.M., Flodin, S., Flores, A., Graslund, S., Hammarstrom, M., Johansson, A., Johansson, I., Kotenyova, T., Lehtio, L., Nilsson, M.E., Nordlund, P., Nyman, T., Olesen, K., Persson, C., Sagemark, J., Thorsell, A.G., Tresaugues, L., Van Den Berg, S., Weigelt, J., Welin, M., Wikstrom, M., Wisniewska, M., Schuler, H. Human Tyrosine Aminotransferase FAU. Structural Genomics Consortium (SGC) CRDT 2008
25. Duff SM, Rydel TJ, McClerren AL, Zhang W, Li JY, Sturman EJ, Halls C, Chen S, Zeng J, Peng J, Kretzler CN, Evdokimov A. The enzymology of alanine aminotransferase (AlaAT) isoforms from Hordeum vulgare and other organisms, and the HvAlaAT crystal structure. Arch Biochem Biophys. 2012;528(1):90-101
26. Han Q, Cai T, Tagle DA, Robinson H, Li J. Substrate specificity and structure of human aminoadipate aminotransferase/kynurenine aminotransferase II. Biosci Rep. 2008;28(4):205-215
27. Han Q, Cai T, Tagle DA, Li J. Structure, expression, and function of kynurenine aminotransferases in human and rodent brains. Cell Mol Life Sci. 2010;67(3):353-368
28. Han Q, Ding H, Robinson H, Christensen BM, Li J. Crystal structure and substrate specificity of *Drosophila* 3,4-dihydroxyphenylalanine decarboxylase. PLoS One. 2010;5(1):e8826
29. Liang J, Han Q, Ding H, Li J. Biochemical identification of residues that discriminate between 3,4-dihydroxyphenylalanine decarboxylase and 3,4-dihydroxyphenylacetaldehyde synthase-mediated reactions. Insect Biochem Mol Biol. 2017;91:34-43
30. Ortega-Castro J, Adrover M, Frau J, Salva` A, Donoso J, Mun˜oz F. DFT Studies on Schiff Base Formation of Vitamin B6 Analogues. Reaction between a
Pyridoxamine-Analogue and Carbonyl Compounds. journal of physical chemistry a. 2010;114(13):4634-4640

31. Maley JR, Bruice TC. Catalytic reactions involving azomethines. XII. Transamination of 1-methyl-3-hydroxy-4-formylpyridinium chloride. Arch Biochem Biophys. 1970;136:187-192
32. Phillips RS, Lima S, Khristoforov R, Sudararaju B. Insights into the mechanism of Pseudomonas dacunhae aspartate beta-decarboxylase from rapid-scanning stopped-flow kinetics. Biochemistry. 2010;49(24):5066-5073
33. Bertoldi M, Gonsalvi M, Contestabile R, Voltattorni CB. Mutation of tyrosine 332 to phenylalanine converts dopa decarboxylase into a decarboxylation-dependent oxidative deaminase. J Biol Chem. 2002;277(39):36357-36362
34. Hu Y, Dietrich D, Xu W, Patel A, Thuss JA, Wang J, Yin WB, Qiao K, Houk KN, Vederas JC, Tang Y. A carbonate-forming Baeyer-Villiger monooxygenase. Nat Chem Biol. 2014;10(7):552-554
35. Barry SM, Kers JA, Johnson EG, Song L, Aston PR, Patel B, Krasnoff SB, Crane BR, Gibson DM, Loria R, Challis GL. Cytochrome P450-catalyzed L-tryptophan nitration in thaxtomin phytotoxin biosynthesis. Nat Chem Biol. 2012;8(10):814-816
36. Teufel R, Miyanaga A, Michaudel Q, Stull F, Louie G, Noel JP, Baran PS, Palfey B, Moore BS. Flavin-mediated dual oxidation controls an enzymatic Favorskii-type rearrangement. Nature. 2013;503(7477):552-556
37. Chang WC, Dey M, Liu P, Mansoorabadi SO, Moon SJ, Zhao ZK, Drennan CL, Liu HW. Mechanistic studies of an unprecedented enzyme-catalysed 1,2-phosphono-migration reaction. Nature. 2013;496(7443):114-118
38. Abell LM, Schloss JV. Oxygenase Side Reactions of Acetolactate Synthase and Other Carbanion-Forming Enzymes. Biochemistry. 1991(30):7883-7887
39. Du YL, Singh R, Alkhalaf LM, Kuatsjah E, He HY, Eltis LD, Ryan KS. A pyridoxal phosphate-dependent enzyme that oxidizes an unactivated carbon-carbon bond. Nat Chem Biol. 2016;12(3):194-199
40. Kaminaga Y, Schnepp J, Peel G, Kish CM, Ben-Nissan G, Weiss D, Orlova I, Lavie O, Rhodes D, Wood K, Porterfield DM, Cooper AJ, Schloss JV, Pichersky E, Vainstein A, Dudareva N. Plant phenylacetaldehyde synthase is a bifunctional homotetrameric enzyme that catalyzes phenylalanine decarboxylation and oxidation. J Biol Chem. 2006;281(33):23357-23366
41. Vavricka C, Han Q, Huang Y, Erickson SM, Harich K, Christensen BM, Li J. From L-dopa to dihydroxyphenylacetaldehyde: a toxic biochemical pathway plays a vital physiological function in insects. PLoS One. 2011;6(1):e16124
42. Kelley LA, Sternberg MJ. Protein structure prediction on the Web: a case study using the Phyre server. Nat Protoc. 2009;4(3):363-371
43. Torrens-Spence MP, Liu P, Ding H, Harich K, Gillaspy G, Li J. Biochemical evaluation of the decarboxylation and decarboxylation-deamination activities of plant aromatic amino acid decarboxylases. J Biol Chem. 2013;288(4):2376-2387
44. Fetzner S, Steiner RA. Cofactor-independent oxidases and oxygenases. Appl Microbiol Biotechnol. 2010;86(3):791-804

Chapter 3

Biochemical identification of residues that discriminate between 3,4-dihydroxyphenylalanine decarboxylase and 3,4-dihydroxyphenylacetaldehyde synthase-mediated reactions

Jing Liang [a], Qian Han [b], Haizhen Ding [a], Jianyong Li [a, *]

[a] Department of Biochemistry, Virginia Polytechnic Institute and State University, Blacksburg, VA24060, United States

[b] Laboratory of Tropical Veterinary Medicine and Vector Biology, and Hainan Key Laboratory of Sustainable Utilization of Tropical Bioresources, Institute of Agriculture and Forestry, Hainan University, Haikou 570228, Hainan, China

[*] Correspondence to Prof. Jianyong Li (lij@vt.edu; Tel: 540-231-5779; Fax: 540-231-9070)

Reprinted from Insect Biochemistry and Molecular Biology, Vol 91, Page. 34-43 (2017), with permission from Elsevier.

Abstract

In available insect genomes, there are several L-3,4-dihydroxyphenylalanine (L-dopa) decarboxylase (DDC)-like or aromatic amino acid decarboxylase (AAAD) sequences. This contrasts to those of mammals whose genomes contain only one DDC. Our previous experiments established that two DDC-like proteins from *Drosophila* actually mediate a complicated decarboxylation-oxidative deamination process of dopa in the presence of oxygen, leading to the formation of 3,4-dihydroxyphenylacetaldehyde (DHPA), CO_2, NH_3, and H_2O_2. This contrasts to the typical DDC-catalyzed reaction, which produces CO_2 and dopamine. These DDC-like proteins were arbitrarily named DHPA synthases based on their critical role in insect soft cuticle formation. Establishment of reactions catalyzed by these AAAD-like proteins solved a puzzle that perplexed researchers for years, but to tell a true DHPA synthase from a DDC in the insect AAAD family remains problematic due to high sequence similarity. In this study, we performed extensive structural and biochemical comparisons between DHPA synthase and DDC. These comparisons identified several target residues potentially dictating DDC-catalyzed and DHPA synthase-catalyzed reactions, respectively. Comparison of DHPA synthase homology models with crystal structures of typical DDC proteins, particularly residues in the active sites, provided further insights for the roles these identified target residues play. Subsequent site-directed mutagenesis of the tentative target residues and activity evaluations of their corresponding mutated enzymes determined that active site His192 and Asn192 are essential signature residues for DDC- and DHPA synthase-catalyzed reactions, respectively. Oxygen is required in the DHPA synthase- mediated process and this oxidizing agent is reduced to H_2O_2 in the process. Biochemical assessment established that H_2O_2, formed in DHPA synthase-mediated process, can be reused as oxidizing agent and this active oxygen species is reduced to H_2O, thereby avoiding

oxidative stress by H_2O_2. Results of our structural and functional analyses provide a reasonable explanation of mechanisms involved in DHPA synthase-mediated reactions. Based on the key active site residue Asn192 (identified in *Drosophila* DHPA synthase) and high primary sequence identity with DDC, we were able to distinguish all available insect DHPA synthases from DDC sequences.

Keywords

Decarboxylase; *Drosophila*; aromatic acetaldehyde synthase; decarboxylation**;** oxidative deamination.

3.1 Introduction

Aromatic amino acid decarboxylase (AAAD) is present in most living organisms from bacteria to humans. Mammalian AAAD is often named 3,4-dihydroxyphenylalanine (dopa) decarboxylase (DDC). This enzyme also catalyzes decarboxylation of 5-hydroxytryptophan. Affected by this annotation in mammalian and also by its ability to catalyze decarboxylation of other aromatic amino acids, DDC and AAAD were used interchangeably and their utilization seems essentially the preference of individual authors in literature (1). In mammals, dopamine and serotonin function as key neurotransmitters and also the substrates for other essential neuroactive compounds, including norepinephrine, epinephrine, and melatonin. Therefore, DDC has been extensively studied in mammals, particularly in humans. Similar to humans, DDC from insects is responsible for the formation of some key neurotransmitters, but moreover insect DDC has more other special functions, such as immune responses (2), eggshell and cuticle hardening

(3). As a result, this enzyme needs to be highly regulated in insects and there have been more studies concerning DDC regulation in insects than that in mammals (1, 3-5).

While there is one DDC-like or AAAD sequence in mammals, there are several DDC-like proteins in all sequenced insects. For example, *Drosophila melanogaster* has five and mosquitoes have 6-7 genes sharing conserved sequences (generally identity >40%) in their genomes. As more genomes of different insect species are available, it becomes clear that essentially all sequenced insect genomes contain an AAAD protein family. The typical DDC in insects displays similar amino acid sequence, structure, molecular weight, substrate selectivity and catalytic properties as its mammalian counterpart, i.e., homodimer with the molecular weight of each monomer around 55 kDa, active to both dopa and 5-hydroxytryptophan and optimum pH is around 7.0 (4). Compared to the extensively studied typical DDC, there have been limited studies of other DDC-like or AAAD proteins in insects. One might wonder why insects need more AAADs than mammals.

Progress in insect neurochemistry provided some explanation for insects to have multiple AAAD proteins. In addition to typical DDC, there are tyrosine decarboxylases in insect DDC-like protein family. Contrary to mammals, insects have specific receptors for tyramine and octopamine and these two compounds play some fundamental physiological roles in insects (6, 7), particularly neurotransmission in central nervous system (6) and reproduction (7). In general, insects have two tyrosine decarboxylase (TyDC) sequences with TyDC1 expressed throughout the body and primarily in non-neural abdominal organs whereas TyDC2 is expressed in the adult brain and nerve cord (7). Identification of TyDC genes was initially made through genetic approaches plus detection of their endogenous products (7). TyDC1 or TyDC2 sequences usually

share high identity across insect species and contain 570-700 residues. Although no critical characterization has been made for TyDC (such as K_m, V_{max}, substrate specificity), its identities could be based on moderate identity (usually ~30-50%) to the typical DDC, higher sequence identity across insect species with functionally identified TyDC and relatively larger protein size than the size of typical DDC (470-500 residues). 3,4-Dihydroxyphenylacetaldehyde (DHPA) synthase is another member of insect DDC-like protein family. In *Drosophila*, studies of DHPA synthase gene were initiated during 1974 (8, 9). Investigators first noticed that some *Drosophila* were vulnerable (9) or resistant (8) to α-methyl dopa (AMD) added to their food supplies. Subsequently they were able to link the vulnerable or resistant phenotype with a DDC-like gene because partial loss of its function due to mutation (9) or elevated expression (8) resulted in the observed phenotype. Historically, this DDC-like gene was named AMD resistant gene in *D. melanogaster*. Analysis of AMD resistant protein determined that its mutation affected formation of *Drosophila* colorless flexible cuticle structures, which contrasts to the role of DDC in rigid cuticle melanization and sclerotization (10-12). *Drosophila* mutants with homozygous mutations of AMD resistant gene die during embryo development stage (10, 11, 13), a time that coincides with active transcription of AMD resistant gene and larval cuticle deposition (11). These early studies imply the role of AMD resistant gene in cuticle formation.

In our previous study (14), we determined that AMD resistant protein also uses L-dopa as substrate like DDC, and this enzyme has higher activity toward L-dopa than that toward AMD. The enzyme also needs oxygen to complete its catalytic cycle, which produces DHPA, NH_3, CO_2 and H_2O_2 as products (Figure 3.1). AMD is one medicine for treating high blood pressure, and the resistance to AMD may not be the true function of this protein. Furthermore, our previous

results show that DHPA is highly reactive and easily cross-links with proteins. Based on the role of DHPA in protein crosslinking, combined with the defects of flexible cuticle formation caused by AMD resistant gene mutation, we name AMD resistant protein as DHPA synthase (14). Using similar strategies, we also determined that two of the DDC-like genes in *Aedes aegypti* mosquito are DHPA synthases (14). The function of DHPA synthase in DHPA production and the reactivity of this compound correlate well with earlier observations in soft cuticle defects in *Drosophila* mutants having a mutated coding gene for the AMD-resistant protein (10).

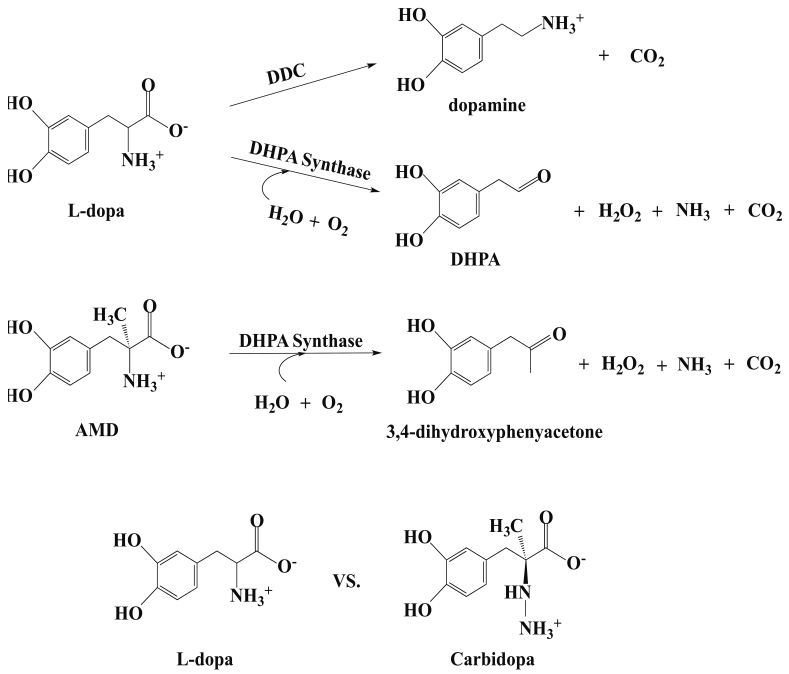

Figure 3.1: Reactions catalyzed by DDC and DHPA synthase and the comparison between L-dopa and carbidopa.

In contrast to TyDC, DHPA synthase has similar protein size and high sequence identity (>40%) to DDC in essentially any given species. The identification of DHPA synthase in *Drosophila* and mosquito enzymes has been based primarily on experimentations (e.g. protein expression and characterization), which is labor intensive. For newly sequenced insect genomes, the annotation

of their DDC (or DDC-like gene) is most likely based on those previously sequenced model species. This study is aimed at **1)** establishing a criterion unequivocal for identification of insect DHPA synthase, **2)** elucidating the mechanism of DHPA synthase-mediated process and **3)** utilizing the criterion to distinguish DHPA synthase from DDC sequences.

3.2 Materials and Methods

3.2.1 Materials

L-dopa, dopamine, pyridoxal-5'-phosphate (PLP), and other chemicals were from Sigma. The IMPACT^{TM}-CN expression system and restriction enzymes were from New England Biolabs (Ipswich, MA).

3.2.2 Primary sequence comparison

BLAST was used to search NCBI protein database using either DHPA synthase previously determined or using *Drosophila* DDC for comparison. Similar blast search with *Drosophila* DHPA synthase or DDC also was done against individual annotated insect genomes to determine the possibility if DHPA synthase could be distinguished from typical DDC in given species based on primary sequence comparison.

3.2.3 Homology modeling

To elucidate the structural differences between DDC and DHPA synthase, some homology models of DHPA synthase were generated using several structures from pig (PDB: 1JS6) (15) or human histidine decarboxylase (4E1O) (16) as the templates. The homology models generated from Phyre2 (17), ModWeb (18), Swiss-Model (19-23) and FUGUE (24) were submitted to Swiss-Model evaluation tools (19-23), including Procheck (25), Anolea (26), QMEAN6 (27, 28). ProSA-web (29, 30) and Verify 3D checks (31) were also performed to select a relatively qualified model. The complex of PLP and carbidopa was from pig DDC (PDB: 1JS3) (15). The DDC crystal structure and the model file were visualized with PyMOL (The PyMOL Molecular Graphics System, Version 1.7.4 Schrödinger, LLC.).

3.2.4 cDNA synthesis and amplification of DDC and DHPA synthase coding regions

Insect total RNA sample was extracted from *D. melanogaster* larvae and pupae using TRIZOL reagent (Invitrogen, Carlsbad, CA) and following the steps of its protocol and was used for synthesizing the first strand cDNA. Gene specific primers (Table 3.1) based on codons of DHPA synthase (NP_476592) and DDC (NP_724164), respectively, were synthesized and used for amplifying their respective coding regions. Amplified full-length DHPA synthase and DDC coding regions were ligated into IMPACT^{TM}-CN expression vector pTYB12, respectively.

Primer	Sequence	Usage
DHPA synthase-F-Nde I	5'-AAA CAT ATG GAT GCC AAG GAG TTT CG-3'	Cloning of DHPA synthase full coding region
DHPA synthase-R-XhoI	5'-AAA CTC GAG TCA CTG AGA TTT CTC GTG CG-3'	
DHPA synthase-F-SapI-N192H	5'-AAA GCT CTT CAC ATA GCT GCA TTG AGA A-3'	Site-directed mutagenesis of N192H of DHPA synthase
DHPA synthase-R-SapI-N192H	5'-AAA GCT CTT CAA TGA CTC TGG TCC GAG G-3'	
DHPA synthase-F-SapI-C194S	5'-AAA GCT CTT CAA GCA TTG AGA AGG CTG G-3'	Site-directed mutagenesis of C194H of DHPA synthase
DHPA synthase-R-SapI-C194S	5'-AAA GCT CTT CAT CGG CTG TTA CTC TGG T-3'	
DHPA synthase-F-SapI-S147T	5'-AAA GCT CTT CAA CCG CTA GCG AGG CTG T-3'	Site-directed mutagenesis of S147T of DHPA synthase
DHPA synthase-R-SapI-S147T	5'-AAA GCT CTT CAT GGT CCC TGG ATC ACC C-3'	
DHPA synthase-F-SapI-Y80F	5'-AAA GCT CTT CAT TTC CCA CCA GCA CCT C-3'	Site-directed mutagenesis of Y80F of DHPA synthase
DHPA synthase-R-SapI-Y80F	5'-AAA GCT CTT CAA AAG TAG GCA TGC ATG T-3'	
DDC-F-NdeI	5'-AAA CAT ATG GAG GCG CCG GAG TT-3'	Cloning of DDC full coding region
DDC-R-EcoRI	5'-AAA GAA TTC TTA CTG CTC CTG TTC CAT CT-3'	
DDC-F-SapI-H192N	5'-AAA GCT CTT CAA ACT CAT CCG TGG AGC G-3'	Site-directed mutagenesis of H192N of DDC
DDC-R-SapI-H192N	5'-AAA GCT CTT CAG TTA GCC TGG TCG AGG C-3'	
DDC-F-SapI-S194C	5'-AAA GCT CTT CAT GCG TGG AGC GGG CTG G-3'	Site-directed mutagenesis of S194C of DDC
DDC-R-SapI-S194C	5'-AAA GCT CTT CAA CGT GAG TGA GCC TGG T-3'	
DDC-F-SapI-T147S	5'-AAA GCT CTT CAA GCG CCA GTG AGT CCA C-3'	Site-directed mutagenesis of T147S of DDC
DDC-R-SapI-T147S	5'-AAA GCT CTT CAT CGG CCC TGG ATG ACA C-3'	
DDC-F-SapI-F80Y	5'-AAA GCT CTT CAT ATC CCA CGG CCA ACT C-3'	Site-directed mutagenesis of F80Y of DDC
DDC-R-SapI-F80Y	5'-AAA GCT CTT CAA TAG TAG GCA TGA AAG T-3'	

Table 3.1: Primer sequences used in this study.

3.2.5 Protein expression and purification

The protein expression and purification follow the method for DDC expression (4). Recombinant plasmids (pTYB12 vector, IMPACT^{TM}-CN expression system) containing enzyme cDNA were transformed into *Escherichia coli* (*E. coli*) ER2566 competent cells. Transformed bacterial colonies were selected and used to express the proteins in large scale (12-20 liters of *E. coli*). Starting from overnight culture, the individual colony was grown at 37 °C for 3.5 h and protein expression was induced by adding 0.3-0.5 mM IPTG at 15 °C and cultured at this temperature with shaking for 24 h. The recombinant proteins were extracted from cells and applied to chitin beads column. The recombinant proteins, bound to the chitin beads through chitin binding

domain in fusion protein, were flushed quickly with cleavage buffer containing 50 mM β-mercaptoethanol and 40 mM PLP. Then the flow is stopped within 1 hour of quick flush and the column is incubated at 23^{o}C for 24 hours to cleave the chitin-binding domain. The designed proteins were then eluted from the column and concentrated using a Centricon YM-50 concentrator in a 25 mM Tris-HCl buffer containing 40 mM PLP. The buffer composition and detailed methods for protein expression and purification follow the IMPACT^{TM}-CN instruction manual. The proteins were further purified by an anion exchange column and gel filtration column (4). Protein purity was analyzed by the SDS-PAGE. The concentration of proteins was determined using a Bio-Red protein assay kit (Hercules, CA) and a concentration gradient of bovine serum albumin was generated as a standard.

3.2.6 Analyses of DDC and DHPA synthase activity

DDC activity assay was based on dopamine formed in L-dopa and enzyme reaction mixtures as described in previous reports (4, 14). Typically, a given reaction mixture 100 μl (pH=7) containing DDC, L-dopa and 40 μM PLP was prepared in 150 mM phosphate buffer and incubated at 25 ^{o}C and reaction was stopped by adding an equal volume of 0.8 M formic acid. The reaction mixture then was centrifuged at 15,000 g for 10 min at 5 ^{o}C. An aliquot of the supernatant (usually 4 to 8 μl) was injected for analysis by reverse-phase HPLC with electrochemical detection (HPLC-ED). The oxidation potential of the working electrode was maintained at 750 mV versus an Ag/AgCl reference electrode. A mobile phase, consisting of 50 mM citrate buffer (pH 3.2), 0.5 mM sodium octyl sulfate as a dynamic ion-pairing agent and 14% acetonitrile, was used during chromatography (flow rate: 0.33 ml per min). Quantitation of

dopamine was based on standard curve generated using authentic dopamine standard at the same chromatographic conditions. Standard was run before and after each activity assay.

DHPA synthase activity assay was based primarily on H_2O_2 formed in DHPA synthase and L-dopa reaction mixture. In DHPA synthase-mediated reactions, each catalytic cycle produces one molecule of DHPA, H_2O_2, NH_3 and CO_2, respectively and the stoichiometric ratio of individual products in principle makes it possible to quantitate any one of its products to represent the catalytic rate of the enzyme. A H_2O_2 quantitation kit was used for the assay based on manufacturer's protocol (Thermo Scientific) and activity was based on the amount of H_2O_2 formed during the first 5 min. DHPA, formed in L-dopa and enzyme mixture, could be resolved by reverse-phase HPLC and be detected by electrochemical detector, but DHPA behaved as a broad peak during HPLC separation (its acetaldehyde functional group might react with water or polymerize in aqueous solution dynamically as formaldehyde once it is in aqueous solution) (14). When necessary to illustrate the relative amount of DHPA formed in a reaction mixture, the reaction mixture (after a period of incubation) was treated with an equal volume of methanol saturated with $NaBH_4$ for 4 min and then the reaction mixture was then analyzed by HPLC-ED. $NaBH_4$ effectively reduces DHPA to 3,4-dihydroxyphenylethanol that eluted as a sharp peak during HPLC-ED analysis.

3.2.7 Sited-directed mutagenesis

Based on comparison of DHPA synthase homology model with DDC structure (PDB: 3K40) (4), several target residues were mutated to other residues. Recombinant vectors containing DHPA

synthase or DDC coding sequence were used to generate mutated sequence using site-directed mutagenesis protocol (Agilent Technology). The frame and orientation of the mutations were verified by DNA sequencing.

3.2.8 Kinetics analyses

For decarboxylation activity assay, enzymes were mixed with 0.2 - 8 mM L-dopa. The total volume of reaction mixtures were 100 μl and prepared in 150 mM phosphate buffer (pH, 7.0) and incubated in a water bath of 25 °C. PLP (40 μM) was also added to the reaction mixtures according to the report (4). The enzyme used for wild-type DDC and DHPA synthase kinetics assay were 0.3 μg and 4 μg per 100 μl reaction mixture respectively. The enzyme concentrations of mutated DDC H192N and mutated DHPA synthase N192H for detecting the kinetics of decarboxylation-oxidative deamination were 10 μg per 100μl reaction mixture while the concentrations for detecting the kinetics of decarboxylation were 2 μg and 5 μg per 100 μl reaction mixture respectively. The reactions were stopped at each 5 min intervals (5 min, 10 min and 15 min) by adding an equal volume of 0.8 M formic acid. Then the mixture was centrifuged and supernatants of the reaction mixtures were analyzed by HPLC-ED. The commercial dopamine was used to produce the standard curves before and after sample analysis. To determine the kinetic properties of DHPA synthase, the same reaction condition with decarboxylation activity assay was used and the reaction rate of DHPA synthase was based on H_2O_2 formed in reaction mixtures. The kinetic parameters were solved using the Michaelis-Menten equation by non-linear regression of SigmaPlot from SYSTAT.

3.3 Results

3.3.1 Sequence comparison

With maximum number of sequences displayed set at 500, a BLAST search of the NCBI non-redundant protein database using DHPA synthase from either mosquito or *Drosophila* enlisted protein sequences all showed the level of identity around or above 50% (not shown). The majority of sequences are either named DDC or AAAD. Similar results were obtained when either *Drosophila* or mosquito DDC sequence was used to BLAST the database. The level of similarity between DHPA synthase and DDC in several insect model species was illustrated in Figure 3.2. It seemed that when a DDC in a given insect species has been experimentally verified, the other DDC-like sequence from the same species (sharing ~50% sequence identity with DDC) could be predicted as a DHPA synthase with reasonable confidence (although such prediction somewhat lacks scientific basis). Unequivocal identification of DHPA synthase appeared problematic if the DDC sequence has not been experimentally verified. Our sequence comparison did not lead to any concrete indicator to classify a sequence as DDC or DHPA synthase in most insect species.

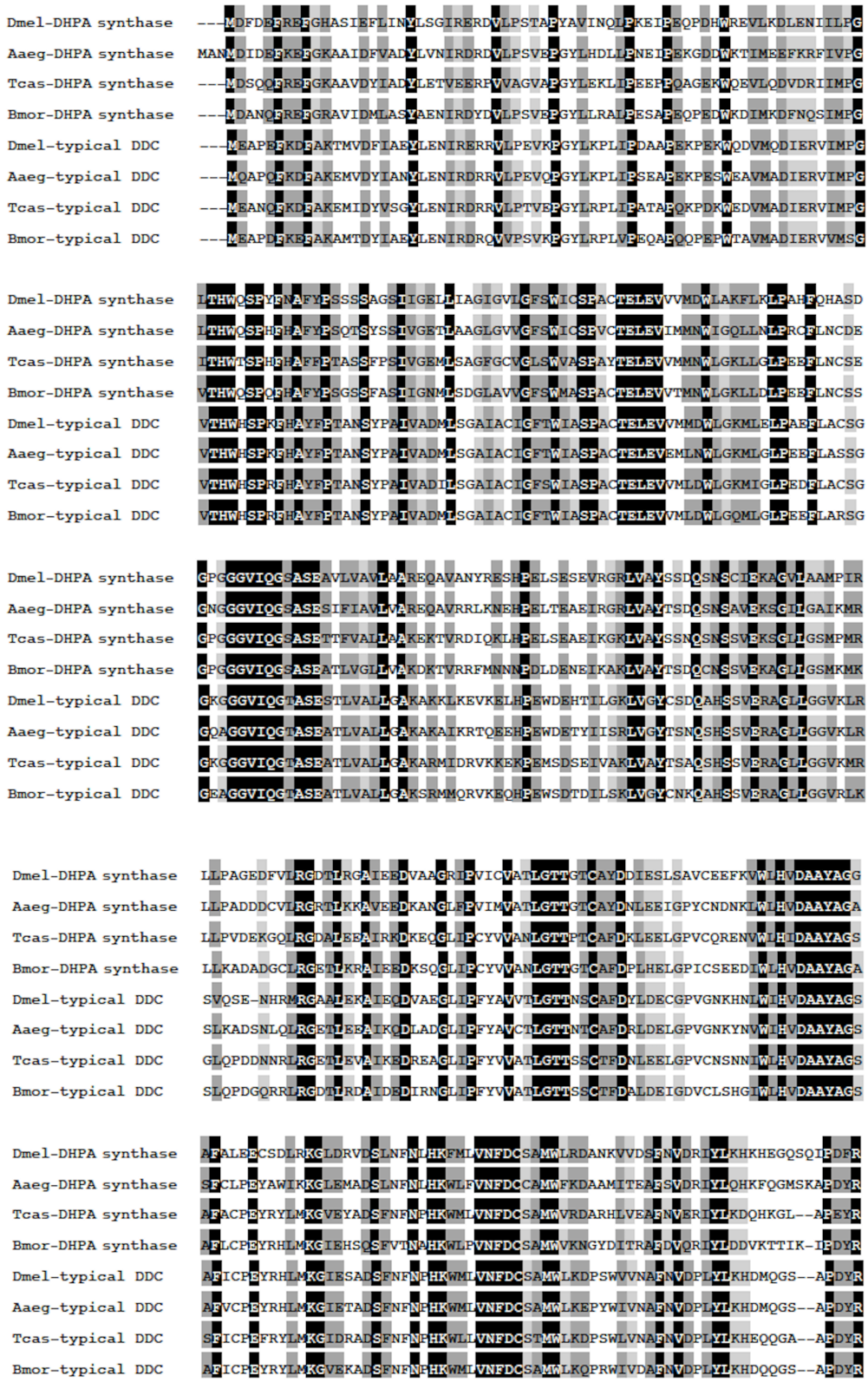
Dmel-DHPA synthase
Aaeg-DHPA synthase
Tcas-DHPA synthase
Bmor-DHPA synthase
Dmel-typical DDC
Aaeg-typical DDC
Tcas-typical DDC
Bmor-typical DDC

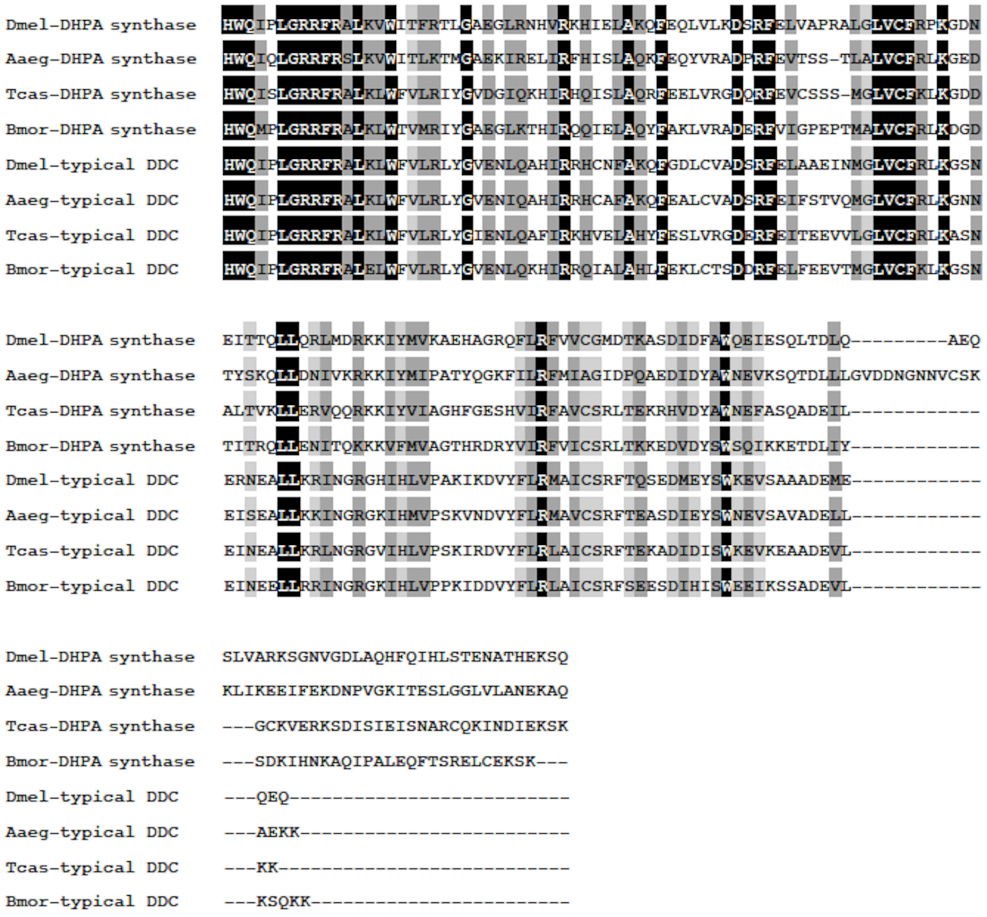

Figure 3.2: Sequence alignment showing the similarity of DDC and DHPA synthase from different insect species. **The conservation of residues is shown by gradually darkened boxes, light grey box with conservation of weak groups, dark grey box with conservation of strong groups and black box with fully conserved residues. The sequence alignment of *Drosophila melanogaster* (Dmel) DHPA synthase (NP_724162), *Aedes aegypti* (Aaeg) DHPA synthse (EAT37247), *Tribolium castaneum* (Tcas) DHPA synthase (XP_008193582.1) and *Bombyx mori* (Bmor) DHPA synthase (XP_004931016.1), in comparison with *Drosophila melanogaster* DDC (NP724164), *Aedes aegypti* DDC (XP_001648264), *Tribolium castaneum* DDC (NP_001096056.1), *Bombyx mori* DDC (NP_001037174.1) is shown. The DHPA synthase shows ~ 50% identity with typical DDC, which is similar to the identity (~50%) the DHPA synthase enzymes share with each other across the species.**

3.3.2 Homology model of *Drosophila* DHPA synthase protein

Drosophila DHPA synthase homology models were generated using the pig DDC (PDB: 1JS3) (15) and human histidine decarboxylase (PDB: 4E1O) (16) as templates. Although the histidine decarboxylase (HDC) shares slightly less (44%) sequence identity with DHPA synthase as compared with the pig DDC (45%), a catalytic loop region, important for catalysis, was seen clearly in the HDC structure. The homology model, judged with best quality by model evaluation tools, was used to compare with *Drosophila* crystal structure (PDB: 3K40) (4). The modeled structures of DHPA synthase were quite similar to DDC (PDB: 3K40) (4) from the same species and present as a homodimer (Figure 3.3 A-C).

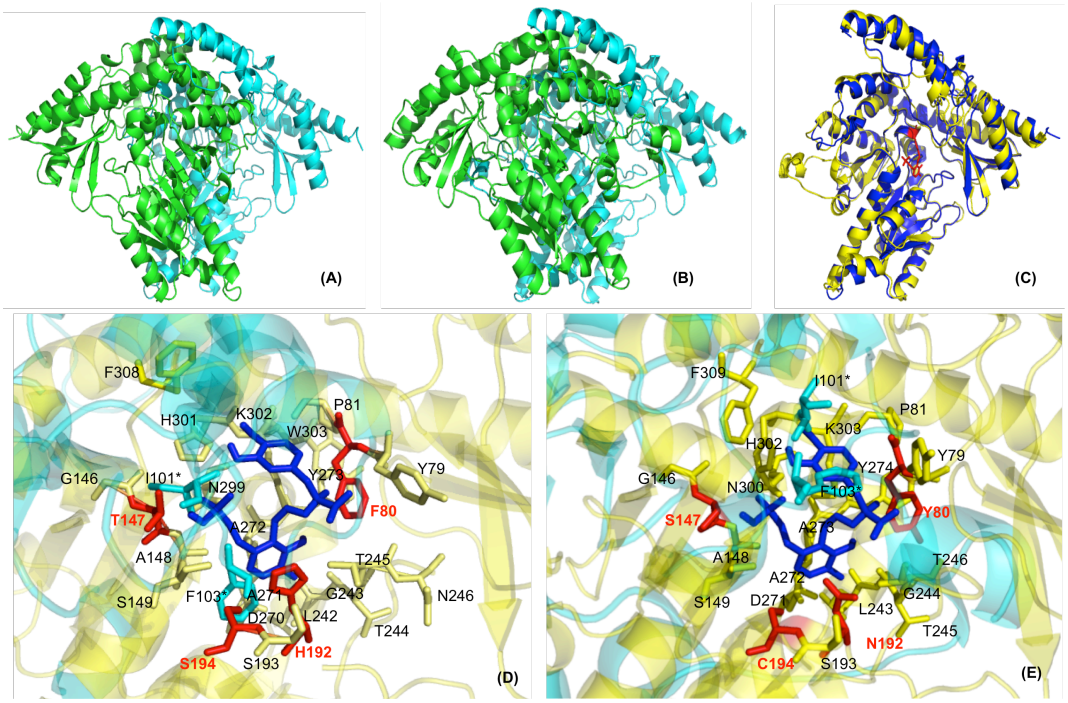

Figure 3.3: Comparison of overall structures and active site conformations of DDC and DHPA synthase. **Overall structure of DDC (PDB:3K40) (4) (A) and a modeled structure of DHPA synthase (B); chain A and chain B of both enzymes are colored in green and cyan, respectively. Superimposed DDC monomer is in blue and DHPA synthase monomer is in yellow (C); internal aldimine (from PDB 3K40) (4) in the superimposed structure is colored in red. For the active sites of DDC (D) and DHPA synthase (E), chain A is colored in yellow**

and chain B is colored in cyan and the residues within 6 Å are shown in sticks and labeled; the external aldimine ligand (from PDB 1JS3) (15) is shown in blue sticks; and the residues conserved in both enzymes are shown in yellow sticks (from chain A) and cyan (labeled with *, from chain B) with un-conserved residues are shown in red sticks.

3.3.3 The active sites of *Drosophila* DDC and DHPA synthase

To evaluate their catalysis and key residues involved, it was necessary to analyze the complex structure (native enzyme associated with substrate or substrate analog) so that the interactions of the active site residues with ligand could be critically evaluated. Coordinates of carbidopa were available from pig DDC (PDB: 1JS3) (15) and were used in the modeling analysis (Figure 3.3) (the compound is similar to L-dopa except for the additional methyl group and N-N bond) (Figure 3.1). For many enzymes, substrate binding often induces conformational changes, but comparison of a native pig DDC (PDB: 1JS6) (15) and its complex with carbidopa (PDB: 1JS3) (15) indicated that positional change in the active site residues seemed small. Some conformational changes (0.1 - 0.3 Å of Cα atoms) were noticed, but this change did not seem large enough to invalidate the prediction of active site residues through their proximity to the ligand. With the ligand in active sites, it seemed clear that the active sites of DDC and DHPA synthase appeared to be mainly composed of residues from one chain and some residues from the other chain (Figure 3.3D & 3.3E).

Based on modeled DHPA synthase structure and *Drosophila* DDC structure, most active site residues in DHPA synthase were conserved as compared to those in DDC (see Figure 3.3D & 3.3E) and they appeared to interact with the ligand through charge, hydrogen bond or hydrophobic interaction. Among the active site residues, Phe80, Thr147, His192 and Ser194 in

DDC (Figure 3.3D) contrasted to residues Tyr80, Ser147, Asn192 and Cys194 in DHPA synthase (Figure 3.3E). Based on this initial active site analysis, functionally verified *Drosophila* and mosquito DHPA synthase sequences were aligned with functionally verified insect DDC separately and then together to verify if the selected active site residues were conserved in DDCs, DHPA synthases or both (Figure 3.4). These sequence analyses confirmed the conservation of Tyr80, Ser147, Asn192 and Cys194 in DHPA synthase and Phe80, Thr147, His192 and Ser194 in DDC.

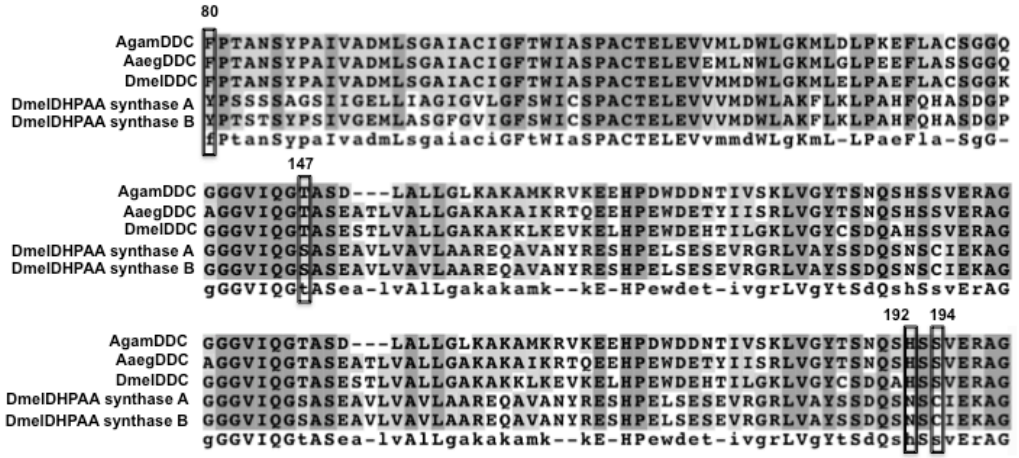

Figure 3.4: Partial sequence alignment of DDC and DHPA synthase. **Partial sequence alignment of *Aedes aegypti* DDC (AaegDDC) (XP_001648264), *Drosophila melanogaster* DDC (DmelDDC, NP724164), *Drosophila melanogaster* DHPA synthase A (DmelDHPA synthase A, NP_476592), *Drosophila melanogaster* DHPA synthase B (DmelDHPA synthase B, NP_724162) and *Anopheles gambiae* DDC (AgamDDC, AAC16249) is shown. The initial target residues that might be important for DDC activity and DHPA synthase activity are highlighted with box.**

After this residue/sequence verification, the side chain positions of these target residues to ligand, particularly to carbidopa Cα, were carefully analyzed. In DHPA synthase, Tyr80, Ser149, Asn192 and Cys194 seemed to interact with the external aldimine primarily through hydrogen

bonds. In DDC, Thr147 and Ser194 also seemed to interact with ligand through hydrogen bond formation, but Phe80 interacted with the ligand primarily through hydrophobic interaction and His192 primarily through charge interactions. Among these active site residues, the Asn192 and His192 (occupied same position in the two enzymes) showed major contrast in terms of their interactions with the ligand. Based on the structures, the side chain of His192 or Asn192 was also the closest to Cα group of the ligand. Phe80 and Tyr80 were another pair that contrasted in chemical properties with Phe80 primarily through hydrophobic interaction and the Tyr80 via hydrogen bond formation, but the pair was not close to Cα group of the ligand.

3.3.4 A N192H mutation in DHPA synthase elevated decarboxylation pathway

The active site Asn192 in DHPA synthase and His192 in DDC stood out in the above structural analyses and mutational study was first targeted to Asn192 or His192. A mutated DHPA synthase N192H was first produced and the purity of recombinant protein as shown in Figure 3.5 and yield (2.5 - 4 mg protein per liter cell culture with OD_{600} ~0.7) were sufficient for the following experiments. The biochemical behaviors of this mutation were compared with those of its wild-type enzyme. The wild-type DHPA synthase catalyzed decarboxylation-oxidative deamination as the major pathway, indicated by 3,4-dihydrophenylethanol (DHPE) peak from DHPA reduced by $NaBH_4$ (Figure 3.6A), but trace amount of dopamine was also observed (Figure 3.6A). When mutated DHPA synthase N192H was analyzed under identical conditions, its typical DDC activity (based on dopamine production) was greatly increased (from negligible to becoming a major product) (Figure 3.6B) as compared to wild-type DHPA synthase (Figure 3.6A).

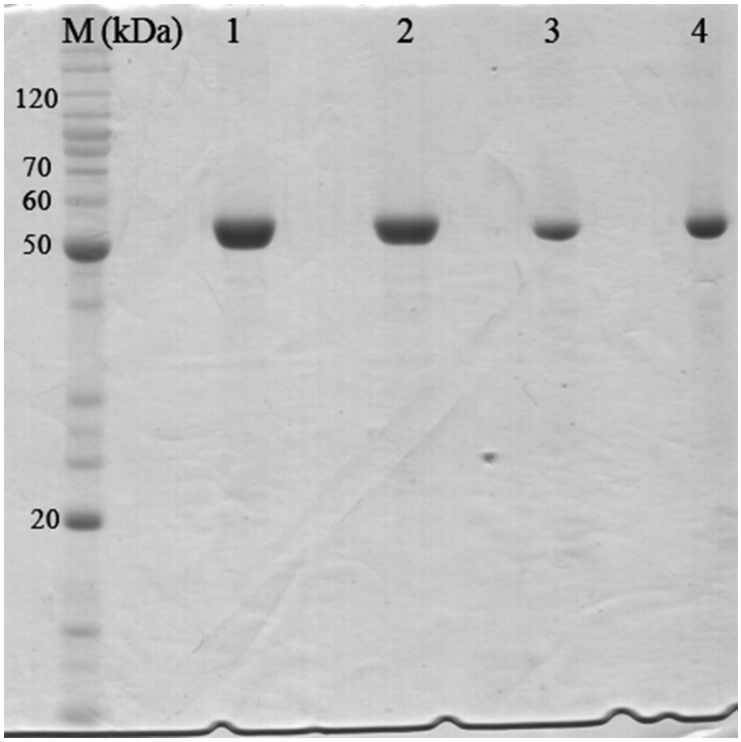

Figure 3.5: The SDS-PAGE gel for purified protein. **M, Protein Marker. 1, the DHPA synthase wild-type enzyme. 2, the mutated DHPA synthase N192H. 3, DDC wild-type enzyme. 4, the mutated DDC H192N.**

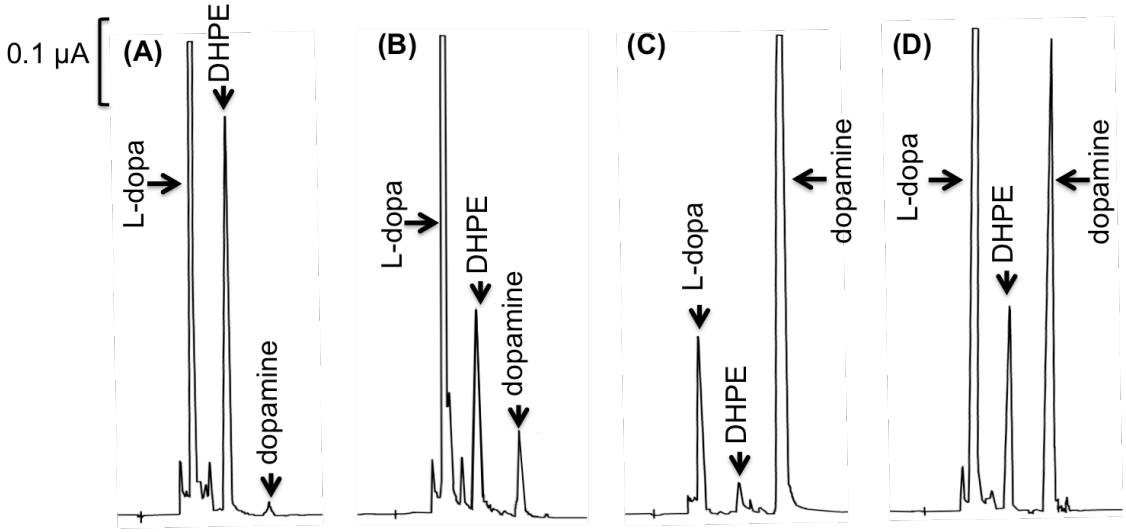

Figure 3.6: HPLC-ED chromatograms showing the relative amounts of DHPA and dopamine formed in their corresponding reaction mixtures. **A reaction mixture of 100 µl, containing 2 mM L-dopa and 35 µg wild-type DDC, or DHPA synthase or their mutated enzymes, was**

prepared in 150 mM phosphate buffer (pH, 7.0) and incubated at 25 °C for 15 min and the reaction was stopped by adding an equal volume of methanol saturated with $NaBH_4$. DHPA formed in the reaction was reduced to 3,4-dihydroxyphenylethanol (DHPE) by $NaBH_4$. Chromatogram A with wild-type DHPA synthase; Chromatogram B with mutated DHPA synthase N192H; Chromatogram C with wild-type DDC; and Chromatogram D with mutated DDC H192N.

3.3.5 A H192N mutation in DDC resulted in a mutated DDC with both DDC and DHPA synthase activity

His192 was stringently conserved in all functionally verified DDC proteins (including many predicted DDC sequences). Wild-type DDC catalyzed primarily decarboxylation from L-dopa to dopamine, but a small DHPA peak (reduced to be DHPE) was also noticeable (Figure 3.6C). When His192 was mutated to Asn192, the mutated DDC H192N showed decreased DDC activity and apparent elevation of the oxidative deamination reaction (Figure 3.6D), suggesting that Asn192 in DHPA synthase plays a major role in aromatic acetaldehyde production.

3.3.6 Kinetic analyses of wild-type DDC, DHPA synthase and their corresponding mutations

The rate of typical decarboxylation reaction by DDC was more than 10-fold (V_{max} of DDC= 3,350 nmol min^{-1} mg^{-1}) higher than the rate of DHPA synthase-catalyzed reaction (V_{max} of DHPA synthase= 270 nmol min^{-1} mg^{-1}). This major difference in activity rate is likely intimately related to their catalytic characteristics, which is discussed in the discussion section. The affinity of DHPA synthase for L-dopa was slightly higher than that of DDC (Table 3.2). Due to difficulties in controlling oxygen concentration, the affinity of this enzyme to oxygen was not determined.

Kinetic analysis also intensified the notion that Asn192 and His192 play roles in DHPA synthase-mediated process and DDC-catalyzed reaction, respectively. In the mutated DHPA synthase N192H, its DHPA synthase activity decreased, while its decarboxylase activity increased an order of magnitude (see Tables 3.3). In the mutated DDC H192N, its DDC activity decreased ~12-fold (V_{max} is 3357 nmol versus 285 nmol dopamine min^{-1} mg^{-1}), but the DHPA synthase activity of this DDC H192N increased many folds from mutation and reached 51% of wild-type DHPA synthase level (139 nmol DHPA min^{-1} mg^{-1} in mutated DDC H192N). Based on the rate of catalysis, this mutated DDC H192N was somewhat equivalent to that of wild-type DHPA synthase in DHPA production.

Enzyme	Activity	K_m (mM)	V_{max} (nmol/min/mg protein)
DHPA synthase	Decarboxylation-oxidative deamination activity	0.88±0.10	270.41±17.23
DDC	Decarboxylation activity	1.26±0.047	3357.08±25.55

Table 3.2: Kinetic parameters of wild-type DHPA synthase and DDC. **The parameters were measured as described in experimental procedures with L-dopa concentration varying from 0.2 to 8 mM. Values were calculated using the non-linear fitting and values represent mean ± S.E. (n=3).**

	Decarboxylation activity		Decarboxylation-oxidative deamination activity	
Enzyme	K_m (mM)	V_{max} (nmol/min/mg protein)	K_m (mM)	V_{max} (nmol/min/mg protein)
DHPA synthase (WT)	Not detected		0.88±0.10	270.41±17.23
N192H DHPA synthase	1.60±0.28	78.14±3.20	1.23±0.21	163.13±9.75
DDC (WT)	1.26±0.05	3357.08±25.55	Not detected	
H192N DDC	1.03±0.04	285.36±8.33	0.82±0.05	139.58±8.07

Table 3.3: Kinetic parameters of wild-type and mutated DHPA synthase and DDC enzymes. **The parameters were measured as described in experimental procedures with L-dopa concentration varying from 0.2 to 8 mM. Values were calculated using the non-linear fitting and values represent mean ± S.E. (n=3). Please note the wild-type enzymes kinetics to L-dopa have already been shown in Table 3.2 and are listed in this table for the purpose of comparison.**

3.3.7 Mutational analyses of other active site residues in DDC and DHPA synthase

Structural analysis also reviewed changes of other active site residues i.e., Phe80 versus Tyr80, Thr147 versus Ser147 and Ser194 versus Cys194 in DDC and DHPA synthase respectively. The same residue swapping through site-directed mutation was done for both enzymes, but activity assays showed no noticeable change in catalytic specificity (i.e., DDC showed considerable DHPA synthase activity or vice versa), except for some variation in activity rates. The mutated DDC S194C and mutated DHPA synthase C194S, as well as mutated DDC F80Y and mutated DHPA synthase Y80F showed similar activity (differences are within 12.3%) with their wild-type enzymes while mutated DDC T147S and mutated DHPA synthase S147T showed only activity variation within 7%.

3.3.8 Participation of H_2O_2 in the oxidative deamination reaction

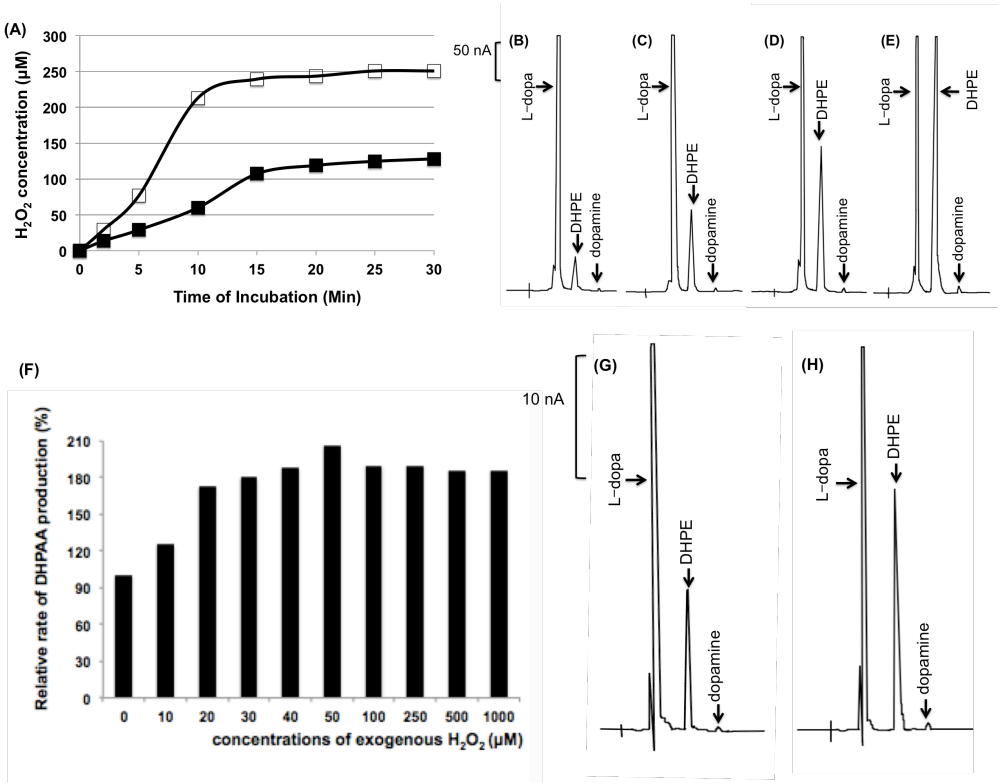

Figure 3.7: H_2O_2 formation versus DHPA production and effect of H_2O_2 on DHPA formation. **DHPA synthase activity based on H_2O_2 production versus incubation time and enzyme concentration (A). In line graph (A), the amount of DHPA synthase used was 9 µg (solid square) and 18 µg (open square) per 200 µl reaction mixture, respectively. All reaction mixtures contained 150 mM phosphate buffer (pH 7.0) and 5 mM L-dopa and were incubated at 25 °C. Chromatograms illustrate relative amounts of DHPA formed based on HPLC-ED detection in reaction mixtures at 5 (B), 10 (C), 20 (D) and 30 (E) min after incubation respectively. Chromatograms B-E show the DHPA formed in reaction mixture (200 µl) containing 35 µg wild-type DHPA synthase and 5 mM L-dopa at 5 (B), 10 (C), 15 (D), 30 (E) min after incubation. Relative rate of DHPA formed in the absence and presence of different concentration of indicated exogenous H_2O_2 (F) in the reaction mixtures (100 µl) containing 1 mM L-dopa and 15 µg wild-type DHPA synthase. Chromatographs shows relative amount of DHPA formed without (G) and with 50 µM H_2O_2 (H) in reaction mixtures (200 µl) containing 9 µg and 2 mM L-dopa.**

During linearity analysis in validating the H_2O_2 assay method, it was noticed that after a seemingly linear H_2O_2 production period, formation of the compound appeared to be somewhat stalled (Figure 3.7A), but within 10 min incubation period, the amount of accumulated H_2O_2 was approximately proportional to incubation time and protein amounts (Figure 3.7A). The dissolved oxygen concentration was around 0.3 mM in aqueous solutions (which fluctuates slightly depending upon atmospheric pressure). This result was initially suspected due primarily to depletion of substrates (primarily oxygen) or product accumulation to some less extent. To be on the safe side, the rate determination for previous kinetic analysis of the wild-type and mutated enzymes was based on H_2O_2 produced during the first 5 min. Subsequently, it was noticed that the curve of H_2O_2 production was in general agreement with HPLC-ED results during the initial 10 min (Figure 3.7B and 3.7C), but the production of DHPA continuously increased following initial 10 min period based on HPLC-ED analysis (Figure 3.7D and Figure 3.7E), which apparently did not agree with data based on H_2O_2 production (Figure 3.7A).

The above results suggest that H_2O_2 formed in the reaction mixture likely is being re-used in a DHPA synthase-mediated reaction during early linearity tested, doubling the protein amounts increased approximately twice the amount of H_2O_2 production during the first 10 min incubation period, but the H_2O_2 accumulation curves looked somewhat hyperbolic (see Figure 3.7A). To verify if H_2O_2 was indeed involved in oxidative deamination in DHPA synthase, different concentrations of exogenous H_2O_2 (0, 10, 20, 30, 40, 50, 100, 250, 500, and 1000 μM) were incorporated into the reactions and initial rate (derived from first 5 min incubation) was calculated. It was found that 50 μM concentration of H_2O_2 showed best activity rate for DHPA

synthase (Figure 3.7F). No further increase in rate of DHPA production by the enzyme was observed beyond 50 μM of H_2O_2.

3.3.9 Application of Asn192 for DHPA synthase identification

Order name	*Species*	DDC	DHPA synthase
Hemiptera	*Acyrthosiphon pisum*	XP_001950555	XP_001950143.1
	Diuraphis noxia	XP_015364475.1	XP_015374550.1
	Cimex lectularius	XP_014253190	XP_014259570.1
Hymenoptera	*Apis mellifera*	XP_394115.2	XP_006563197.1
	Apis dorsata	XP_006610829.1	XP_006610830.1
	Apis florea	XP_012344147.1	XP_003690124.1
	Bombus terrestris	XP_003399661.1	XP_003399659.1
	Bombus impatiens	XP_003491885.1	XP_003491883.1
	Megachile rotundata	XP_003704691.2; XP_012143780.1	XP_003704683.1
	Habropoda laboriosa	XP_017787631.1	XP_017787636.1
	Eufriesea mexicana	XP_017766874.1	XP_017766882.1
	Linepithema humile	XP_012226027.1	XP_012226256.1
	Pogonomyrmex barbatus	XP_011632998.1	XP_011633014.1
	Trachymyrmex zeteki	XP_018301533.1	XP_018301567.1
Diptera	*Drosophila melanogaster*	NP_724164.1	NP_724162.1; NP_476592.1
	Drosophila arizonae	XP_017859858.1	XP_017858927.1
	Drosophila mojavensis	XP_002002172.1	XP_002002174.1
	Drosophila yakuba	XP_002090668.1	XP_002090666.1; XP_015052399.1
	Drosophila eugracilis	XP_017069573.1	XP_017069575.1; XP_017069576.1
	Drosophila elegans	XP_017116621.1	XP_017117131.1; XP_017117132.1
	Drosophila suzukii	XP_016934704.1	XP_016927121.1; XP_016927129.1
	Aedes aegypti	XP_001648264.1	XP_001661056.1; XP_001661057.1
	Anopheles gambiae	XP_319841.3	XP_319838.3
	Anopheles darlingi	ETN60761.1	ETN60762.1
	Anopheles sinensis	KFB39134.1	KFB39133.1
Lepidoptera	*Bombyx mori*	NP_001037174.1; XP_012549896.1	XP_004931016.1
	Papilio machaon	NP_001303952.1; XP_014369966.1	XP_014370039.1
	Papilio xuthus	NP_001299156.1; KPI93750.1	NP_001299624.1; KPI93764.1
	Papilio polytes	NP_001298595.1	XP_013133917.1
	Amyelois transitella	XP_013188831.1	XP_013188794.1
	Plutella xylostella	XP_011550805.1	XP_011548131.1
	Danaus plexippus	EHJ63554.1	EHJ67528.1
	Operophtera brumata	KOB76562.1	KOB58186.1
Isoptera	*Zootermopsis nevadensis*	KDR23678.1	KDR23679.1
Coleoptera	*Tribolium castaneum*	NP_001096056.1; EFA03481.1	XP_008193582.1; XP_973068.2
	Anoplophora glabripennis	XP_018569156.1	XP_018569158.1; XP_018569153.1
	Aethina tumida	XP_019878068.1; XP_019877884.1	XP_019877885.1; XP_019877892.1
	Dendroctonus ponderosae	XP_019761571.1	XP_019761605.1; ENN76340.1

Table 3.4: The NCBI accession numbers of DDC and possible DHPA synthase in different model species from different insect orders. **Only species with sequenced genomes and annotations are listed.**

Based on the presence of Asn192 in conjunction with high similarity to DDC, we were able to distinguish DHPA synthase from DDC in NCBI (https://www.ncbi.nlm.nih.gov/protein). Table 3.4 illustrates individual DDC and DHPA synthase with NCBI accession numbers in sequenced insect species from different insect orders. Our data suggest that DHPA synthase is present in most sequenced insect genomes (if not all). Some insect species have one DHPA synthase (such as species from Hemiptera and Hymenoptera) and some species have two separate DHPA synthase genes.

3.4 Discussion and Conclusions

Insect DDC and DHPA synthase share high sequence similarity. Based on available insect genomes, there are at least one typical DDC and one DHPA synthase. Considering the universal presence of DDC in all animal species, insect DDC likely is more ancient and DHPA synthase was derived from DDC during environmental adaptation. In any given species their DDC and DHPA synthase share about 50% identity. The level of their sequence identity seems high enough to be classified as the same protein if they were from different species, but the situation appears sufficiently different if they are from the same species. When the typical DDC has been established, the other DDC-like enzyme should be DHPA synthase in the same species. If neither is functionally verified, one most likely has some difficulty to tell the two enzymes apart (see Figure 3.1 for examples). Our results in this study provided an effective means to distinguish DHPA synthase from DDC based on the relatively high sequence identity (~50%) to DDC and

the presence of the signature Asn192 residue in its sequence. The identification of essential function of Asn192 in DHPA synthase also provided some basis that enabled us to compare and contrast its similarities and differences in catalytic mechanism with those of DDC. This promoted our comprehension of DHPA synthase-mediated reaction and also led some better understanding of DDC-catalyzed reaction.

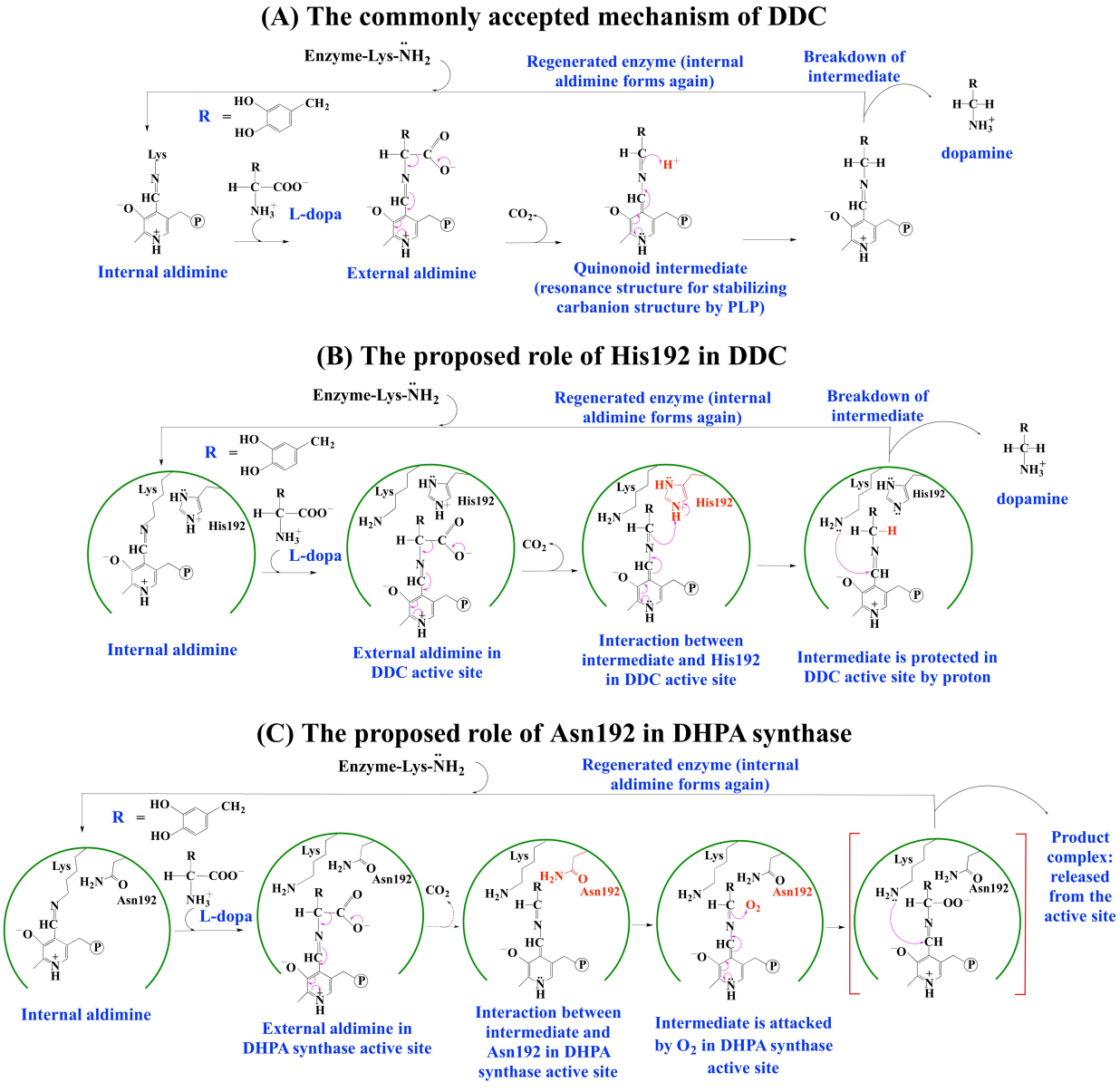

Figure 3.8: The commonly accepted mechanism of DDC and the proposed role of His192 and Asn192 in DDC and DHPA synthase respectively.

Both DDC and DHPA synthase are PLP-containing enzymes and share high sequence identity and both use L-dopa as a substrate. These two enzymes contain a conserved Lys302 or Lys303 residue and a Schiff-base structure (named internal aldimine) is formed through the aldehyde group of PLP and the ε-amino group of the conserved lysine residue. Binding of L-dopa substrate promotes breaking up of the Schiff-base structure and formation of a new Schiff-base structure. This process is commonly termed transimination and the PLP-substrate complex, thus formed, named external aldimine. The DDC-catalyzed mechanism has been extensively studied (http://proteopedia.org/wiki/index.php/DOPA_Decarboxylase). It has been generally accepted that delocalization of electron density toward PLP moiety and intermediate orientation allows for the stereospecific decarboxylation at Cα, releasing the carboxyl group and formation of a quinonoid intermediate. Ensuing protonation of Cα of the intermediate by a residue or species in the active site somewhat stabilizes the catecholamine moiety. Subsequent interactions between Lys302 and the protonated intermediate promote Schiff-base exchange or transimination process, releasing dopamine and formation of internal aldimine (Figure 3.8A). This commonly accepted mechanism is rational, but the species/residue, promoting this quinonoid intermediate protonation, remains obscure. Our data from comparative analysis provide some tangible basis to suggest that His192 is the one functioning on protonation of the quinonoid intermediate (Figure 3.8B). Our comparative studies established a key residue in DDC catalysis and complemented the decarboxylation mechanism.

In DHPA synthase, the same transimination process, like DDC, apparently proceeds in the enzyme. The mechanism, leading to carboxyl group breaking off, also could be explained by the

same mechanism like DDC as well. Once quinonoid intermediate is formed, however, DHPA synthase likely has problem in mediating a rapid protonation of the intermediate. In DHPA synthase, Asn192 occupies the same position as His192. Compared with histidine in DDC, the poor ability of asparagine residue in charge interaction makes it difficult to protonate the quinonoid intermediate. Moreover, based on modeled structures, no other residues, capable of mediating charge-interactions, are in close proximity to Cα of the quinonoid intermediate to enhance its protonation. The quinonoid intermediate, unable to be protonated and being intrinsically reactive, needs other means to stabilize or react, which leads to oxygen addition (Figure 3.8C). This oxygen addition induces electron movement toward it, which shifts back the imine structure. This makes it possible for Schiff-base to undergo transimination process with active site lysine residue, leading to formation of internal aldimine and releasing a product complex (Figure 3.8). The product complex, once released from active site into buffer, disintegrate into H_2O_2, NH_3 and DHPA in aqueous solution.

The predicted DHPA synthase-mediated process is based on careful examination of the active site structure of the enzyme and consideration of the high reactivity/instability of the quinonoid intermediate. For most enzymes, substrate binding often induces conformational changes (particularly active site), which isolates the active site from solvent. Protonation of quinonoid intermediate is considered a critical step to lead some electron and structural rearrangements (resume the imine structure) so that a transimination between Lys302 and protonated quinonoid intermediate could proceed. Inability to rapidly promote quinonoid intermediate by Asn192 and limitation in charge interaction from buffer induces oxygen addition. Another driving force likely is high reactivity/instability of the quinonoid intermediate. This could be explained from

the minor DHPA pathway in DDC. Even with predicted role in rapid protonation of the quinonoid intermediate by His192 in DDC, a small fraction of the intermediate still escaped from the typical decarboxylation route (Figure 3.6C). Oxygen addition to Cα induces some electron delocalization, which makes the intermediate resumes its Schiff-base structure (double bond resumes between carbon of the original PLP aldehyde group and amino group in the intermediate), which promotes similar transimination process, formation of internal aldimine and releasing product complex (Figure 3.8).

It is difficult to propose precisely the structure of the product complex and the real one might be different from the assumed one in brackets in the diagram (Diagram 3.1). Although the disintegration of the product complex might occur right after a transimination process in the active site, it likely proceeds after being released from the active site. As discussed, enzyme active site likely is quite different from a buffer environment. In most enzymes, substrate binding often induces some conformational changes, which isolates the active site from solvent (For example, often there are limited electron densities within crystal structures, which one could attribute to water molecules). This likely is particularly true for PLP-mediated reactions. It is well known that PLP mediates a variety of reactions and charge interaction often plays a central role in different reactions. However, if charge interactions depend largely on anion and cation in buffer, PLP-mediated enzymatic reactions would not be specific. Isolation of buffer upon substrate binding likely accounts for the specificity of enzymatic reactions because random interactions through diffusion by buffer components are minimized. The breakdown of the product complex involves acid-base mediation and hydrolysis, which should proceed easily in a buffer environment (Diagram 3.1).

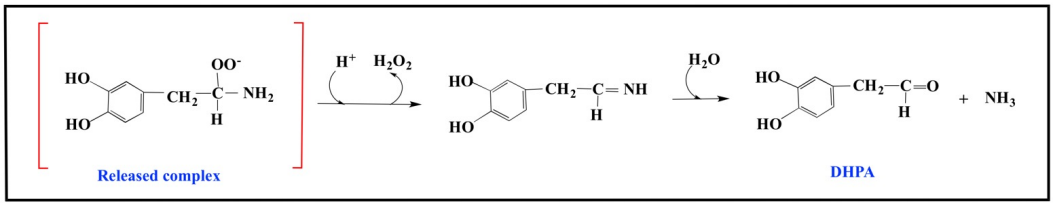

Diagram 3.1:The proposed hydrolysis of released complex in buffer.

In summary: Results of our comparative study lead to a reliable approach in distinguishing DHPA synthase from DDC in insects. Our comparative analyses of DDC and DHPA synthase result in a better understanding of DHPA synthase-mediated process and complemented mechanisms of DDC-catalyzed reaction as well. Our data about general presence of DHPA synthase in insects and the role of this enzyme in cuticle formation should provide the momentum toward a comprehensive understanding of the functional evolution of this essential insect enzyme. However, some details (such as the structure of oxygen-dopamine complex and the individual steps of its breaking down process) remain to be verified in DHPA synthase catalysis. While there is every reason to consider the major effect of Asn192 in DHPA production and His192 in dopamine formation in DHPA synthase and DDC, respectively, mutation of Asn192 to His192 in DHPA synthase or His192 to Asn192 in DDC did not lead to complete switch one way or other in the catalytic reactions. The operation of both DHPA and dopamine pathways in their mutated proteins suggest that other active site residues play subtle roles in their respective reaction, but the influences of these individual residues appears to be difficult ascertain or quantify through mutation analysis. Nonetheless, the Asn192 residue in conjunction with high similarity to DDC seems sufficient to establish DHPA synthase identity.

Potential conflicts of interest

The authors declare that they have no conflicts of interest with the contents of this article.

3.5 Acknowledgements

This work was supported by Department of Biochemistry and College of Agriculture; Life Science at Virginia Tech; US Department of Agriculture; and National Natural Science Foundation of China [31472186].

3.6 References

1. Hodgetts RB, O'Keefe SL. Dopa decarboxylase: a model gene-enzyme system for studying development, behavior, and systematics. Annu Rev Entomol. 2006;51:259-284
2. Christensen BM, Li J, Chen CC, Nappi AJ. Melanization immune responses in mosquito vectors. Trends Parasitol. 2005;21(4):192-199
3. Andersen SO. Insect cuticular sclerotization. Insect Biochem Mol Biol. 2010;40(3):166-178
4. Han Q, Ding H, Robinson H, Christensen BM, Li J. Crystal structure and substrate specificity of *Drosophila* 3,4-dihydroxyphenylalanine decarboxylase. PLoS One. 2010;5(1):e8826
5. Hiruma K, Riddiford LM. Hormonal Regulation of Dopa Decarboxylase during a Larval Molt. Dev Biol. 1985(110):509-513
6. Borowsky B, Adham N, Jones KA, Raddatz R, Artymyshyn R, Ogozalek KL, Durkin MM, Lakhlani PP, Bonini JA, Pathirana S, Boyle N, Pu X, Kouranova E, Lichtblau H, Ochoa FY, Branchek TA, Gerald C. Trace amines: identification of a family of mammalian G protein-coupled receptors. Proc Natl Acad Sci U S A. 2001;98(16):8966-8971
7. Cole SH, Carney GE, McClung CA, Willard SS, Taylor BJ, Hirsh J. Two functional but noncomplementing Drosophila tyrosine decarboxylase genes: distinct roles for neural tyramine and octopamine in female fertility. J Biol Chem. 2005;280(15):14948-14955
8. Sherald AF, Wright TRF. The Analog Inhibitor, alpha-Methyl Dopa, as a Screening Agent for Mutants Elevating Levels of Dopa Decarboxylase Activity in *Drosophila melanogaste*. Molec gen Genet 1974(133):25-36

9. Sparrow JC, Wright TRF. The Selection for Mutants in *Drosophila melanogaster* Hypersensitive to alpha-Methyl Dopa, a Dopa Decarboxylase Inhibitor. Molec gen Genet 1974(130):127-141
10. Wang D, Marsh JL. Developmental regulation of the alpha-methyldopa hypersensitive gene of Drosophila melanogaster. Dev Biol. 1995;168:598-612
11. Marsh JL, Erfle MP, Leeds CA. Molecular localization, developmental expression and nucleotide sequence of the *alpha-methyldopa hypersensitive* gene of *Drosophila*. Genetics Society of America. 1986;114:453-467
12. Black BC, Pentz ES, Wright TRF. The alpha methyl dopa hypersensitive gene, *l(2)amd*, and two adjacent genes in *Drosophila melanogaster*: Physical location and direct effects of amd on catecholamine metabolism. Molec gen Genet. 1987;209:306-312
13. Sparrow JC, Wright TRF. The selection for mutants in *Drosophila melanogaster* Hypersensitive to alpha-melthyl dopa, a dopa decarboxylase inhibitor. Molec gen Genet. 1974;130:127-141
14. Vavricka C, Han Q, Huang Y, Erickson SM, Harich K, Christensen BM, Li J. From L-dopa to dihydroxyphenylacetaldehyde: a toxic biochemical pathway plays a vital physiological function in insects. PLoS One. 2011;6(1):e16124
15. Burkhard P, Dominici P, Borri-Voltattorni C, Jansonius JN, N. MV. Structural insight into Parkinson's disease treatment from drug-inhibited DOPA decarboxylase. Nat Struct Biol. 2001;8(11):963-967
16. Komori H, Nitta Y, Ueno H, Higuchi Y. Structural study reveals that Ser-354 determines substrate specificity on human histidine decarboxylase. J Biol Chem. 2012;287(34):29175-29183
17. Kelley LA, Sternberg MJ. Protein structure prediction on the Web: a case study using the Phyre server. Nat Protoc. 2009;4(3):363-371
18. Pieper U, Webb BM, Barkan DT, Schneidman-Duhovny D, Schlessinger A, Braberg H, Yang Z, Meng EC, Pettersen EF, Huang CC, Datta RS, Sampathkumar P, Madhusudhan MS, Sjolander K, Ferrin TE, Burley SK, Sali A. ModBase, a database of annotated comparative protein structure models, and associated resources. Nucleic Acids Res. 2011;39(Database issue):D465-474
19. Arnold K, Bordoli L, Kopp J, Schwede T. The SWISS-MODEL workspace: a web-based environment for protein structure homology modelling. Bioinformatics. 2006;22(2):195-201
20. Biasini M, Bienert S, Waterhouse A, Arnold K, Studer G, Schmidt T, Kiefer F, Cassarino TG, Bertoni M, Bordoli L, Schwede T. SWISS-MODEL: modelling protein tertiary and quaternary structure using evolutionary information. Nucleic Acids Res. 2014;42(Web Server issue):W252-258
21. Guex N, Peitsch MC, Schwede T. Automated comparative protein structure modeling with SWISS-MODEL and Swiss-PdbViewer: a historical perspective. Electrophoresis. 2009;30 Suppl 1:S162-173
22. Kiefer F, Arnold K, Kunzli M, Bordoli L, Schwede T. The SWISS-MODEL Repository and associated resources. Nucleic Acids Res. 2009;37(Database issue):D387-392
23. Schwede T. SWISS-MODEL: an automated protein homology-modeling server. Nucleic Acids Res. 2003;31(13):3381-3385
24. Shi J, Blundell TL, Mizuguchi K. FUGUE: sequence-structure homology recognition using environment-specific substitution tables and structure-dependent gap penalties. J Mol Biol. 2001;310(1):243-257

25. Laskowski RA, MacArthur MW, Moss DS, Thornton JM. PROCHECK: a program to check the stereochemical quality of protein structures. Journal of Applied Crystallography. 1993;26(2):283-291
26. Melo F, Feytmans E. Assessing Protein Structures with a Non-local Atomic Interaction Energy. J Mol Biol. 1998;277:1141-1152
27. Benkert P, Tosatto SC, Schomburg D. QMEAN: A comprehensive scoring function for model quality assessment. Proteins. 2008;71(1):261-277
28. Benkert P, Kunzli M, Schwede T. QMEAN server for protein model quality estimation. Nucleic Acids Res. 2009;37(Web Server issue):W510-514
29. Sippl MJ. Recognition of Errors in Three-dimensional structures of proteins. Proteins. 1993;17:355-362
30. Wiederstein M, Sippl MJ. ProSA-web: interactive web service for the recognition of errors in three-dimensional structures of proteins. Nucleic Acids Res. 2007;35(Web Server issue):W407-410
31. Luthy R, Bowie JU, Eisenberg D. Assessment of protein models with three-dimensional profiles. Nature. 1992;356(5):83-85

Chapter 4

Substrate Selectivity of *Anopheles gambiae* Tyrosine Decarboxylase

Jing Liang [a], Qian Han[b], Haizhen Ding [a], Jianyong Li [a*]

[a] Department of Biochemistry, Virginia Polytechnic Institute and State University, Blacksburg, VA24060, United States

[b] Laboratory of Tropical Veterinary Medicine and Vector Biology, Hainan Key Laboratory of Sustainable Utilization of Tropical Bioresources, Institute of Agriculture and Forestry, Hainan University, Haikou, 570228, Hainan, China.

[*] Correspondence to Prof. Jianyong Li (lij@vt.edu; Tel: 540-231-5779; Fax: 540-231-9070)

Abstract

In sequenced invertebrate genomes, there are usually two genes named tyrosine decarboxylase 1 (TyDC1) and TyDC2, respectively, and they are believed responsible for producing tyramine. Tyramine is the only precursor for producing octopamine, and both tyramine and octopamine are major neurotransmitters in insects. While there is no doubt that tyramine is produced by TyDC, the biochemical behaviors of insect TyDC have not been clearly established. This study concerns the biochemical properties of this insect TyDC1 in comparison with well-established insect dopa

decarboxylase (DDC). Our data revealed that the insect TyDC1, similar to DDC, showed two visible absorbance peaks with λ_{max} at around 340 nm and 422 nm (typical for aromatic decarboxylases), but its 422 nm peak is much greater than its 340 nm peak, which contrasts to other characterized aromatic amino acid decarboxylases (including DDC). In addition, substrate screening against different aromatic amino acids established that TyDC1 catalyzes efficiently L-tyrosine to tyramine, but the enzyme also has a substantial activity to L-dopa. This contrasts with insect and mammalian DDC that has no detectable activity to L-tyrosine. Kinetic analysis revealed that TyDC1 has a relatively high affinity to both tyrosine and dopa at a sub-millimolar range as compared to the millimolar range of DDC to dopa. Homology modeling provided clues for active site residues that might affect its visible spectrum and its activity on both L-tyrosine and L-dopa. Subsequent site-directed mutations of TyDC1 gene indicated that its active site residue Asn304 appears primarily responsible for its spectral characteristics and higher affinity to L-tyrosine than that to L-dopa. An active site residue Ser353 has the major impact on substrate selectivity. In addition, mutation of His193, a conserved residue in DDC and TyDC, to an alanine decreased substantially its decarboxylation activity, but this mutated enzyme displayed considerable oxidative deamination activity, leading to 3,4-dihydroxylphenylacetaldehyde, H_2O_2, and NH_3 formation. Our results provide not only the basic characteristics of insect TyDC but also insight into the mechanism of its substrate selectivity and functional evolution.

4.1 Introduction

Tyramine and octopamine are two neurotransmitters whose physiological roles are predicted to be critical in invertebrates, particularly in insects (1, 2). In addition to their roles as

neurotransmitters, tyramine and octopamine play specific but essential physiological roles in insects, such as reproduction, sensitization to stimuli, and modulation of peripheral organs (1-3). Tyramine is believed to be especially involved in appetite regulation, olfaction, and neuromuscular control, response to cocaine, and post-mating inactivation (through pheromone) (1-3). Numerous efforts have been made towards cloning, identification and functional verification of tyramine and octopamine receptors in insects and these efforts have led to some tangible evidence for their G-protein coupled receptor status (2). Some receptors are specific only for tyramine or for both tyramine and octopamine (2, 4-7). Based on research data, the importance of tyramine and octopamine in invertebrates, particularly in insects, has been clearly established. It is expected that as research continues, further evidence for their proposed physiological functions and possibly new functions will emerge.

There have been a number of studies dealing with genes responsible for the production of tyramine and octopamine. In insects, DDC has been the most or at least one of the most extensively studied aromatic amino acid decarboxylases (AAAD). Based on sequence data, there are several sequences sharing high identity (>30%) to DDC in any given sequenced insect genome. These coding sequences generally were classified as DDC-like proteins or AAAD to be more inclusive. In *Drosophila*, it was found that some mutants failed to be sensitized by cocaine, and examination of their brain extracts determined that they had low tyramine concentration (3). Real-time PCR analyses indicated some positive correlation between low RNA level of DDC-like sequences and diminished tyramine and octopamine levels in the mutants (3). The two DDC-like sequences were termed tyrosine decarboxylase-1 (TyDC1) and tyrosine decarboxylase-2 (TyDC2) in *Drosophila* and their mutant phenotypes could be partially or

completely rescued by driving the expression of TyDC2 and/or TyDC1 by genetic approaches (8). These studies provided important functional information about insect TyDC and some basis to classify these DDC-like proteins as TyDC. The temporal and spatial profiles of both TyDC1 and TyDC2 have been analyzed in detail in typical model species, including *Drosophila melanogaster* (8, 9) and *Phormia regina* (10).

Compared to functional elucidation of tyramine and octopamine, the studies related to proteins responsible for production of tyramine and octopamine are limited. For example, it is unknown whether insect TyDC, like its DDC counterpart, works exclusively on tyrosine. Insect DDC catalyzes decarboxylation of L-dopa and 5-hydroxytryptophan without any activity toward L-tyrosine. Based on this observation, one might have taken for granted to presume that its TyDC might have activity only on tyrosine. Apparently, there is a lot to learn about the biochemical and biophysical properties of insect TyDC at the protein levels. The major difficulty in determining the biochemical properties has been the amount of insect TyDC available for critical analysis. Although TyDC is indispensable, it is expressed in specific tissues or organs and the level of its protein is low. This causes great difficulty to purify TyDC for biochemical studies. Although it might be possible to achieve some estimation about the TyDC from partially purified samples (e.g. tissue extract or homogenates of whole insects), one would hesitate to attribute the detected activities exclusively to TyDC. Development of protein expression techniques has revolutionized protein functional elucidation. However, the current protein expression technologies still have limitations. No matter how sophisticated a research laboratory might have been, many proteins simply could not be functionally expressed (particularly those low abundant regulatory proteins

that expressed in specific tissues/cells). The predicted insect TyDC sequences seem to fall into this category.

To better understand the insect TyDC1 and TyDC2, through extensive optimization, we successfully expressed an *Anopheles gambiae* TyDC (XP_308521). Sequence comparison indicated that this TyDC sequence belongs to insect TyDC1, sharing ~65% identity with predicted TyDC1 across insect species so far. Therefore, its biochemical properties should be representative of insect TyDC1 enzymes as a whole. In this communication, we aim to address the spectra characteristics and substrate selectivity of this enzyme and the residues involved in its specific spectral and substrate selectivity characteristics.

4.2 Materials and Methods

4.2.1 Chemicals

L-dopa, dopamine, L-tyrosine, m-tyrosine, o-tyrosine, tyramine, 5-hydroxytryptophan (5-HTP), L-5-hydroxytryptamine, PLP, and other chemicals were products from Sigma-Aldrich company (St. Louis, MO). The IMPACT^{TM}-CN expression system and restriction enzymes were from New England Biolabs (Ipswich, MA).

4.2.2 Generation of the wild-type cDNA and mutated cDNA fragments

Total RNA sample was extracted from *Anopheles gambiae* using TRIZOL reagent from Invitrogen (Carlsbad, CA) and following its protocol. The extracted RNA was used for synthesizing the first strand cDNA. Gene specific primers were synthesized and used for

amplifying the fragment of TyDC1 coding regions. The coding region fragment was ligated into IMPACT^{TM}-CN expression vectors, which were also used as the template to generate mutations using primers of site-directed mutagenesis listed. The frame and orientation of the mutated sequences were verified by DNA sequencing.

4.2.3 Expression and Purification of wild-type and mutated TyDC1 enzymes

Escherichia coli (*E. coli*) ER2566 competent cells (IMPACT^{TM}-CN expression system) were transformed with recombinant plasmids (pTYB12) containing wild-type TyDC1 and mutated TyDC1 cDNA. The following protein expression and purification use similar method for DDC expression and purification (11). Transformed bacterial colonies were grown overnight at 37 °C. Then overnight culture was transferred to fresh medium and grown at 37 °C for 3.5 h and then was induced with IPTG (final concentration: 0.3 mM to 0.5 mM) and cultured with shaking at 15 °C for 48 hours. The soluble fusion protein was extracted and applied to chitin bead column because the fusion protein contains one chitin-binding domain. Then the column was quickly flushed with 3 bed volumes of cleavage buffer containing 50 mM β-mercaptoethanol and 40 μM PLP. The quick flush should be finished within 1 hour, and the flow is stopped. The column is incubated at 24 ^{o}C for 40 hours to cleave the chitin-binding domain and release the protein. The protein was concentrated using a Centricon YM-50 concentrator in a 25 mM Tris-HCl buffer containing 40 μM PLP and purified by an anion exchange column and gel-filtration chromatography. Mutated proteins were expressed and purified in the same way. The composition of buffers and the detailed methods used in the protein expression process are in the instruction manual of IMPACT^{TM}-CN (New England Biolabs Inc. Version 2.1). Purity of proteins was analyzed by SDS-PAGE gel. The protein concentration was determined following

the protocol of the Bio-Red assay kit (Hercules, CA) and a concentration gradient of bovine serum albumin was generated as a standard.

4.2.4 Substrate selectivity

A reaction mixture of 100 μl was prepared in 150 mM phosphate buffer (pH, 7) containing 5 μg wild-type enzyme or mutated enzyme, 2 mM L-dopa, L-tyrosine, 5-HTP, m-tyrosine, o-tyrosine and 40 μM PLP. The reaction mixture was incubated at 25 ^{o}C for 5 minutes, 10 minutes and 15 minutes and an equal volume of 0.8 M formic acid was added into to stop the reaction. The reaction mixture was centrifuged and 5 μl supernatant was analyzed by HPLC with electrochemical detection (HPLC-ED).

4.2.5 Kinetic Analysis

For decarboxylation activity assay, enzymes were mixed with 0.02 - 10 mM different substrates, respectively, in 150 mM phosphate buffer (pH, 7.0) and incubated at 25 °C. Substrate concentration was varied until enzymes were saturated. 40 μM PLP was also added into buffer (11). The reactions were stopped at time intervals (5 min, 10 min and 15 min) by adding an equal volume of 0.8 M formic acid. Then the mixture was centrifuged and 5 μl supernatant was injected into HPLC-ED for analysis. The commercial tyramine, dopamine, 5-hydroxytryptamine were used to generate standard curves, respectively, for their relative substrates. The kinetic parameters were solved using the Michaelis-Menten equation.

4.2.6 Homology modeling

TyDC1 was modeled by Phyre2 (12), ModWeb (13), Swiss-Model (14-18) and FUGUE (19) and models were submitted for evaluation using Swiss-Model evaluation tools(14-18), ProSA-web (20, 21) and Verify 3D checks (22). The model file was viewed by PyMOL (The PyMOL Molecular Graphics System, Version 1.7.4 Schrödinger, LLC.). The external aldimine formed by PLP and carbidopa was from the pig DDC by superimposing (PDB: 1JS3) (23) and the internal aldimine formed by PLP and lysine residue was from *Drosophila* DDC (PDB: 3K40) (11). The residues from the flexible loop region of DDC were also modeled and superimposed with 3K40 (11) for comparison.

4.3 Results

4.3.1 TyDC spectral characteristics, substrate selectivity and kinetic properties in comparison with those of DDC

After extensive optimization, TyDC1 was successfully expressed using *E. coli* cells. During protein extraction, a low concentration of PLP (40 μM) (11) was incorporated into solubilization buffer and buffers used for affinity chromatographies, which ensured the association of the PLP cofactor with the enzyme. No exogenous PLP was added into the ionic exchange and gel filtration buffers and therefore TyDC was resolved from free PLP. Purified TyDC showed two apparent absorbance peaks in visible region with λ_{max} at around 340 nm and 422 nm, respectively, and the absorbance at around 422 nm is higher (Figure 4.1A). Presence of absorbance peak in visible region at physiological pH conditions is common to all PLP containing enzymes, but the number of peaks and their λ_{max} vary depending upon the

environments of PLP. When a DDC (accession number: AAC16249.1) from the same species (*Anopheles gambiae*) was expressed and purified in the same manner in an identical buffer, the intensity of its 340 nm peak apparently is higher than its 422 nm peak (Figure 4.1B). After purified TyDC was dialyzed overnight, no apparent decrease of its visible spectra and no ratio change of the 340/422 nm peaks were observed, suggesting that PLP associated with its polypeptide rather tightly in TyDC.

Purified TyDC1 was first screened for substrate selectivity with each of the aromatic amino acids, including phenylalanine, L-tyrosine, L-dopa, tryptophan and 5-hydroxytrophan. Among the aromatic amino acids tested, TyDC1 showed the highest activity to tyrosine, but also displayed a considerable activity to L-dopa (83% the rate of tyrosine decarboxylation) (Table 4.1). This contrasts to insect DDC that has no detectable activity to L-tyrosine (Table 4.1). No activities to phenylalanine, tryptophan and 5-hydroxytryptophan were detected. Kinetic analysis revealed that insect TyDC1 showed relatively high affinity to tyrosine and L-dopa (Table 4.1). For example, the K_m of insect TyDC1 to tyrosine was more than 10-fold lower than that of insect DDC to L-dopa and its overall catalytic efficiency on tyrosine and dopa was more than 50- and 20-fold higher respectively to that of DDC to L-dopa.

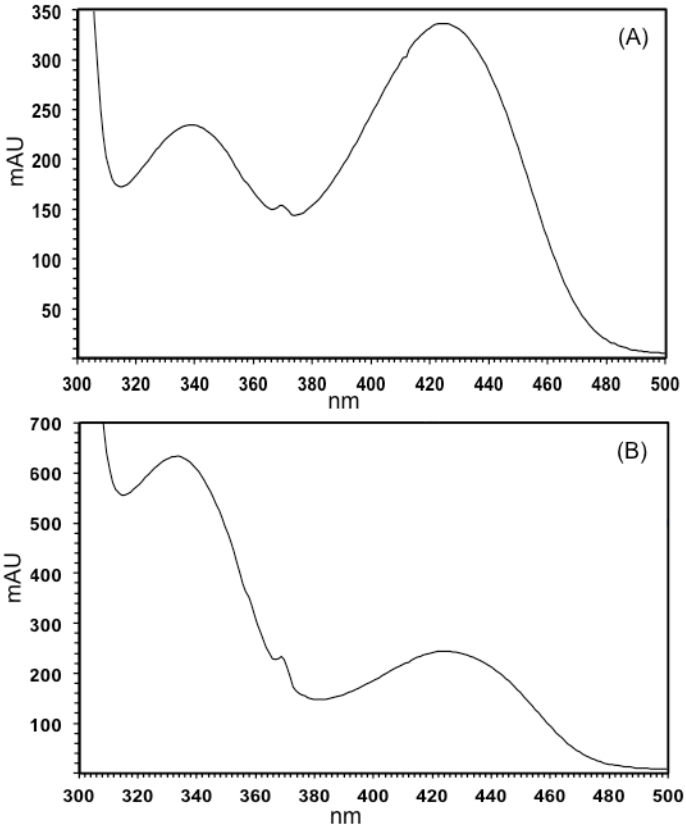

Figure 4.1: The spectra of PLP (with λ_{max}) in purified TyDC (A) and DDC (B) at pH 7.0. **The presence of absorbance peaks at around 340 nm and 422 nm indicates PLP binding. The differences of the levels of two peaks in DDC and TyDC are shown.**

	TyDC				DDC			
	K_m (mM)	K_{cat} (min^{-1})	V_{max} (nmol/min/mg)	k_{cat}/K_m ($min^{-1}mM^{-1}$)	K_m (mM)	K_{cat} (min^{-1})	V_{max} (nmol/min/mg)	k_{cat}/K_m ($min^{-1}mM^{-1}$)
L-tyrosine	0.10±0.01	514.45±58.09	4761.75±537.70	5266.44	-	-	-	-
L-dopa	0.17±0.02	427.18±49.77	3953.86±460.65	2484.32	1.30±0.05	127. 02±2.2	2250.05±30.01	97.71

Table 4.1: The kinetics of wild-type *Anopheles gambiae* TyDC comparing with kinetics of DDC from the same species.

4.3.2 Active site residues that potentially affect spectral characteristics and substrate selectivity of TyDC as compared with those in DDC

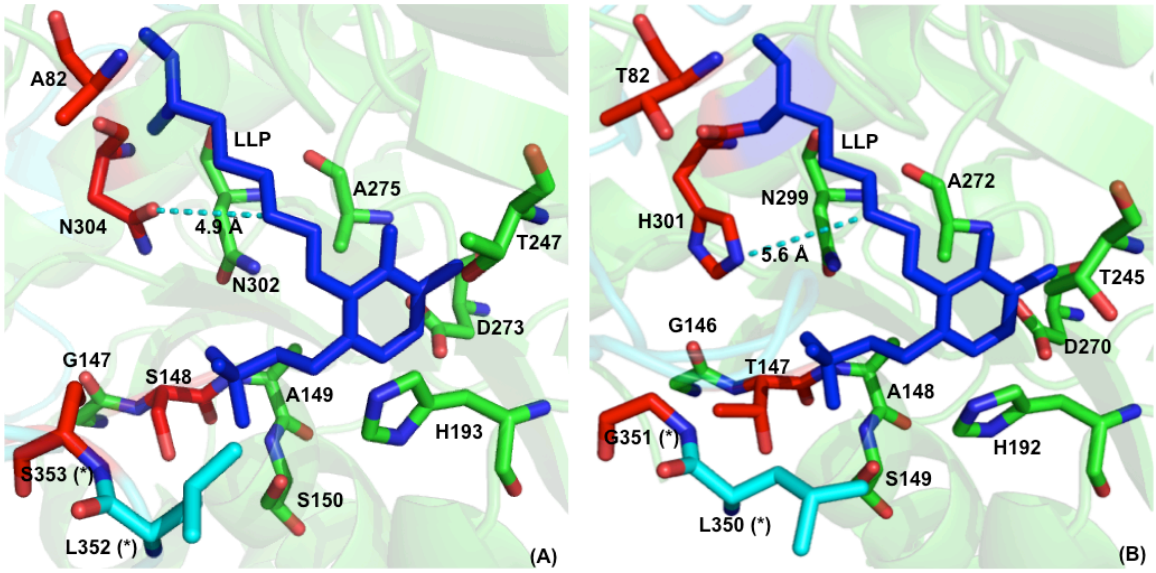

Figure 4.2: The active sites of TyDC (A) and DDC (B) with internal aldimine. **Chain A is colored in green and chain B is colored in cyan in both enzymes. The internal aldimine from DDC crystal structure (PDB: 3K40) (11) is shown in blue sticks. The residues interacting with internal aldimine are shown in sticks and labeled with residue names. The residues shared in common by both enzymes are shown in green sticks (from chain A) and cyan (from chain B, labeled with *). The different residues, but conserved in each enzyme, are shown and labeled in red. The distances between Asn304 (in TyDC) or His301 (in DDC) and internal aldimine ε-carbon were shown in cyan dashed lines. G351 and L350 from chain B in DDC are generated from a DDC model.**

The spectral characteristics of PLP-containing enzymes were first due to presence of PLP-moiety itself and also the interactions of active site with the co-factor. The spectral dissimilarity of TyDC as compared to DDC suggested some differences in the interactions between the two enzymes. TyDC shared good sequence identity to DDC (~50 %). Several homology models of TyDC were built based on different templates and compared with DDC crystal structure (PDB: 3K40) (11). While the overall structures of the two enzymes were quite similar, several different

active site residues, occupying similar positions and having similar orientation, were noticed, which include Ala82, Ser148, Asn304 and Ser353 in TyDC and its corresponding residues Thr82, Thr147, His301 and Gly351 at equivalent positions in DDC (Figure 4.2). Among these similar position residues, Ala82 in TyDC interacted with internal aldimine primarily through hydrophobic interaction and Thr82 in DDC primarily through hydrogen bond interaction; Ser148 in TyDC and Thr147 in DDC interacted with the internal aldimine through the same hydrogen bond formation; Ser353 in TyDC and Gly351 seemed to act similarly, but Gly351 seemed to lead more active site space in DDC than that of Ser353 in TyDC; and Asn304 in TyDC could establish hydrogen bond interaction, while its counterpart His301 in DDC through charge interaction.

Among the 4 pairs of different residues, the Asn304 in TyDC active site contrasted with its counterpart residue of His301 in DDC in terms of interactions with their internal aldimine. Asn304 could easily interact with the internal aldimine through hydrogen bond, while His301 could network with it through charge interaction. Therefore, His301 could have some major effect on electrochemical status of the internal aldimine. Based on the structural models, the side chain of Asn304 in TyDC or His301 in DDC was close to lysine residue (Lys302 in DDC and Lys305 in TyDC) involved in the internal aldimine complex formation, particularly the Schiff-base group of the internal aldimine. It has generally been considered that the 330-340 and 420-430 absorbance peaks were due to the presence of enolamine and ketoenamine tautomers. If true, Asn304 in TyDC likely favored the production of its ketoenamine form (λ_{max}: around 422 nm), while His301 in DDC likely promoted the formation of enolamine tautomer (λ_{max}: around 340 nm) in DDC.

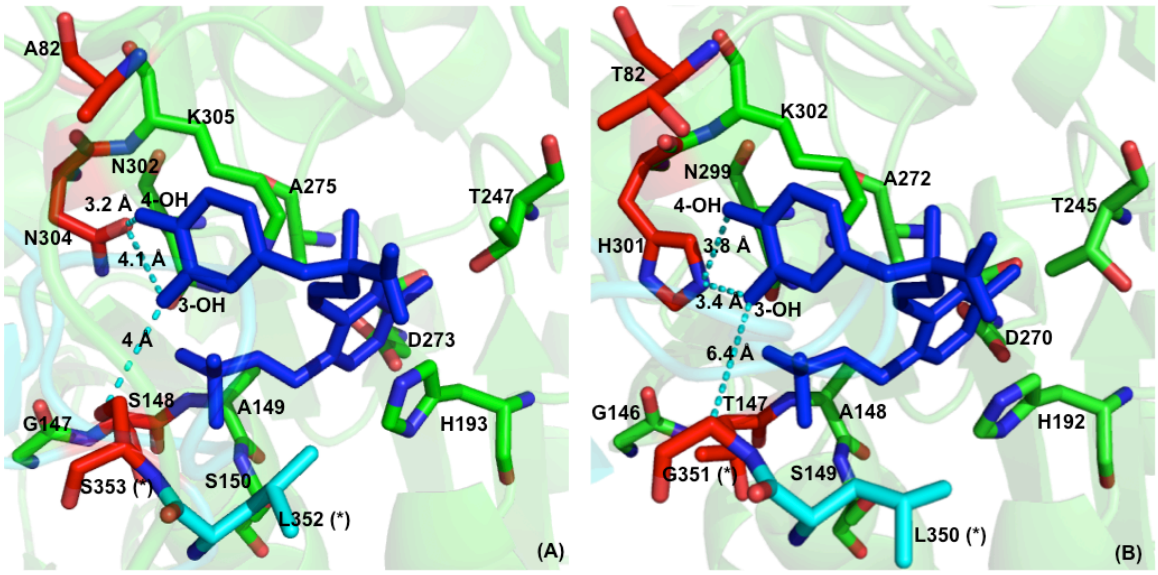

Figure 4.3: The active sites of TyDC (A) and DDC (B) with external aldimine. **Chain A is colored in green and chain B is colored in cyan in both enzymes. The external aldimine from pig DDC crystal structure (PDB: 1JS3) (23) is shown in blue sticks. The residues interacting with internal aldimine are shown in sticks and labeled with residue names. The residues shared in common by both enzymes are shown in green sticks (from chain A) and cyan (from chain B, labeled with *). The different residues, but conserved in each enzyme, are shown and labeled in red. The distances between carbidopa 3-OH and 4-OH to Asn304 (in TyDC) versus His301 (in DDC) and Ser353 (in TyDC) versus Gly351 (in DDC) were shown in cyan dashed lines.**

In addition to the spectra differences between TyDC and DDC, another difference is the substrate selectivity. Thus, the substrate selectivity and its structural basis are also analyzed. TyDC model was superimposed with pig DDC complex structure with external aldimine formed by PLP and carbidopa (23) to analyze the active site residues and was compared with DDC (Figure 4.3). Structural analysis indicated that among the residues that were different in two enzymes but occupy similar position and had similar orientation. Ala82 in TyDC interacted with the phenolic ring of substrate through hydrophobic interaction while Thr82 in DDC primarily through hydrogen bond with 4-OH group of L-dopa. Ser148 in TyDC and Thr147 in DDC were

more close to PLP than to L-dopa and both interacted with PLP through hydrogen bond. Ser353 in TyDC and Gly351 in DDC seems leading to bigger space in DDC than that in TyDC. Asn304 in TyDC versus His 301 in DDC interacted with substrate through hydrogen bond and charge interaction, respectively. Therefore, among those differentiated residues between TyDC and DDC, Ser353 in TyDC versus Gly351 in DDC and Asn304 in TyDC versus His301 in DDC standed out because of the differences in interactions and active site spaces to allow substrate binding, respectively. Although Ala82 in TyDC and Thr82 in DDC also interacted with substrate not in the same manner, the moieties they interacted with are phenolic ring and 4-OH group of substrate respectively (Figure 4.3) which are shared in common in both dopa and tyrosine and thus are not the one affecting substrate selectivity.

4.3.3 N304H mutation affected the kinetics and spectra of TyDC

As indicated by structural analysis, Asn304 and His301 might be the residues primarily responsible for the displayed spectral characteristics in TyDC and DDC, respectively. To ascertain this, efforts were made to mutate Asn304 to His304 in TyDC and His301 (equivalent to Asn304 position) to Asn301 in DDC, respectively. The mutated TyDC N304H was successfully expressed, but the mutated DDC H301N failed to be expressed. Spectral analysis of purified TyDC1 N304H protein revealed a large 340 nm peak and a small 422 nm peak (Figure 4.4), which became indeed similar to that of wild-type DDC (Figure 4.1B). This provided experimental evidence for suggesting that the interaction of Asn304 with internal aldimine was primary for TyDC spectral characteristics.

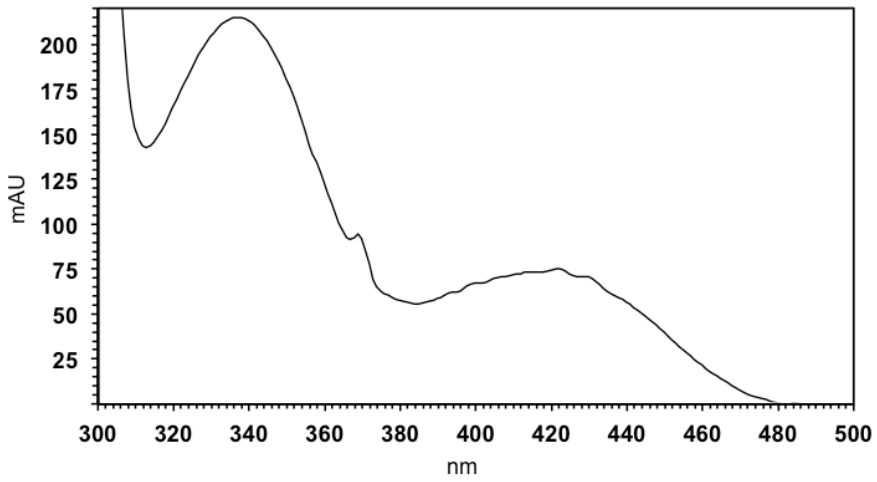

Figure 4.4: The spectra of PLP (with λ_{max}) in purified TyDC N304H protein under pH 7.0.

Another apparent difference of TyDC as compared to DDC has been the substrate selectivity. The close proximity of Asn304 to internal aldimine suggested that this residue likely would be close to substrate moiety of external aldimine and therefore might affect substrate binding/catalysis. Structural analysis of modeled TyDC structure complexed with carbidopa (a dopa analog) suggested that Asn304 was closer to 4-OH (3.2 Å) than 3-OH groups (4.1 Å) of carbidopa (Figure 4.3A). In contrast, examination of a DDC structure with carbidopa ligand indicated His301 was closer to the 3-OH group (3.4 Å) than 4-OH group (3.8 Å) of carbidopa moiety (Figure 4.3B). The distance should be shorter with presence of external aldimine formed by PLP and real substrate (L-dopa or L-tyrosine) because of an extra $–NH_2$ group and $–CH_3$ group in carbidopa. Thus, to verify the predicted possibility to be involved in substrate binding/catalysis, N304H was examined toward different substrates and the kinetics were detected.

	TyDC WT or N304H mutation	K_m (mM)	K_{cat} (min^{-1})	Vmax (nmol/min/mg)	K_{cat}/K_m ($min^{-1}mM^{-1}$)
L-tyrosine	WT	0.10±0.01	514.45±58.09	4761.75±537.70	5266.44
	N304H	4.54±0.53	47.51±5.44	428.03±61.50	10.46
L-dopa	WT	0.17±0.02	427.18±49.77	3953.86±460.65	2484.32
	N304H	0.12±0.02	4.93±0.20	45.59±1.81	41.49

Table 4.2: Kinetics of TyDC wild-type enzyme and N304H to L-tyrosine and L-dopa. **Please note that the wild-type TyDC kinetics to L-dopa and L-tyrosine have already been shown in Table 4.1 and are listed in this table for the purpose of comparison.**

Biochemical analysis of this TyDC N304H showed that the substrate selectivity was not affected, but there were apparent changes in its kinetic properties (Table 4.2). The mutated TyDC N304H enzyme showed a considerably low affinity to tyrosine reflected by more than 40-fold increased K_m as compared with the wild-type and at the same time greatly reduced its activity (more than 10-fold) of tyrosine decarboxylation as compared to that of wild-type enzyme. The catalytic activity of the mutated enzymes was also reduced greatly to L-dopa, but it showed a better affinity to the compound as indicated by the lower K_m (0.12 mM) as compared with that of wild-type enzyme (0.17 mM) (Table 4.2).

4.3.4 The substrate selectivity of the mutated TyDC S353G

The TyDC N304H enzyme showed a more than 40-fold decrease in its affinity to tyrosine, but its affinity to L-dopa was increased slightly (from 0.17 mM to 0.12 mM). This suggested that although N304H mutation in TyDC did not help in catalysis, it enhanced L-dopa binding. Ser353

in TyDC and Gly351 in DDC was another pair of different residues in similar position at their respective active site, but glycine residue appeared to occupy less space, thereby making slightly more room for incoming substrate than that of serine. Mutation of the active site residue Ser353 of TyDC to Gly did not lead to noticeable spectral change, but Ser353 and Gly351 are conserved in TyDC and DDC respectively and they are also in the interacting range with the substrate. Ser353 versus Gly has the possibility to be involved in substrate binding due to the fact that Ser353 can interact with 3-OH group of carbidopa through hydrogen bond and Gly makes the space bigger and more hydrophobic. Thus, Ser353 versus Gly may be involved in substrate selectivity by affecting the substrate binding space and hydrophobicity and S353G was screened for substrate selectivity of each compound. S353G lowered the activity to L-dopa and L-tyrosine, but increased activity to m-tyrosine and o-tyrosine. Moreover, S353G mutation enabled TyDC to use 5-HTP as a substrate (Table 4.3).

	TyDC WT or S353G mutation	K_m (mM)	K_{cat} (min^{-1})	V_{max} (nmol/min/mg)	K_{cat}/K_m ($min^{-1}mM^{-1}$)
L-tyrosine	WT	0.10±0.01	514.45±58.09	4761.75±537.70	5256.44
	S353G	1.32±0.02	51±0.23	394.45±1.80	38.66
L-dopa	WT	0.17±0.02	427.18±49.77	3953.86±460.65	2484.32
	S353G	0.36±0.01	46.54±3.32	359.93±36.41	127.99
o-tyrosine	WT	3.96±0.83	2.70±0.06	24.97±0.52	0.68
	S353G	0.42±0.05	58.92±3.96	545.39±51.84	141.88
m-tyrosine	WT	6.63±0.71	2.18±0.21	32.28±3.09	0.33
	S353G	0.38±0.01	5.06±0.17	39.14±1.30	13.36
5-HTP	WT	No decarboxylation activity			
	S353G	1.59±0.30	0.39±0.04	2.99±0.34	0.24

Table 4.3: The substrate selectivity of S353G mutation compared with wild-type enzyme. **Please note the wild-type enzyme kinetics to L-dopa and L-tyrosine have already been shown in Table 4.1 and are listed in this table for the purpose of comparison.**

As compared with wild-type enzyme, S353G also showed the highest activity to L-tyrosine and the K_{cat} to L-dopa was around 91 % its K_{cat} to L-tyrosine. However, the K_{cat} to L-tyrosine and L-dopa was lowered to 9.91 % and 10.89 % of the original activities of wild-type enzyme. At the same time, the K_{cat} to m-tyr and o-tyr was increased 2.32 and 21.82 times, respectively. Due to Gly is conserved in DDC at the equivalent position with Ser353 and DDC can use 5-HTP as another substrate in addition to L-dopa, the activity of mutated TyDC S353G to 5-HTP was also determined. Intriguingly, the mutated TyDC S353G generated activity to 5-HTP, contrasting to the no activity in the wild-type enzyme, although the activity is low and V_{max} is only 2.99 nmol min^{-1} mg^{-1}.

4.3.5 H193 is involved in decarboxylation

Substrate selectivity comparison of active site residues between TyDC and DDC indicated that most of the residues, making up of their active site and interacting with PLP, were the same or similar. For example, based on TyDC homology model and DDC crystal structure, His193 in TyDC and His192 in DDC were similar in spatial orientation and interacted with the internal aldimine and external aldimine through charge interaction and π-π stacking.

Sequence alignment and structural analysis indicates that His193 is in close proximity with the Schiff base of the external aldimine. Thus, His193 is possibly involved in decarboxylation and thus was mutated to Ala to remove all the hydrophilic and aromatic effect of His and also the ability of His193 as a good proton donor and acceptor while Ala has no ability to form hydrogen

bond or serve as a proton donor and acceptor. The H193A reduced the decarboxylation activity to L-dopa and L-tyrosine more than one magnitude and increased acetaldehyde synthase activity to L-dopa and to L-tyrosine (Figure 4.5), indicating the important role His193 plays in keeping the typical decarboxylation pathway.

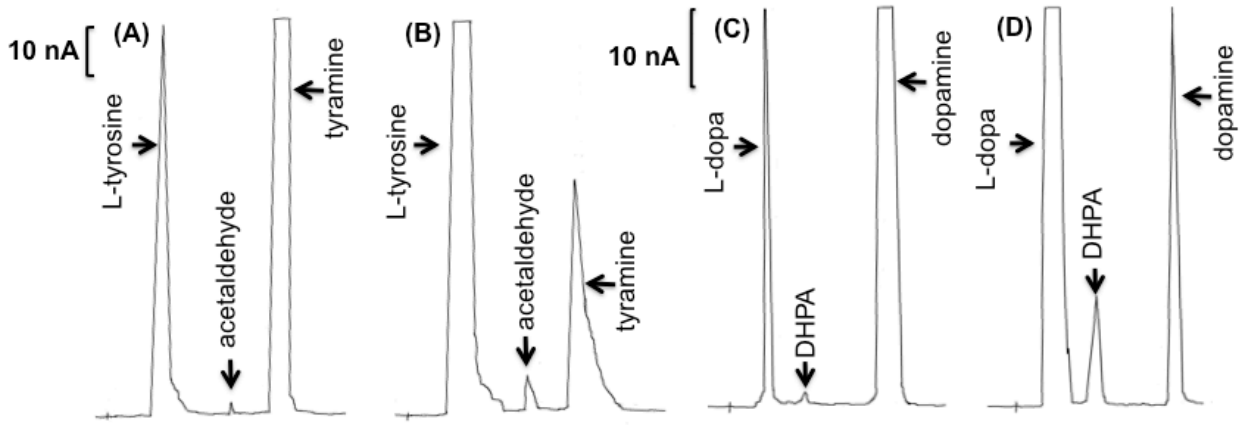

Figure 4.5: The chromatogram indicating activity of wild-type TyDC enzyme and H193A to L-dopa and L-tyrosine. **The wild-type TyDC and H193A activity to L-tyrosine are shown in A and B respectively with the same scale bar. C and D shows the wild-type TyDC and H193A activity to L-dopa respectively with another scale bar as added.**

4.4 Discussion

There have been numerous research and publications related to insect neurotransmitter dopamine or tyramine/octopamine, especially the synthesis, function, regulation of those insect neurotransmitters (1, 2, 11). As the first step to catalyze the production of tyramine, which is the substrate to produce octopamine, TyDC is of great importance in tyramine/octopamine pathway. However, there are no reports on the substrate selectivity or catalytic properties due to the difficulty to express the functional insect TyDC. The tyramine/octopamine's physiological role is

presumably critical for invertebrate, but not for vertebrate (1, 2). Thus, the biochemical understanding of TyDC is extremely indispensable because the substrate selectivity or catalysis is closely related to its physiological functions.

Although the insect homogenate can be analyzed toward tyrosine for a feeling of TyDC activity, with the high concentration of DDC and other proteins and components in the homogenate, it is hard to clearly characterize TyDC activity, for example, whether it is also active to dopa or 5-HTP. As contrast to its critical role, the biochemical characteristics of TyDC is not reported and far from clearly clarified. In this study, we reported the first functionally expressed insect TyDC, XP_308521.3 from *Anopheles gambiae*. There were two *Drosophila* tyrosine decarboxylases and were annotated as TyDC1 (NP_610226.2) and TyDC2 (NP_724489.1). Sequence alignment suggested that XP_308521.3 should belong to TyDC1 because of higher identity with TyDC1 (65.7 %) than with TyDC2 (49.8 %).

Through biochemical analysis of the expressed wild-type TyDC, as compared with DDC, we found two apparent differences between TyDC and DDC. First, the spectral analysis of TyDC indicated that TyDC spectra has predominant absorption at 422 nm (215 mAU v.s. 300 mAU for λ_{max} at around 340 nm and 422 nm respectively) while 340 nm absorption predominates in DDC (around 630 mAU v.s 230 mAU for λ_{max} at around 340 nm and 422 nm respectively). Second, another characteristic that TyDC differentiates from DDC is the substrate selectivity and the high affinity of TyDC to the substrates.

To fully understand the spectra and substrate selectivity differences, homology models of TyDC were generated and compared with DDC structure. In terms of spectra characteristics, our homology modeling and structural comparison provided some target residues. Subsequent site-directed mutagenesis and ionic exchange purification results indicated that the spectra of DDC and TyDC are affected by interaction between PLP and active site residues, especially with Asn302 in TyDC and His301 in DDC.

Free PLP displays a predominantly visible absorbance peak with λ_{max} around 390 nm with the value changing slightly depending on pH of the buffer. Once the PLP is anchored in PLP-dependent enzymes, due to interactions between PLP and the active site residues, absorption is observed from 300 nm to 500 nm, but the peak number and the λ_{max} vary in different enzymes. It has been known that ketoenamine and enolamine tautomers showed the λ_{max} at 420-430 nm and 330-340 nm, respectively. Therefore, it seems that active site residues in TyDC likely favored the production of its ketoenamine tautomer while His301 in DDC likely leads to more enolamine formation. However, only forming different tautomers, or the substitution on the pyridine ring is not the indeed reason contributing to the PLP absorbance. It is known that PLP's absorbance is due primarily to its pyridine ring, while the substitutions on the pyridine ring, including the interactions between substitutions and active site residues, contribute to the varying of the absorbance. In addition, the broad peak, instead of a sharp peak, indicates that the process is undergoing equilibrium and could not be simply attributed to formation of either only enolamine or only ketoenamine tautomer. Thus, we propose that the Asn304 versus His301 affect the spectra through effect on the electron distribution of PLP aromatic ring, even it is true that the interactions may also lead to different predominant tautomers.

The role of Asn304 in TyDC and His301 in DDC on affecting the spectra is supported by the following aspects. First, the wild-type TyDC and DDC showed the spectra differences but high identity in sequence, high similarity for both the overall structure and most of the active site residues, indicating the possibilities of small changes in the active site, especially those interacting with internal aldimine, are probably responsible for the spectra differences. Second, based on the structural analysis, the proximity of Asn304 in TyDC and His301 in DDC to the Lys 305 and Lys302 respectively makes it possible for interaction with internal aldimine. Third, sequence alignment suggested that Asn304 was highly conserved in identified TyDC and His301 was highly conserved in identified DDC. When Asn304 in TyDC was mutated to His, the mutated TyDC N304H makes the spectra similar to that of DDC. Asn304, other than forming hydrogen bond easily with internal aldimine (formed by Lys with PLP), is hard to enable charge interactions with internal aldimine, while His301 in DDC could have charge interaction to affect the PLP ring electron density.

In addition to the spectra differences, in contrast to DDC, which has activity to L-dopa and 5-HTP, our TyDC1 has no activity to 5-HTP, but catalyzes the decarboxylation of not only L-tyrosine but also L-dopa with high affinity reflected by K_m of sub-millimolar range, which contrasts the K_m (milimolar range) of DDC. Moreover, TyDC to both tyrosine and dopa is more active than DDC to dopa indicated by the result that K_{cat} of TyDC to tyrosine and dopa is 4.1 and 3.5 times the K_{cat} of DDC to dopa respectively. Compared with DDC, TyDC catalyzes the decarboxylation of tyrosine and dopa with higher affinity and activity, which we believe is related to its especially critical role to produce the predominant neurotransmitter

tyramine/octopamine presumably specific for insects. Our analyses of DDC and TyDC expression profile show that the DDC expresses at a relatively high level in different developmental stages as compared with TyDC expression (data not shown). The low expression level but high affinity and high activity of TyDC probably prevent the depletion of the essential amino acid tyrosine but maintain the production of tyramine/octopamine neurotransmitter essentially for insects. TyDC should be highly regulated to maintain sufficient concentration of neural tyrosine and otherwise the depletion of the essential amino acid tyrosine will lead to adverse functional consequences for the cell. On one hand, tyrosine is the substrate or precursor for not only tyramine/octopamine synthesis but also dopamine formation. The low expression level of TyDC may prevent severe depletion of tyrosine and also make the tyrosine still available for the tyrosine hydroxylase. On the other hand, the high affinity and activity of TyDC assure the efficient synthesis of tyramine/octopamine even with a relatively low expression of TyDC. Moreover, the ability of TyDC to catalyze decarboxylation of L-dopa probably could also contribute to dopamine synthesis need in cells as well. It looks like the cell needs more dopamine through not only higher expression level of DDC but also the activity of TyDC towards dopa. This may attribute to the more important role of DDC not only in neurotransmitter production but also in sclerotization while TyDC is mainly involved in neurotransmitter production.

The substrate selectivity is closely related to the function of TyDC and DDC in synthesis of neurotransmitters tyramine, dopamine and serotonin. Thus, to fully understand the substrate selectivity differences and the residue involved, after comparing homology model of TyDC with DDC, we were able to identify possible substrate binding residues of TyDC. Further site-directed

mutagenesis and activity assay excluded other residues but indicated that two residues, Asn304 and Ser353, are primarily involved in the substrate binding of TyDC.

Ser353 is conserved in TyDC while Gly is conserved in DDC at the equivalent position. The mutated TyDC S353G enabled TyDC to catalyze decarboxylation of 5-HTP, which is the substrate of DDC but not wild-type TyDC. Although the K_{cat} of the S353G is smaller than expected, the 1.59 mM K_m of S353G indicated the relative reasonable affinity generated to 5-HTP, which is comparable to affinity (indicated by the K_m of 1.3 mM) of DDC to L-dopa. This suggests that the Ser353 is involved in the substrate selectivity of TyDC to exclude 5-HTP as a substrate while Gly enables the utilization of 5-HTP as substrate. Our homology modeling and structural analysis further indicated that Gly as compared with Ser353, without $–CH_2$-OH side chain, makes additional space (Figure 4.3) available for 5-HTP indole ring, which is bigger than the dopa and tyrosine benzene ring. In addition to the effect to allow TyDC to use 5-HTP as a substrate, the mutated enzyme S353G also decreased the binding affinity and activity to L-tyrosine and dopa, but increased the affinity and activity to o-tyrosine and m-tyrosine to make the enzyme have highest affinity and activity to o-tyrosine (Table 4.3).

The substrate selectivity changed by S353G mutated enzyme indicates that Ser353 versus Gly351 are the residues for excluding using 5-HTP as a substrate, but it is not the residue determining the enzyme substrate affinity toward tyrosine or L-dopa because both affinities to L-tyrosine and L-dopa are decreased by S353G mutated enzyme as reflected by the increased K_m values. Instead, another pair of residues, Asn304 versus His301 stands out in kinetics analyses. Asn304 is conserved in all *in vivo* functionally verified TyDC while His conserved in all the

DDC at the equivalent position. By mutating Asn304 to His301 in TyDC, the K_m toward tyrosine was increased from 0.1 mM to 4.54 mM while the K_m toward dopa was decreased from 0.17 mM to 0. 12 mM, indicating the better affinity of TyDC N304H to dopa than to tyrosine, which is in contrast with highest affinity toward tyrosine in the wild-type TyDC. The K_m of mutated enzyme N304H and wild-type TyDC indicates that the Asn304 enables higher affinity to tyrosine while His301 enables higher affinity to dopa. Homology model of TyDC and crystal structure of DDC provides a reasonable explanation that Asn304 side chain $–NH_2$ is closer to the 4-OH group (3.2 Å) of carbidopa than to the 3-OH group (4.1 Å). In contrast, in DDC, the His301 side chain –NH- is closer to the 3-OH group (3.4 Å) of carbidopa (Figure 4.3). The tyrosine has 4-OH group while dopa has both 3-OH and 4-OH group. The ability of Asn304 to form hydrogen bond in a shorter distance with the 3-OH group may contribute to the higher affinity with tyrosine in wild-type TyDC and in DDC the His301 is closer to 3-OH group, which only exist in substrate dopa, to form hydrogen bond.

In addition to the residues involved in spectra and substrate selectivity, we also identified that His192 residue is critical for tyrosine decarboxylation. Site-directed mutation, H192A, significantly decreased the decarboxylation activity (Figure 4.5), indicating that His192 is involved in the decarboxylation catalysis. At the same time, the acetaldehyde synthesis activity of H192A is increased (Figure 4.5), indicating the importance of His192 in maintaining the typical decarboxylation pathway.

In summary, the first insect TyDC enzyme has been functionally expressed, and its substrate specificity and spectra characteristics have been determined in this study. Our data about the

high affinity and catalytic activity of TyDC and also its ability to catalyze both dopamine and tyramine formation more efficiently than DDC should provide the insight toward a comprehensive understanding of the function of this essential insect enzyme and also provide an insight of TyDC evolution. However, some details (such as the exact 3-D electron distribution on PLP ring in wild-type DDC, TyDC and mutated enzymes) remain to be verified. While spectra and K_m of our mutated and wild-type enzymes does indicate that the Asn304 in TyDC versus His301 in DDC has major effect for not only the spectra differences but also the affinity differences toward tyrosine or dopa, mutation of Asn304 to His in TyDC did not lead to a higher K_{cat} toward L-dopa instead of L-tyrosine, but the mutated enzyme N304H of TyDC does make the K_{cat}/K_m for L-dopa is ~4 times of that for L-tyrosine. Also taken the ability of using both dopa and tyrosine by their wild-type and mutated enzymes, all these facts indicate that other active site residues may also have a role in substrate binding, but the effect of these individual residues is subtle and hard to be quantified through mutation analysis one by one. Nevertheless, our data provided a reasonable biochemical basis to propose that Asn304 in TyDC versus His301 in DDC has major role in differentiating their spectra and also more importantly aid in more affinity to tyrosine and dopa respectively while Ser353 is the residue to affect substrate selectivity, especially make the active site smaller to exclude 5-HTP as a substrate. In addition, His192 is important for decarboxylation activity. Our comparative analyses of DDC and TyDC result a better understanding of TyDC spectra and substrate selectivity and key residues involved as well and provide one insight of how the TyDC biochemical characteristics may contribute to the balance between the tyramine/octopamine formation and dopamine formation starting from the same substrate tyrosine.

4.5 References

1. Roeder T. Tyramine and octopamine: ruling behavior and metabolism. Annu Rev Entomol. 2005;50:447-477
2. Lange AB. Tyramine: from octopamine precursor to neuroactive chemical in insects. Gen Comp Endocrinol. 2009;162(1):18-26
3. McClung C, Hirsh J. the trace amine tyramine is essential for sensitization to cocaine in Drsophila. Curr Biol. 1999(9):853-860
4. Blenau W, Baumann A. Molecular and pharmacological properties of insect biogenic amine receptors: lessons from Drosophila melanogaster and Apis mellifera. Arch Insect Biochem Physiol. 2001(48):13-38
5. Saudou F, Amlaiky N, Plassat J-L, Borrelli E, Hen R. Cloning and characterization of a Drosophila tyramine receptor. The EMBO Journal. 1990(9):3611-3617
6. Robb S, Cheek TR, L.Hannnan F, M.Hall L, M.Midgley J, D.Evans P. Agonist-specific coupling of a cloned Drosophila octopamine/tyramine receptor to multiple second messenger systems. The EMBO Journal. 1994;13(6):1325-1330
7. Cazzamali G, Klaerke DA, Grimmelikhuijzen CJ. A new family of insect tyramine receptors. Biochem Biophys Res Commun. 2005;338(2):1189-1196
8. Cole SH, Carney GE, McClung CA, Willard SS, Taylor BJ, Hirsh J. Two functional but noncomplementing Drosophila tyrosine decarboxylase genes: distinct roles for neural tyramine and octopamine in female fertility. J Biol Chem. 2005;280(15):14948-14955
9. Blumenthal EM. Isoform- and cell-specific function of tyrosine decarboxylase in the Drosophila Malpighian tubule. J Exp Biol. 2009;212(Pt 23):3802-3809
10. Ishida Y, Ozaki M. Aversive odorant causing appetite decrease downregulates tyrosine decarboxylase gene expression in the olfactory receptor neuron of the blowfly, Phormia regina. Naturwissenschaften. 2012;99(1):71-75
11. Han Q, Ding H, Robinson H, Christensen BM, Li J. Crystal structure and substrate specificity of *Drosophila* 3,4-dihydroxyphenylalanine decarboxylase. PLoS One. 2010;5(1):e8826
12. Kelley LA, Sternberg MJ. Protein structure prediction on the Web: a case study using the Phyre server. Nat Protoc. 2009;4(3):363-371
13. Pieper U, Webb BM, Barkan DT, Schneidman-Duhovny D, Schlessinger A, Braberg H, Yang Z, Meng EC, Pettersen EF, Huang CC, Datta RS, Sampathkumar P, Madhusudhan MS, Sjolander K, Ferrin TE, Burley SK, Sali A. ModBase, a database of annotated comparative protein structure models, and associated resources. Nucleic Acids Res. 2011;39(Database issue):D465-474
14. Arnold K, Bordoli L, Kopp J, Schwede T. The SWISS-MODEL workspace: a web-based environment for protein structure homology modelling. Bioinformatics. 2006;22(2):195-201
15. Biasini M, Bienert S, Waterhouse A, Arnold K, Studer G, Schmidt T, Kiefer F, Cassarino TG, Bertoni M, Bordoli L, Schwede T. SWISS-MODEL: modelling protein tertiary and quaternary structure using evolutionary information. Nucleic Acids Res. 2014;42(Web Server issue):W252-258

16. Guex N, Peitsch MC, Schwede T. Automated comparative protein structure modeling with SWISS-MODEL and Swiss-PdbViewer: a historical perspective. Electrophoresis. 2009;30 Suppl 1:S162-173
17. Kiefer F, Arnold K, Kunzli M, Bordoli L, Schwede T. The SWISS-MODEL Repository and associated resources. Nucleic Acids Res. 2009;37(Database issue):D387-392
18. Schwede T. SWISS-MODEL: an automated protein homology-modeling server. Nucleic Acids Res. 2003;31(13):3381-3385
19. Shi J, Blundell TL, Mizuguchi K. FUGUE: sequence-structure homology recognition using environment-specific substitution tables and structure-dependent gap penalties. J Mol Biol. 2001;310(1):243-257
20. Sippl MJ. Recognition of Errors in Three-dimensional structures of proteins. Proteins. 1993;17:355-362
21. Wiederstein M, Sippl MJ. ProSA-web: interactive web service for the recognition of errors in three-dimensional structures of proteins. Nucleic Acids Res. 2007;35(Web Server issue):W407-410
22. Luthy R, Bowie JU, Eisenberg D. Assessment of protein models with three-dimensional profiles. Nature. 1992;356(5):83-85
23. Burkhard P, Dominici P, Borri-Voltattorni C, Jansonius JN, N. MV. Structural insight into Parkinson's disease treatment from drug-inhibited DOPA decarboxylase. Nat Struct Biol. 2001;8(11):963-967

Chapter 5

Conclusion

PLP-dependent enzymes are involved in diverse enzymatic reactions of many critical biological processes. Due to the close structure-function relationship and the important physiological functions of PLP-dependent enzymes, the PLP-dependent enzymes have become the foci for structural-functional study and the mechanism study. Among the PLP-dependent enzymes, aromatic amino acid decarboxylase catalyzes the production of aromatic amines, some of which are essential neurotransmitters (e.g., dopamine, serotonin, histamine, etc.) (Chapter 2).

This study is focused on the biochemical characterization of aromatic amino acid decarboxylases L-3, 4-dihydroxyphenylalanine (dopa) decarboxylase (DDC) and tyrosine decarboxylase (TyDC) and one 3,4-dihydroxyphenylacetaldehyde (DHPA) synthase. DDC is responsible for decarboxylation of L-dopa and 5-hydroxytryptophan to produce dopamine and serotonin respectively, and DDC is also involved in more physiological processes in insects. TyDC catalyzes the first step (L-tyrosine decarboxylation) in tyramine/octopamine synthesis pathway, the physiological functions of which are considered to be essential for insects specifically. We identified that some annotated DDC, DDC-like proteins or aromatic amino acid decarboxylases actually catalyze oxygen involved decarboxylation-oxidative deamination to produce 3,4-dihydroxyphenylacetaldehyde (DHPA) synthase, CO_2, H_2O_2 and NH_3, which is in contrast with the typical non-oxidative decarboxylation catalyzed by DDC. Due to the functions of DHPA in

crosslinking of proteins in the process of flexible cuticle formation, these proteins are annotated as DHPA synthase (Chapter 3).

Our research conducted a comparative study between DHPA synthase and DDC by sequence alignment, structural analysis, and site-directed mutagenesis. DDC catalyzes the typical non-oxidative decarboxylation while DHPA synthase catalyzes oxygen involved decarboxylation-oxidative deamination. Our structural analysis and site-directed mutagenesis results indicated the presence of conserved Asn residue and His residue in the active site of DHPA synthase and DDC respectively could discriminate the DHPA synthase and DDC-mediated reactions. Based on our result, we proposed a mechanism for explaining the role of His residue and Asn residue in DDC and DHPA synthase-catalyzed reaction respectively. We also found that oxygen involved in the reaction would be reduced to H_2O_2 and the produced H_2O_2 could be reused as an oxidizing agent to lower the accumulation and oxidative stress of H_2O_2. Furthermore, based on the signature residues, we are able to identify more real DHPA synthase from DDC even they are annotated as DDC-like proteins in the database. Our results indicated that most of the sequenced insect genomes (if not all) had at least one DHPA synthase (Chapter 3).

With the sequencing of insect genomes, there are a group of enzymes annotated as tyrosine decarboxylases in insect genomes, but no biochemical evaluation of those enzymes has been reported in terms of the enzymatic catalysis property and substrate selectivity. The problem is because expression of functionally active TyDC is difficult and we expressed the first recombinant insect TyDC. Therefore, based on the successful expression of the first functional insect TyDC, we analyzed the PLP spectra, substrate selectivity and kinetic properties of wild-

type TyDC. Wild-type TyDC is active to both L-dopa and L-tyrosine and has higher substrate affinity and catalytic activity than those of DDC to L-dopa. Through comparative study with DDC by sequence alignment, structural analysis and comparison, and site-directed mutagenesis, we identified that one active site Ser353 in DDC is mainly involved in substrate specificity by affecting the space of the active site. Next to the Lys residue that is in charge of PLP binding through internal aldimine formation, there is one Asn304 residue conserved in TyDC while a conserved His residue at the equivalent position. This pair of residues is in charge of the spectra differences and also substrate binding affinity (dopa versus tyrosine) of DDC and TyDC. This study for the first time provides a better understanding of the enzymatic characteristics of insect tyrosine decarboxylase and provides the basis for the further functional research of tyrosine decarboxylase in tyramine/octopamine synthesis pathway (Chapter 4).

This dissertation is mainly focused on the structure-function relationship of the PLP-dependent enzymes, but some results could also inspire some interesting research of other fields in the future. First, the identification of high reactivity of DHPA and the biochemical analyses of DHPA synthase provides a basis for achieving a comprehensive understanding of the insect flexible cuticle formation, especially how the toxic process could be balanced. The DHPA formed is quite reactive for protein crosslinking through a way similar to that of formaldehyde in tissue fixation, but there has been no report regarding the detailed biochemical characteristics and mechanism of insect DHPA synthase before our study. Our results of insect DHPA synthase indicate that the whole catalytic process is quite slow and the produced H_2O_2 is reused as the oxidizing agent in the process. Through a slow reaction rate and the ability to reuse H_2O_2, insects could utilize the reaction product DHPA for flexible cuticle protein crosslinking and at the same

time to avoid the toxicity and oxidative stress caused by the accumulation of DHPA and H_2O_2 respectively. Due to the high reactivity, it is predicted that DHPA must be excluded from the circulation to the whole body of insects. It is also worthwhile to test whether the DHPA synthase could be a protein material for cuticle formation through crosslinking by produced DHPA into the cuticle protein matrix, and DHPA synthase could also be a target for controlling insect-borne diseases. Moreover, the proposed mechanism of DHPA synthase in this study also raise other questions as to how the oxygen is activated through the process, whether the quinonoid intermediate will have some radical characteristics, and whether there are some conformational changes during this slow reaction to enable catalysis. Second, based on our biochemical analysis of the first functionally expressed insect TyDC, TyDC can use both dopa and tyrosine as substrate and TyDC has higher substrate affinity and catalytic activity toward L-dopa than those of dopa decarboxylase toward L-dopa. It is intriguing to study whether these characteristics have some physiological meaning, for example, whether TyDC and DDC have different localization or same localization in neurons, whether the tyramine/octopamine specific neuron could also use dopamine as a neurotransmitter. Besides, there are still no crystal structures for the insect TyDC, and the crystallization of TyDC protein will better contribute to the functional analyses of TyDC. Because the physiological role of tyramine is presumably important for insects, the crystal structure of TyDC could also provide some basis for the structure-based strategy for insect-borne disease control.

Nowadays, a better understanding of PLP-dependent enzymes has been achieved. With the availability of more sequenced genomes, more PLP-dependent enzymes will be proposed. With the comparative study on the closely related PLP-dependent enzymes, e.g., study on DDC versus

DHPA synthase in terms of different reactions on the same substrate, or analyses of substrate specificity based on the comparison between DDC and TyDC, a better understanding toward the reaction specificity and substrate selectivity of PLP-dependent enzymes will be achieved.